AN EXPERIMENTAL STUDY OF THE EFFECT OF INSTABILITY ON DYNAMIC DISPLACEMENT RELATIVE PERMEABILITY MEASUREMENTS

APPROVED BY SUPERVISORY COMMITTEE:

_____

_____

AN EXPERIMENTAL STUDY OF THE EFFECT OF INSTABILITY ON DYNAMIC DISPLACEMENT RELATIVE PERMEABILITY MEASUREMENTS

by

SANTANU KHATANIAR, B.TECH.

THESIS

Presented to the Faculty of the Graduate School of

The University of Texas at Austin

in Partial Fulfillment

of the Requirements

for the Degree of

MASTER OF SCIENCE IN ENGINEERING

THE UNIVERSITY OF TEXAS AT AUSTIN

AUGUST 1985

ACKNOWLEDGEMENTS

The author gratefully acknowledges the help of Dr. Ekwere J. Peters for his suggestion of a research topic and his close supervision and guidance throughout the course of this study. The author also thanks Dr. Mark A. Miller for his consent to serve on the supervisory committee.

Finally, the author acknowledges the help of Mr. J. Wortham, Mr. R. E. Hamilton and Dr. B. A. Rouse in setting up the equipment for this study.

ABSTRACT

An experimental study was undertaken to investigate the effects of instability on oil and water relative permeabilities measured by the dynamic displacement method. The calculation of relative permeability from dynamic displacement data assumes a stable displacement of oil by water. This assumption is no longer valid when the displacement becomes unstable. Therefore, the computed relative permeabilities are liable to be incorrect in such a situation.

Dynamic displacement experiments were carried out using unconsolidated sand packs, refined oils and distilled water. Oil and water relative permeability curves were obtained by a standard calculation technique. The degree of instability of the displacements was varied by varying a dimensionless stability number. The higher the stability number, the higher is the degree of instability. One steady state experiment also was carried out to obtain a set of control data.

The results show that instability has a significant effect on both oil and water relative permeability curves, obtained from dynamic displacement data. In gen-

eral, the oil relative permeabilities decreased and the water relative permeabilities increased with increasing stability number. Therefore, it is necessary to conduct dynamic displacement experiments under stable displacement conditions in order to obtain the true relative premeability curves for the fluid-rock system.

TABLE OF CONTENTS

LIST OF TABLES

LIST OF FIGURES

CHAPTER 1

INTRODUCTION

1.1 THE CONCEPT OF RELATIVE PERMEABILITY

The permeability of a porous medium represents the ease with which a fluid can flow through it. Relative permeability is the measure of the ease of flow when more than one fluid is present. Thus, the notion of relative permeability involves more than one fluid flowing through a porous medium in the same direction.

The three fluids that are usually of interest to the petroleum industry are oil, water and gas. Since at least two of these fluids are normally present in a petroleum reservoir, their relative permeabilities must be known in advance for predicting reservoir performance. Laboratory measurements of two and three phase relative permeability made on reservoir rock samples are used for the purpose of performance prediction. Therefore, it is important that these laboratory measurements provide accurate data to ensure correct prediction of reservoir performance. The present study will investigate the accuracy of relative permeabilities measured in the laboratory using the dynamic displacement method. Three

phase systems, however, will not be considered in this study.

Routine laboratory measurements of relative permeability utilize the dynamic displacement method, also referred to as the unsteady state method. This method provides a means of determining relative permeabilities rapidly. In this method, the porous medium, hereinafter referred to as the core, is first saturated with one fluid and this fluid is then displaced by another. Specifically, for an oil-water system, the core is first saturated with oil and the oil is then displaced with water. Relative permeabilities are computed from oil and water production data and pressure drops across the core.

The technique for computing oil-water relative permeabilities from dynamic displacement experiments was developed by Welge(1) and Johnson, Bossler and Naumann(2). Their derivation of the technique was based on the assumption of a stable, Buckley-Leverett(3) type displacement of oil by water. This type of displacement process is characterized by the advancement of water as a sharp front.

1.2 DESCRIPTION OF THE PROBLEM

In the dynamic displacement experiments it is often necessary to use high viscosity oil and/or high displacement rates and sometimes, low interfacial tensions for the following reasons :

1) The oil-water relative permeability curves obtained by the dynamic displacement method are limited only to the saturation values greater than the breakthrough water saturation. Relative permeabilities for saturations less than the breakthrough water saturation cannot be computed from this experiment. Hence, it appears desirable to have low breakthrough recovery followed by a large after-production of the displacing phase so that a wide saturation range can be obtained. High oil viscosity and high water flow rate both help achieve this goal.

2) Gravity segregation and boundary effects are known to have distorting effects on relative permeability measurements. Gravity segregation is caused by different densities of oil and water. Boundary effects arise from capillary discontinuity at the outflow face of the core. Several researchers(4,5) have shown that both boundary effects and gravity segregation can be effectively eliminated by using high displacement rates.

3) Use of a high displacement rate expedites the dynamic displacement experiments.
4) Low interfacial tension relative permeability data are required for modelling several types of enhanced oil recovrey processes. Hence, low tension relative permeabilities also need to be measured in the laboratory.

Unfortunately, high displacement rates, high oil-water viscosity ratio and low interfacial tensions tend to make the displacement of oil by water unstable. An unstable displacement is characterized by the lack of a sharp front of the displacing phase. Instead, the displacing phase advances through the core in the form of well-defined channels referred to as fingers. Thus, instability leads to a breakdown of the assumption of stable, Buckley-Leverett type displacement. Since this assumption constitutes the principal basis of the Welge and Johnson et al.'s technique for calculating relative permeabilities, the computed values are liable to be inaccurate when the displacement is unstable.

1.3 OBJECTIVE OF THIS STUDY

The objective of this study was to conduct an experimental investigation of the effect of instability on oil-water relative permeabilities, as measured by the

dynamic displacement (unsteady state) technique. This will be accomplished by performing waterflood experiments on unconsolidated sandpacks saturated with viscous oils. Different levels of instability, as represented by a dimensionless stability number, will be achieved by varying the displacement rate, sand wettability and oil viscosity. Oil and water relative permeabilities in each case will be computed by the Welge and Johnson et al.'s technique. A set of correct relative permeability data will be obtained by the steady state method for comparison with those obtained from dynamic displacement data. An attempt will also be made to provide an empirical correction method for reducing the effect of instability on dynamic displacement relative permeabilities.

1.4 ORGANIZATION OF THE REPORT

The principal methods for laboratory measurement of oil-water relative permeability curves are summarized in Chapter 2. The reasons for concern regarding possible effects of instability on relative permeabilities measured by the dynamic displacement method are indicated.

Chapter 3 contains a literature review of the major experimental and theoretical developments in the study of laboratory relative permeability measurements.

The factors that have a direct influence on the stability of a displacement are elicited. Experimental investigation of the effects of these factors on relative permeability measurements are reviewed.

The experimental equipment and procedures used in this study are discussed in Chapter 4. A description of the materials and the data analysis technique are also included in this chapter.

Chapter 5 presents the experimental results obtained from this study. These are summarized in the form of tables and graphs. Dynamic displacement relative permeability measurements at various levels of instability are presented and the overall effect of instability on these measurements is illustrated.

Chapter 6 gives a summary of the conclusions that were reached from this study. Some recommendations for future work in this area are made.

Various tables and plots showing details of the work done in this study are included in the Appendices. Appendix A contains tables of recovery and pressure data for each displacement experiment. Tables of computed injectivity data and oil-water relative permeabilities are included in Appendices B and C, respectively. Plots of recovery data, injectivity data and oil-water relative

permeabilities for individual experiments are shown in Appendices D, E and F, respectively.

CHAPTER 2

MEASUREMENT OF RELATIVE PERMEABILITY

Relative permeability is the measure of a porous medium's ability to conduct a fluid in the presence of one or more competing immiscible fluids. It is defined as the ratio of the effective permeability to the absolute permeability of the porous medium. The effective permeability to a given phase, when more than one phase is present, is obtained by applying the well-known Darcy's law to the phase under consideration. Since the maximum value of effective permeablilty is the absolute permeability, which occurs when a given fluid completely saturates the porous medium, values of relative permeability can vary from 0 to a maximum of 1.

There are two basic methods of laboratory measurement of relative permeability:

1) the steady state method

2) the dynamic displacement (unsteady state) method

The steady state method is direct and simple but is extremely time consuming, taking as many as several days for obtaining a single point on the relative permeability-saturation plot. In this method, all the relevant

phases are injected simultaneously into the core at predetermined rates until the pressure drop across the core stabilizes. The effective permeabilities and hence, the relative permeabilities may then be calculated by applying Darcy's law to each flowing phase. This gives a single point on the relative permeability-saturation plot. The whole procedure has to be repeated at different flow rates to complete the plot. The plot may be obtained over the complete saturation range. Several methods such as the Penn State method, the single core dynamic method and the Hassler method(6) essentially make use of the steady state technique with different modifications.

The dynamic displacement or unsteady state method is far less time consuming but is not as direct and simple as the steady state method. A technique to calculate oil and water relative permeabilities from a dynamic displacement experiment data was developed by Welge(1) and Johnson et al.(2). Currently, this is probably the most widely used method for routine laboratory measurement of two phase relative permeabilities.

The dynamic displacement method differs from the steady state method in that the core is first saturated with one fluid which is then displaced with the other, instead of flowing all the fluids simultaneously as in the steady state method. By assuming the displace-

ment to be stable and applying the theory of Buckley and Leverett, Welge(1) developed a method for calculating the ratio of relative permeabilities as a function of saturation at the core outlet. For linear immiscible displacement of one incompressible fluid by another, Welge derived the following relationship to compute the oil-water relative permeability ratio from oil and water production data. For water displacing oil:

$$\frac{k_{rw}}{k_{ro}} = \frac{\mu_w}{\mu_o}\left[\frac{1}{f_{o2}} - 1\right] \qquad (2.1)$$

The quantity f_{o2} is given by the slope of the recovery plot, that is, the plot of Q_o against Q_i:

$$f_{o2} = \frac{dQ_o}{dQ_i} \qquad (2.2)$$

A typical recovery plot for a constant rate waterflood experiment is shown in Figure 2.1. The volume of oil recovered equals that of water injected until the point of water breakthrough so that $f_{o2}=1$ until this point. Thus, from Equation 2.1, the computed pre-breakthrough relative permeability ratios are all zero. This is why the dynamic displacement method is limited only to the

FIGURE 2.1 TYPICAL RECOVERY PLOT

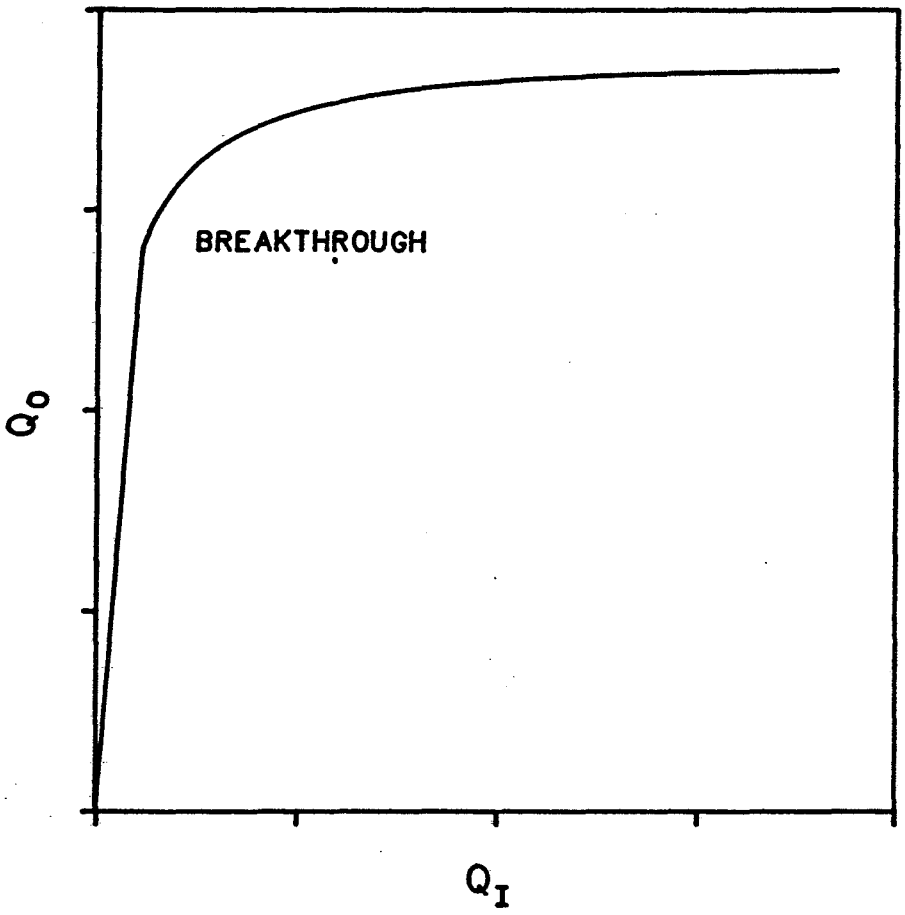

post-breakthrough region. Beyond breakthrough, the water production rate increases and the oil production rate declines continously. Welge(1) also showed that the saturation of the displacing phase at the core outlet can be obtained from the average saturation of the displacing phase in the core as:

$$S_{w2} = S_{wav} - f_{o2}Q_i \tag{2.3}$$

The average saturation can be easily obtained from material balance.

Welge's theory was further extended by Johnson, Bossler and Naumann(2) to permit the calculation of individual oil and water relative permeabilities. By integrating Darcy's law for each phase along the length of the core, Johnson et al. derived the following relationship:

$$\frac{f_{o2}}{k_{ro}} = \frac{d}{d\left[\frac{1}{Q_i}\right]}\left[\frac{1}{Q_i I_r}\right] \tag{2.4}$$

where

$$I_r = \frac{\left[\frac{q}{\Delta P}\right]}{\left[\frac{q}{\Delta P}\right]_{base}}$$

Relative permeability to water could then be computed from oil relative permeability using Welge's equations. Figure 2.2 shows a typical plot of $Q_i I_r$ versus $1/Q_i$. A typical plot of oil and water relative permeabilities is shown in Figure 2.3.

Implementation of the Welge and Johnson et al.'s technique requires the determination of two derivatives at the same value of cumulative water injection. In general, the process of differentiating experimental data by measuring slopes manually may involve significant amount of inaccuracy because of the usual scatter present in the experimental data. In 1978, Jones and Roszelle(7) developed a graphical technique for computing two phase relative permeabilities from dynamic displacement data. Their method, which was essentially equivalent to Johnson et al.'s method, was claimed to be easier to use and more accurate than the latter. However, this method also requires the determination of derivatives by drawing tangents and hence is probably not an effective solution to the basic problem.

FIGURE 2.2 TYPICAL INJECTIVITY PLOT

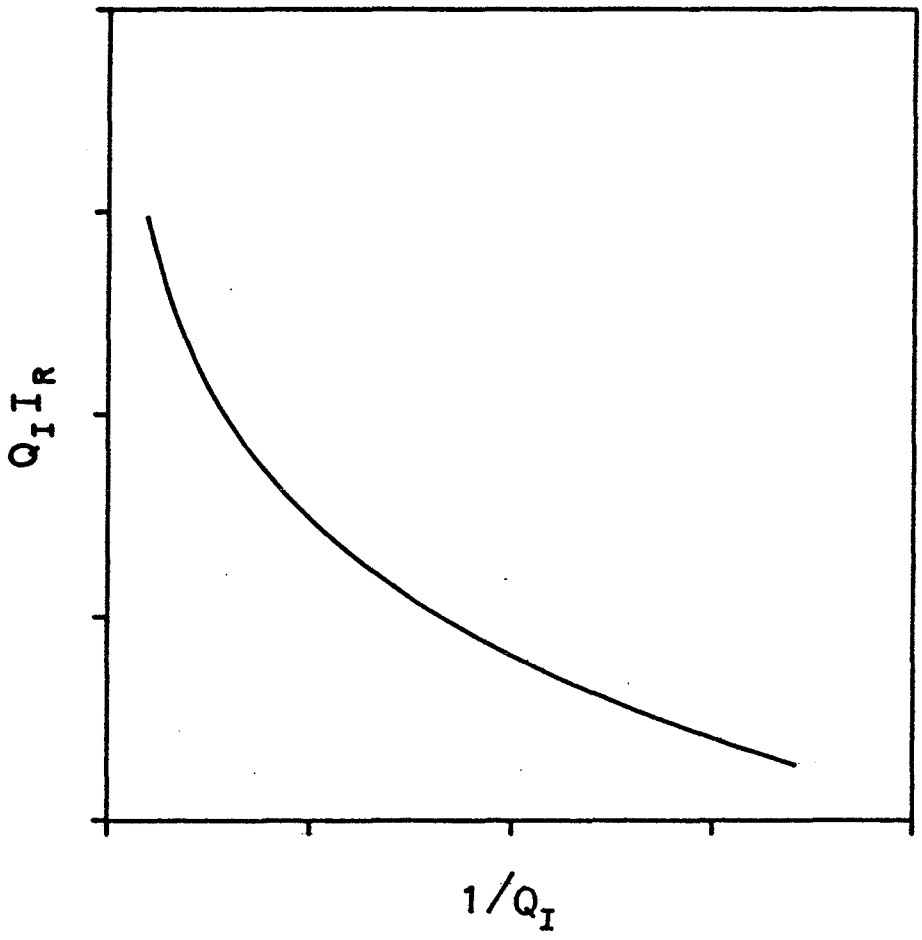

FIGURE 2.3 TYPICAL OIL AND WATER RELATIVE PERMEABILITY CURVES

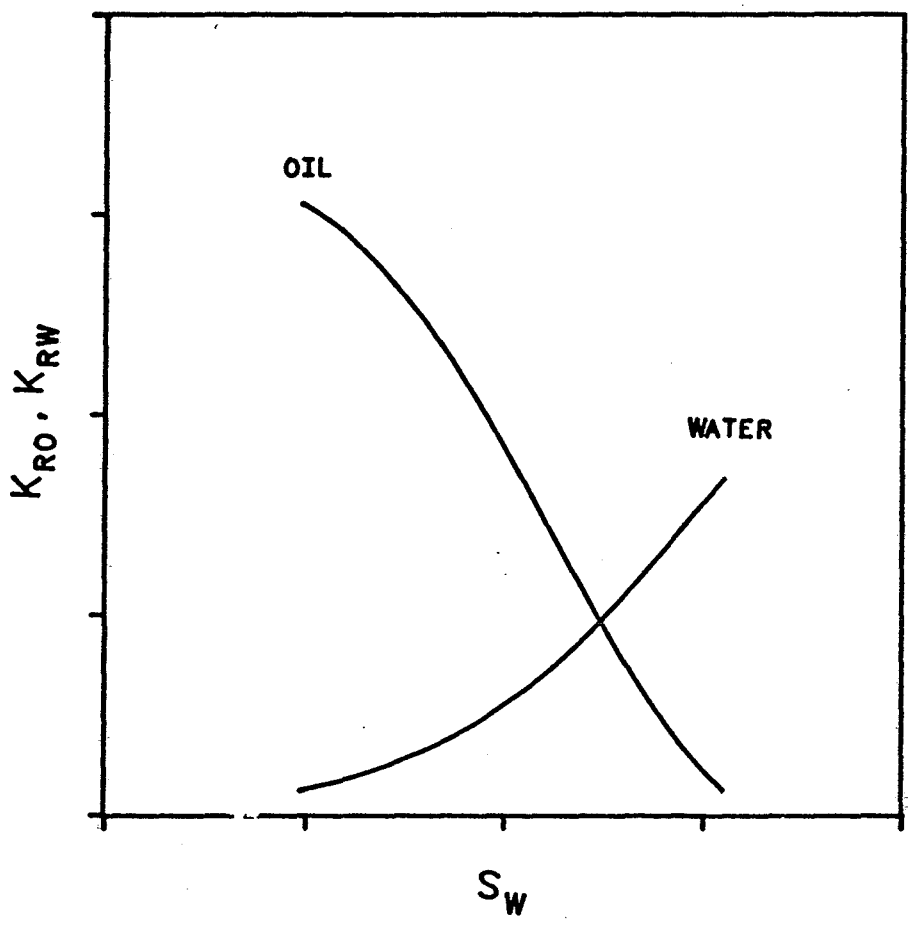

An alternative to the process of smoothing the data and drawing tangents by hand was presented by Miller and Ramey(8). They suggested the use of functional relationships to fit the experimental data. Derivatives were then determined by directly differentiating the functions involved. Thus, the scatter in experimental data was accounted for and the process always yielded smooth relative permeability curves.

CHAPTER 3

REVIEW OF RELATED RESEARCH

3.1 GENERAL

The effect of instability on dynamic displacement oil and water relative permeability measurements has received only limited attention. Past research in this area includes investigation of the effects of flow rate, viscosity ratio, interfacial tension and rock wettability on the steady state and the dynamic displacement relative permeablilty measurements.

Flow rate, viscosity ratio, interfacial tension and rock wettability all have a direct bearing upon the stability of displacements. Several investigators(9-13) have demonstrated that a displacement becomes less stable under any of the following conditions:

1) Increasing flow rate
2) Increasing oil-water viscosity ratio
3) Decreasing interfacial tension
4) Increasing oil wettability

An unstable displacement results in early breakthrough of the displacing phase due to the formation of viscous fingers. The existence of viscous fingers has been demon-

strated in laboratory core flood experiments(9-13). Some researchers(11,14) have expressed concern regarding the accuracy of relative permeability measurements when unstable displacement conditions prevail.

The criterion used in this study to ascertain the stability of displacements was a dimensionless stability number developed by Peters and Flock(13). The stability number was derived by extending a stability theory that was presented earlier by Chouke et al.(12). Although their analysis was based on a piston-like displacement, its validity for Buckley-Leverett type displacements was experimentally demonstrated by Peters and Flock(13). The Peters-Flock stability number for a cylindrical system is given by

$$N_s = \frac{(M - 1)(v - v_c)\,\mu_w\,D^2}{C^*\,k\,\sigma} \qquad (3.1)$$

where

$$v_c = \frac{k\Delta\rho g\cos(\alpha)}{\mu_w\,(M - 1)}$$

The critical value of the stability number was determined to be 13.56. This number and its critical value provide a necessary and sufficient condition for predicting the onset of instability in both oil-wet and water-wet porous

media. If in a given cylindrical system the computed value of the stability number exceeds the critical value under given conditions, then the displacement will be unstable. In addition, the magnitude of the stability number provides qualitative information regarding the severity of instability. If the stability number associated with a displacement is less than the critical value, then the displacement will be stable.

3.2 EFFECT OF RATE

Steady state oil and water relative permeability measurements have, in general, been found not to be affected by flow rate. This can be expected because in steady state measurements both fluids are injected simultaneously into the core. Thus, it is not a displacement process and the question of instability is eliminated. Theoretically, relative permeabilities are functions of saturation only. Therefore, steady state measurements provide correct values of relative permeability at all flow rates.

Early research on steady state relative permeability measurements include those of Osoba et al.(6), Caudle et al.(15) and Sandberg et al.(16). These studies have indicated steady state relative permeabilities to be essentially independent of flow rate in the absence of

boundary effects. Caudle et al., however, reported some effect of initial interstitial water saturation on steady state oil and water relative permeabilities.

In 1953, Rapoport and Leas(17) conducted a theoretical and experimental investigation of the effect of displacement rate on horizontal linear waterflood behavior. By extending the original Buckley-Leverett theory, they derived a scaling coefficient, given by $Lv\mu_w$, that could be used for quantitative determination of Buckley-Leverett type displacement conditions. From a series of constant rate displacement experiments, Rapoport and Leas concluded that Buckley-Leverett type flooding behavior is achieved when the scaling coefficient exceeds a critical value. They reported increases in breakthrough oil recovery with increasing value of the scaling coefficient. The breakthrough recovery was constant once the critical value of the scaling coefficient was exceeded. Similar behavior for water-wet porous media was reported later by Kyte and Rapoport(18).

It is important to distinguish between the Rapoport-Leas criterion and the Peters-Flock stability criterion. The critical value of the Rapoport-Leas scaling group, $Lv\mu_w$, represents the point when capillary forces cease to be significant. The displacement rate required to achieve this might be high enough to cause

the Peters-Flock stability number to exceed its critical value and make the displacement unstable. This is especially true at a high oil-water viscosity ratio. In such a case Buckley-Leverett theory will not be applicable. Such a possibility was first indicated by Calhoun and La Rue(19) in 1951. While the importance of elimination of capillary effects in relative permeability measurements has been emphasized in the past, the possible effects of instability have largely been ignored.

In a recent study, Fulcher et al.(20) presented steady state oil and water relative permeability measurements made on large Berea sandstone cores. Essentially no change in relative permeabilities was observed when flow rate was varied from 80 cc/hr to 400 cc/hr.

In 1982, Sufi et al.(21) reported the effects of displacement rate on dynamic displacement oil and water relative permeability measurements. They carried out dynamic displacement experiments to study the effect of temperature on oil-water relative permeability measurements. It is generally believed that in order to obtain representative relative permeability curves, dynamic displacement experiments must be performed at stabilized flooding conditions so that the assumption of Buckley-Leverett type displacement remains valid. The Rapoport and Leas scaling coefficient based on break-

through recovery provided one criterion for selecting a minimum rate that will eliminate capillary effects. Sufi et al., however, used a different criterion to determine the minimum displacement rate. They obtained relative permeability curves for different displacement rates. The displacement rate was considered sufficient to overcome capillary effects when the relative permeabilities became independent of the displacement rate.

Sufi et al. used unconsolidated Ottawa sandpacks for their experiments. Kaydol oil of 220 centipoise viscosity was displaced with distilled water. The core was first saturated with oil and the oil was then displaced with water under a constant pore pressure of 200 psi.

Oil and water relative permeability curves determined by the dynamic displacement method were found to be affected by displacement rate (Figure 3.1). The oil relative permeabilities increased only slightly with increasing rate, that is, with increasing stability number. The water relative permeabilities, however, exhibited marked change with displacement rate. These were low for low rates and increased rapidly with increasing rate. Both the oil and water relative permeabilities reached a limiting position for displacement rates greater than 240 cc/hr. A similar study at an elevated tem-

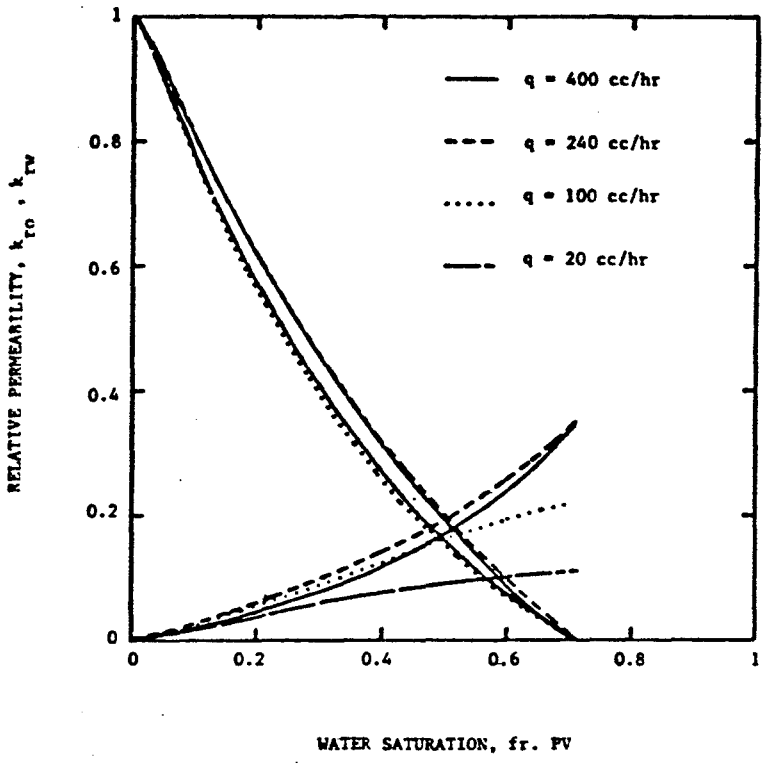

Figure 3.1: Effect of Displacement Rate on Relative Permeabilities Reported by Sufi et al.

perature of 150°F also showed rate dependency below 240 cc/hr. They concluded that the displacement process stabilized at rates above 240 cc/hr. This corresponded to a Rapoport and Leas' $Lv\mu_w$ value of about 6 cm^2-cp/min as the critical value. The critical value computed by Rapoport and Leas for their experiments was about 4 cm^2-cp/min, which is in close agreement with that found in Sufi et al.'s study.

Sufi et al. recognized the problem of viscous fingering by observing a decline in breakthrough recovery with increasing displacement rates. The breakthrough oil recoveries remained constant until a displacement rate of 100 cc/hr was achieved. This was followed by a sharp decline in the breakthrough recovery due to viscous fingering as displacement rates were increased beyond 100 cc/hr. However, at rates above 400 cc/hr, the breakthrough recoveries became constant again, but at a smaller value. A similar breakthrough recovery pattern was observed earlier by Peters(22). However, for Sufi et al.'s system, the dimensionless stability number at a rate of 100 cc/hr is about 10,000 , assuming oil-water interfacial tension of 25 dynes/cm and C^* =5.5 . Since the core was initially saturated with oil this value of C^* should be used, as suggested by Peters and Flock. Even if C^* =306 is used, assuming a water-wet system, the stability number at 100 cc/hr is about 190. Both values are appreciably higher than the critical value of 13.56 proposed earlier by Peters and Flock. It is possible that a different value of the wettability constant be applicable to the Sufi et al.'s system. Still, this value will have to be at least ten times the proposed value for a water-wet system to agree with the theoretical critical stability number.

It is interesting to note that the displacement rate required to achieve stabilized relative permeability curves closely corresponded to the rate where the lower plateau of the breakthrough recovery plot begins. According to the Peters and Flock stability theory, this lower plateau represents extremely unstable displacement conditions. The rate effect on oil and water relative permeabilities observed in these experiments could be due to instability rather than capillary effects, as was concluded by Sufi et al. Also, it is apparent that in this case, it was not possible to satisfy both the Rapoport-Leas and Peters-Flock stability criteria simultaneously. This problem was earlier addressed by Bentsen and Saeedi(23) while discussing waterflooding of high viscosity oils. The displacement rate required to achieve an $Lv\mu_w$ value above the critical may lead to viscous fingering. Sufi et al. agreed that the dynamic displacement relative permeabilities computed from an unstable displacement experiment will not be representative.

3.3 EFFECT OF VISCOSITY RATIO

Steady state relative permeability measurements have, in general, been found not to be affected by oil-water viscosity ratios. The findings of Levine(24)

and Sandberg(16) et al. tend to confirm this. Odeh(25), however, reported variation of steady state oil and water relative permeability curves with viscosity ratio in core samples of less than 1 darcy permeability. Oil relative permeabilities increased with increase in the oil-water viscosity ratio, the variation being maximum at low water saturations. The relative permeabilities to water remained unaffected by viscosity ratio. Odeh's findings were contradicted by Baker(26) and Downie and Crane(27) on the basis of theoretical and experimental considerations. They indicated the possibility of Odeh's results being affected by experimental difficulties.

In a recent study of the effect of the capillary number on oil and water relative permeabilities, Fulcher et al.(20) presented steady state relative permeability data to demonstrate the effect of viscosity ratio. By increasing the wetting phase viscosity by a factor of 1000, they noted a decrease in the non wetting phase relative permeability. This was accompanied by an increase in the wetting phase relative permeability of about the same order.

The effect of oil-water viscosity ratio on dynamic displacement relative permeability measurements was first investigated by Johnson et al.(2), when they first proposed their measurement technique. Three wat-

erfloods were performed on glass bead packs at oil-water viscosity ratios of 1, 5 and 37. All the three sets of relative permeability curves were found to be in close agreement.

In 1973, Lefebvre du Prey(28) carried out an experimental investigation of the effects of several factors, namely, interfacial tension, viscosity and displacement rate (in the dimensionless group $\sigma/\mu v$), wettability and viscosity ratio on oil-water relative permeabilities. The experiments were conducted on three artificial sintered porous media using the dynamic displacement method and relative permeabilities were calculated by the Welge and Johnson et al.'s technique. For each fluid pair, displacements were carried out in two directions, the final state of one displacement being the starting point for the following one. Samples were first saturated with the wetting fluid which was then displaced with the non wetting fluid.

The results indicated a substantial influence of viscosity ratio on the dissymmetry of measured relative permeability curves. The higher the viscosity of one liquid was, the lower was the relative permeability to the other liquid (Figure 3.2). This is in agreement with Fulcher et al.'s findings. Interestingly, Lefebvre du Prey's relative permeability measurements were made by

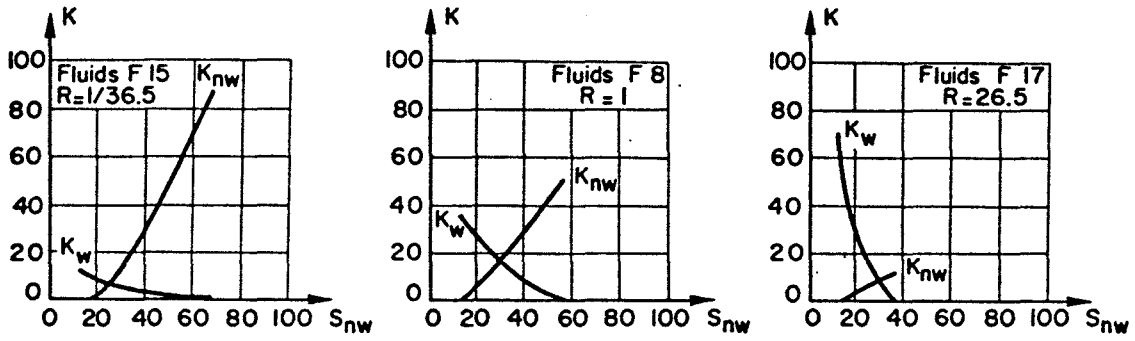

Figure 3.2: Effect of Viscosity Ratio on Relative Permeabilities Reported by Lefebvre du Prey

the dynamic displacement method while Fulcher et al. used the steady state method.

3.4 EFFECT OF INTERFACIAL TENSION

Interfacial tension has, in general, been found to affect both steady state and dynamic displacement relative permeability measurements. Some researchers have investigated the effect of interfacial tension combined with other variables as a capillary number.

Fulcher et al. carried out steady state relative permeability measurements to investigate the effects of capillary number and its constituents. The capillary number was defined as $\mu v/\sigma\phi$. However, from steady state measurements, Fulcher et al. could not arrive at a defi-

nite conclusion regarding the effect of capillary number on oil-water relative permeabilities. They reported no change in oil and water relative permeabilities for interfacial tensions above 2 dynes/cm. Below this value, relative permeabilities to both phases increased with decreasing interfacial tension. At very low interfacial tensions both relative permeability curves tended to become straight lines and assumed an 'X' shape.

Lefebvre du Prey(28) observed the effect of the capillary number, defined as $\sigma/\mu v$, on dynamic displacement oil and water relative permeability measurements in three artificial porous media. From experiments carried out in teflon cores, relative permeabilities to both phases were found to decrease with increasing value of the capillary number (Figure 3.3). The capillary number was varied from 5.1×10^3 to 1.4×10^6 at unit viscosity ratio. This result is in general agreement with the trend reported by Fulcher et al. from steady state measurements.

An increase in the capillary number used by Lefebvre du Prey corresponds to a decrease in the stability number, that is, a less unstable displacement. Thus, his findings agree with those of Sufi et al. to some extent. The decrease in relative permeability observed by Lefebvre du Prey was of the same order for both wet-

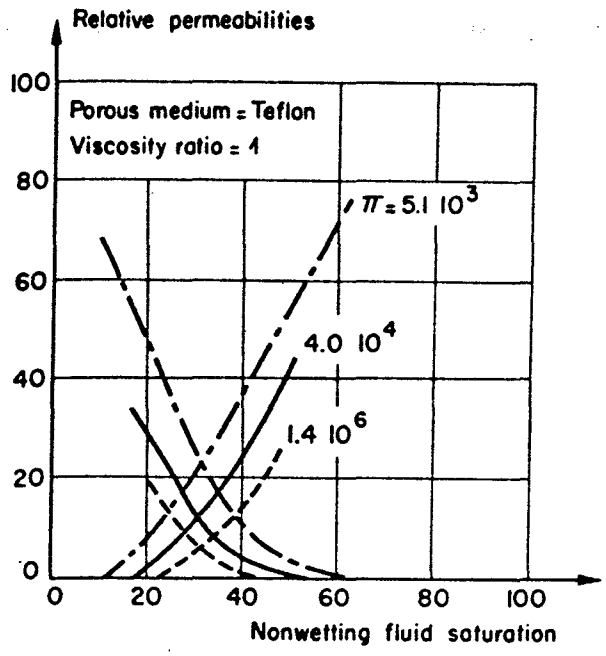

Figure 3.3: Effect of Capillary Number on Relative Permeabilities Reported by Lefebvre du Prey

ting and non wetting phases. Sufi et al. noted only a small decrease in oil relative permeabilities and a large decrease in water relative permeabilities with decreasing stability number.

In 1981, Amaefule and Handy(29) presented both steady state and dynamic displacement relative permeability measurements for different interfacial tensions. Oil water relative permeabilities were measured on Berea sandstone cores. Relative permeabilities were computed

from displacement data by the Welge and Johnson et al.'s method.

Amaefule and Handy's results showed a significant difference between steady state and dynamic displacement relative permeability results. Steady state relative permeabilities exhibited insignificant change until an interfacial tension of 0.1 dynes/cm was reached. Below this value of interfacial tension, both the oil and water relative permeabilities increased with decreasing interfacial tension. This trend agrees with that found by Fulcher et al..

Dynamic displacement oil relative permeabilities decreased and water relative permeabilities increased with decreasing interfacial tension (Figure 3.4). Also, the difference in oil relative permeabilities was more significant at low water saturations. In terms of the stability of the displacement, lower interfacial tension implies a less stable displacement. The increase in water relative permeability was much larger compared to the decrease in oil relative permeability. Thus, the trend of water relative permeabilities agrees well with that found by Sufi et al. The trend of oil relative permeabilities, however, is opposite to that reported by Sufi et al.. In general, dynamic displacement oil relative permeabilities were lower and water

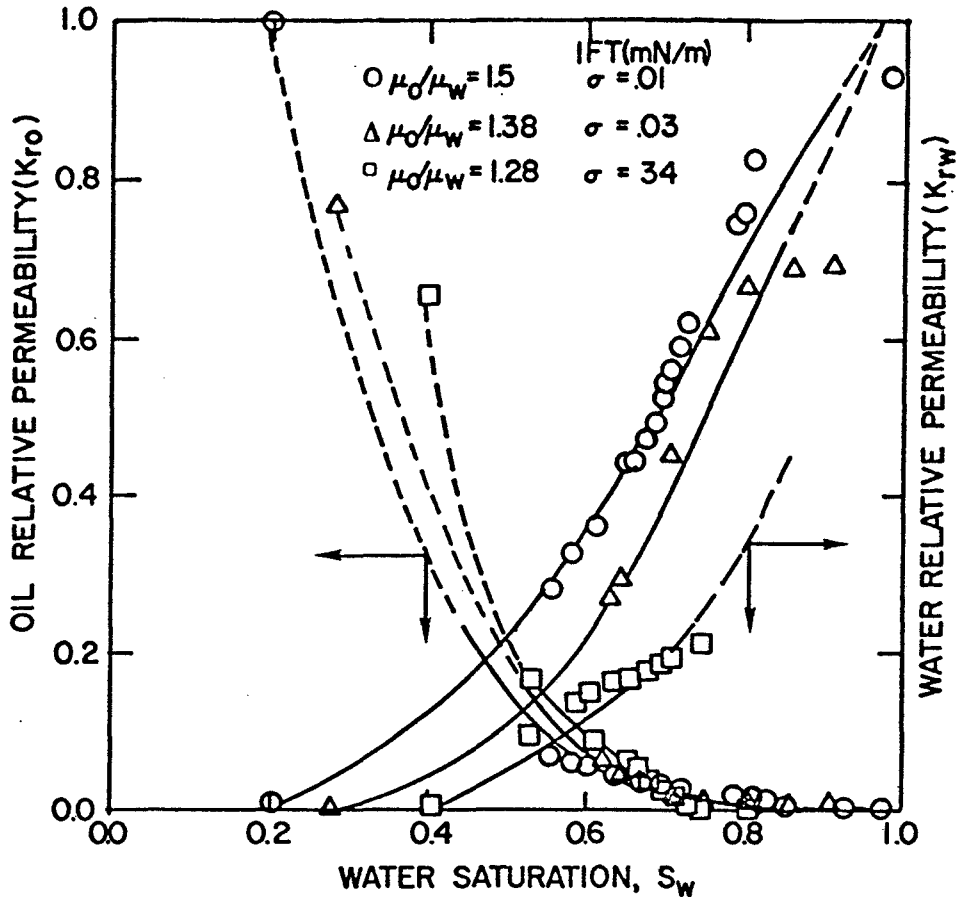

Figure 3.4: Effect of Interfacial Tension on Relative Permeabilities Reported by Amaefule and Handy

relative permeabilities were higher than the corresponding steady state values. The crossover point of dynamic displacement water and oil relative permeabilities shifted towards lower water saturation values with decreasing interfacial tension. This behavior is thought to be representative of increasing oil wetness of the

porous medium. Amaefule and Handy's work also shows that dynamic displacement measurements may differ from the true relative permeabilities depending on flooding conditions.

3.5 EFFECT OF SAND WETTABILITY

The effects of sand wettability and initial water saturation on the displacement process have been reported in the literature. Lefebvre du Prey(28) did not explicitly report the effect of wettability on dynamic displacement relative permeability measurements. However, he did observe a drastic change in the nature of the displacement process with change in wettability. When the displacing phase was nonwetting, breakthrough occurred early followed by a large after-production. When the displacing phase was wetting, the displacement became more piston-like. This is in general agreement with stability theory. When the displacing phase is wetting, the wettability constant C^* is large and this tends to decrease the stability number.

The effect of wettability on steady state oil and water relative permeability measurements was presented by Owens and Archer(30). Experiments were conducted over a wide range of rock wettabilities, as defined by contact angles. A contact angle of 0° is

strongly water-wet media and a contact angle of 180° is strongly oil-wet media. The results indicated that at a given saturation, the relative permeability to oil decreased as the degree of oil wetting increased. Similarly, the water relative permeability decreased with increasing water wettability (Figure 3.5).

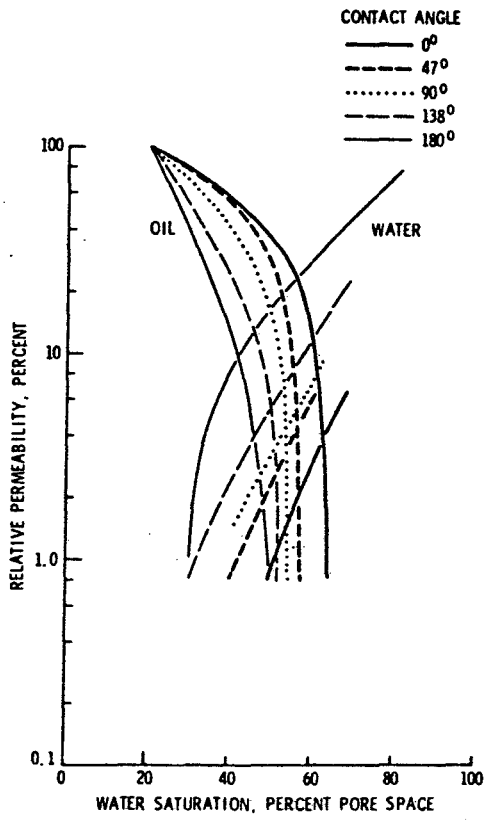

Figure 3.5: Effect of Rock Wettability on Relative Permeabilities Reported by Owens and Archer

A decrease in water wettability and an increase in oil wettability lead to a less stable waterflood. A gradual

and continous reduction in oil displacement efficiency was indicated as the core wettability changed from water-wet to oil-wet.

3.6 SUMMARY

From the foregoing discussion, it is apparent that experimentally determined relative permeabilities depend on the method of measurement as well as on the rock and fluid properties. Oil-water relative permeabilities determined by the dynamic displacement method have been found to be affected by displacement rate, viscosity ratio, interfacial tension and possibly by rock wettability. Since all these parameters have a direct bearing upon the stability of the displacement, it is possible that the basic mechanism behind these effects is instability. The fact that steady state relative permeabilities are generally not affected by flow rate and viscosity ratio lends credence to the above hypothesis. Steady state measurements do not involve a displacement process and hence do not suffer from the problem of instability.

CHAPTER 4

EXPRIMENTAL EQUIPMENT AND PROCEDURE

4.1 FLUIDS

Two oils were used to saturate the core in this study. This permitted carrying out of displacements at two viscosity ratios. The oils used were Dow Corning 200 and Texaco White oil No. 22. The Dow Corning oil is a refined silicon oil with 100 centistokes nominal viscosity. It was used in most of the runs because it has a density close to that of water. This helped to minimize gravity segregation problems. It also does not easily form an emulsion with water. The Texaco White oil had a nominal viscosity of 35 centipoise.

The displacing fluid used in all experiments was distilled water containing very small amounts of DiSodium Fluoroscein dye. At very low concentrations the dye imparted a light green color to the water. It was used to make the water easily discernible from oil so that the water breakthrough could be easily recognized and effluent volumes could be easily measured. For experiments that had initial water saturation, clear

distilled water without any dye was used to establish the initial water saturation.

The properties of the experimental fluids are given in Table 4.1. These properties were measured earlier by Broman(31) who used the same fluids for his stability studies.

TABLE 4.1

FLUID PROPERTIES AT 23.5°C

Fluid	Density (gm/cc)	Viscosity (cp.)	o/w visc. ratio	IFT (dynes/cm)
Distilled water	0.9957	1.011		
Texaco White oil	0.8859	35.31	34.93	21.6
Dow Corning 200	0.9589	108.37	107.19	26.7

4.2 THE FLOW SYSTEM

The flow system consisted of a constant rate pump and alternate flow loops for pumping oil and water independently. A double cylinder Ruska W-II proportioning pump was used to inject oil and water into the core. The pump was capable of delivering fluid at 28 different rates ranging from 2.5 cc/hr/cylinder to 560 cc/hr/cylinder.

The Dow Corning 200 oil and water were kept in separate steel pressure vessels. The Ruska pump displaced Texaco White oil No. 22 into the pressure vessels. This oil is immiscible with and lighter than the Dow Corning 200 oil and water. Therefore, it was injected into the pressure vessels from the top. By placing the two pressure vessels in separate flow loops it was possible to inject water or oil independently.

4.3 CORE HOLDER

A cylindrical core holder, 61.5 cm in length and 4.8 cm in internal diameter, was used for this study. The core holder was made of PVC to provide a smooth interior. To contain the unconsolidated sand pack, two stainless steel end caps were used. Each end cap was fitted with two O'rings which pressed tightly against the inner walls of the core holder to provide a liquid-proof

seal. The end caps were held in place by means of four hand nuts. Each end cap was provided with a central hole 6.4 mm in diameter for fluid entry/exit. The hole was surrounded by a shallow groove of 35 mm diameter where a screen could be held in place by means of an O'ring.

One displacement experiment was also carried out in a short core holder which was 30.3 cm long and 4.8 cm in internal diameter. The other characteristics of the core holder were the same as those of the longer one. The purpose of this run was to push the core out of the core holder at the end of the waterflood in order to visually examine the core sections for the evidence of viscous fingering.

4.4 POROUS MEDIUM

The porous medium used in this study was unconsolidated packs of 100-140 mesh silica sand(Oklahoma No. 1). The average porosity and permeability of the sand packs were approximately 30% and 3.5 darcies, respectively. Sieve analysis of this sand was performed earlier by Broman(31). The results of the sieve analysis are given in Table 4.2.

TABLE 4.2

SIEVE ANALYSIS RESULTS

Mesh size	Grain size (microns)	% stopped by screen
50	300	0.4
100	150	45.4
140	106	44.2
170	90	7.2
	Total:	97.2

4.5 PRESSURE MEASUREMENT SYSTEM

The pressure drops across the core were measured using three Validyne pressure transducers connected to a Validyne digital readout device. The pressure drop was obtained by measuring pressure at the inlet end of the core holder because the outlet end was open to the atmosphere. The digital pressure readout device was cal-

ibrated by applying air pressure and using an accurate Bourden gauge as the refernce.

4.6 EFFLUENT COLLECTION SYSTEM

The produced fluids were collected in 10 cc graduated test tubes using an ISCO Retriever II fraction collector. The outlet end of the core holder was connected to the fraction collector by means of a short piece of 1/4 inch flexible tubing.

4.7 CORE PREPARATION

The sand packs were prepared by tamping the sand filled core holder with a wooden hammer. Peters(22) had noted earlier that this method was rapid and provided as good a pack as that obtained by vibrating the sand filled core holder in a mechanical vibrator for several days.

Nylon screens were placed in the grooves of the end caps to prevent migration of sand out of the core holder. One of the end caps was then inserted into the core holder and secured with hand nuts. The core holder was placed vertically in a clamp with the open end facing up. Sand was poured in small increments and the core holder tamped with hammer until no visible settlement of the sand took place. When the sand level reached a

point somewhat below the top, the other end cap was fitted, making sure that both O'rings went inside the core holder. Thus, the actual length of the core was less than the length of the core holder to allow for the end caps to go in. The cap to cap length of the packed core holder was measured with a meter scale. The total height of the two end caps was subtracted from this value to obtain the true length of the sand pack.

4.8 PROCEDURE FOR RUNS WITHOUT INITIAL WATER

The runs without initial water saturation were carried out by first saturating the core with the appropriate oil (Dow Corning 200 or Texaco White oil 22) and then waterflooding it. While saturating, the core was held vertically to utilize gravity forces for making the advancement of the oil front uniform. Oil was injected at a constant rate from the bottom of the core holder. The same oil injection rate of 80 cc/hr was used in all the runs without initial water. After the core was completely saturated, the effluent from the top was collected in a measuring cylinder. Oil injection was continued until the pressure drop across the core stabilized. The stabilized pressure drop was used to calculate the absolute permeability of the core from Darcy's

law. The pore volume of the core was computed from material balance.

After saturation, the core was held horizontally and water injection was started at constant rate. The effluent was collected in the fraction collector. Since the water was colored, water breakthrough was clearly visible through the flexible tubing at the core outlet. Cumulative water injected, cumulative oil produced and the corresponding pressure drop across the core were noted. Water injection was continued until there was no appreciable oil production.

4.9 PROCEDURE FOR RUNS WITH INITIAL WATER

The procedure for these runs was similar to the procedure for runs without initial water. The core was first saturated with water and then flooded with oil to establish an initial water saturation. A gravity feed method was used to saturate the core with water. The core was held vertically and clear distilled water was allowed to flow into the core under gravity from a graduated burette connected to the bottom of the core holder. When the core was fully saturated with water, its permeability was measured by injecting water at a constant rate. The water in the core was then displaced with oil at a constant rate of 60 cc/hr. The same rate

was used for all runs with initial water. Oil injection was continued until no more water was produced. The effluent was collected in a measuring cylinder and the stabilized pressure drop across the core was noted. The core was then waterflooded at a constant rate as in the non-initial water case. For very low displacement rates, the core was held vertically while waterflooding in order to eliminate the problem of water underrunning the oil.

4.10 PROCEDURE FOR STEADY STATE RUN

In the steady state experiment, an initial water saturation was established by first saturating the core with distilled water and then displacing the water with the Dow Corning oil. Oil flowing at initial water saturation gave the first point of the relative permeability-saturation plot. The ratio of water flow rate to oil flow rate was then successively increased. For each combination of water and oil flow rates, the stabilized pressure drop across the core was noted. Oil and water relative permeabilities were computed from Darcy's law. Water saturation in the core was was computed from material balance.

4.11 DATA ANALYSIS

Oil and water relative permeabilities were computed from the displacement data by using the Welge and Johnson et al.'s technique as outlined in Chapter 2. As was pointed out in that chapter, the method requires the determination of two derivatives. This was performed by fitting smooth functional relationships through the observed data by the least square method and then differentiating these functions. This procedure was suggested by Miller and Ramey(8). They also suggested the following functional relationships:

$$Q_o = A_1 + A_2(\ln Q_i) + A_3(\ln Q_i)^2 \qquad (4.1)$$

$$\ln(Q_i I_r) = B_1 + B_2(\ln Q_i) + B_3(\ln Q_i)^2 \qquad (4.2)$$

These equations fitted the experimental data of this study satisfactorily.

In order to compare the relative permeability curves for the non-initial water systems and the initial water bearing systems, the water saturation was normalized as given below:

$$S_{wn} = \frac{S_{w2} - S_{wi}}{1 - S_{wi} - S_{or}} \qquad (4.3)$$

The oil and water relative permeabilities were plotted as functions of the normalized water saturation.

The dimensionless stability number for each displacement was calculated by using the relationship given in Chapter 3 (Equation 3.1). The values of the wettability constant, C^*, used in these calculations were $C^*=4.44$ for non-initial water systems with either Dow Corning 200 oil or Texaco White oil 22 and $C^*=306.25$ for systems with initial water. The value of C^* for non-initial water systems was determined by Broman(31) using spectral analysis techniques and the C^* for initial water bearing systems was determined earlier by Peters(13). The stability number was calculated with velocities in cm/sec, viscosities in poise, lengths in cm, interfacial tensions in dynes/cm and permeabilities in cm^2.

CHAPTER 5

EXPRIMENTAL RESULTS AND DISCUSSION

5.1 GENERAL

The experimental results are summarized in this chapter. Eleven displacement experiments and one steady state experiment were conducted. The core properties, breakthrough recoveries and ultimate recoveries for each displacement run are presented. The oil and water relative permeabilities calculated from the displacement data are plotted together with the steady state data to demonstrate the effect of unstable displacements on relative permeability measurements.

5.2 CORE PROPERTIES, BREAKTHROUGH AND ULTIMATE RECOVERIES

The core properties for each run are summarized in Table 5.1. The average permeability and porosity of the cores were around 3.5 darcies and 30%, respectively. The stability numbers, breakthrough and ultimate recoveries and displacement conditions for dynamic displacement experiments are presented in Table 5.2. Run No. 1

TABLE 5.1

CORE PROPERTIES

RUN NO.	OIL	L (cm)	ϕ (%)	S_{wi} (%)	K (darcy)	K_{or}	$Lv\mu_w$ $\frac{cm^2 - cp}{min}$
1*	Dow C.	54.7	30.19		3.47		
2	Dow C.	54.8	30.13	11.59	3.40	3.14	
3	Dow C.	54.6	30.34	12.21	3.37	3.09	
4	Dow C.	54.7	30.58	11.90	3.42	3.16	5.04
5	Dow C.	54.9	30.27	10.63	3.38	3.11	10.08
6	Texaco	54.7	29.99	0	3.48		
7	Texaco	54.9	30.08	0	3.43		8.09
8	Dow C.	54.5	30.10	0	3.57		4.02
9	Dow C.	54.5	30.20	0	3.59		6.03
10	Dow C.	54.6	30.14	0	3.54		8.05
11	Dow C.	54.8	30.23	0	3.63		10.10
12	Dow C.	25.9	30.40	0	3.56		7.64

* Steady State Run

TABLE 5.2

DISPLACEMENT SUMMARY

RUN NO.	CORE POSITION	INJECTION RATE (cc/hr)	v_c (cm/s)	N_s	OIL RECOVERY (% IOIP) BT.	FINAL
2	Vert.	25	1.127E-6	35	41.95	55.7
3	Vert.	30	1.117E-6	42	42.14	56.7
4	Horz.	100	0	138	38.28	54.9
5	Horz.	200	0	280	36.11	55.4
6	Vert.	50	1.077E-5	1815	28.83	43.6
7	Horz.	160	0	5980	22.65	42.9
8	Horz.	80	0	7275	13.76	41.7
9	Horz.	120	0	10850	12.62	43.1
10	Horz.	160	0	14670	10.56	42.3
11	Horz.	200	0	17880	10.50	42.0
12	Horz.	320	0	29170	10.56	43.4

was a steady state experiment and the remaining runs were displacement experiments. Three of the displacements were carried out with the core vertical and water was injected from the bottom. This approach was adopted for the low displacement rate runs to avoid gravity segregation. The remaining runs were made with the core horizontal. Run No. 12 was made using the short core holder. The breakthrough recoveries and the ultimate recoveries are plotted against the dimensionless stability number in Figure 5.1 and Figure 5.2, respectively.

5.3 RELATIVE PERMEABILITIES

The dynamic displacement oil and water relative permeabilities for all eleven displacement experiments are shown in Figures 5.3A through 5.3G. In Figures 5.3A through 5.3D, relative permeabilities are plotted against normalized water saturation while in Figures 5.3E through 5.3G, relative permeabilities are plotted against water saturation(unnormalized). The steady state oil-water relative permeability curves are also plotted in the same figures for comparison. There were four displacements with initial water saturation and seven displacements without initial water saturation. Of the latter seven, two were made using Texaco White oil 22. All the other runs were made with the Dow Corning 200

FIGURE 5.1 BREAKTHROUGH RECOVERY

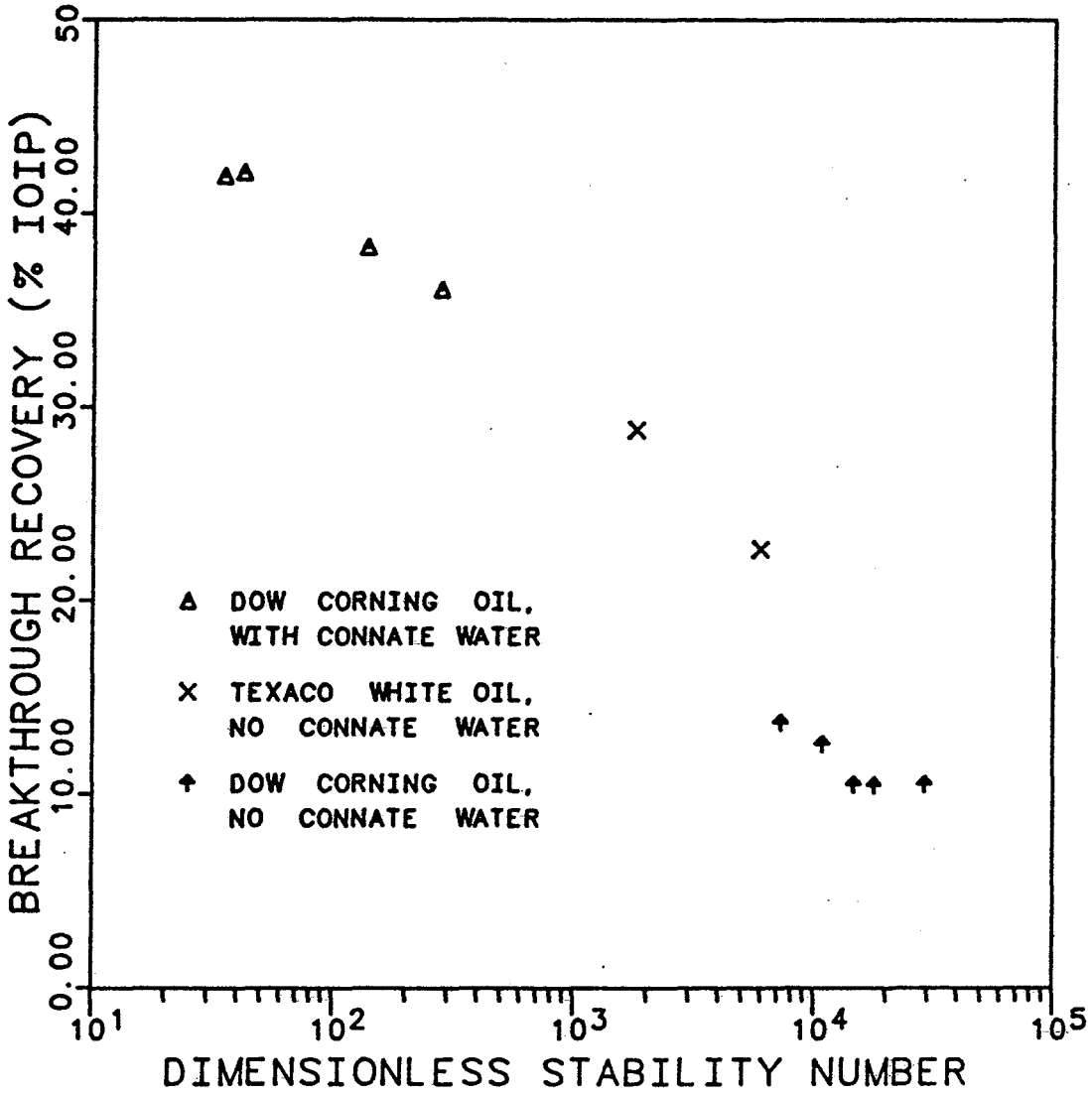

FIGURE 5.2 ULTIMATE RECOVERY

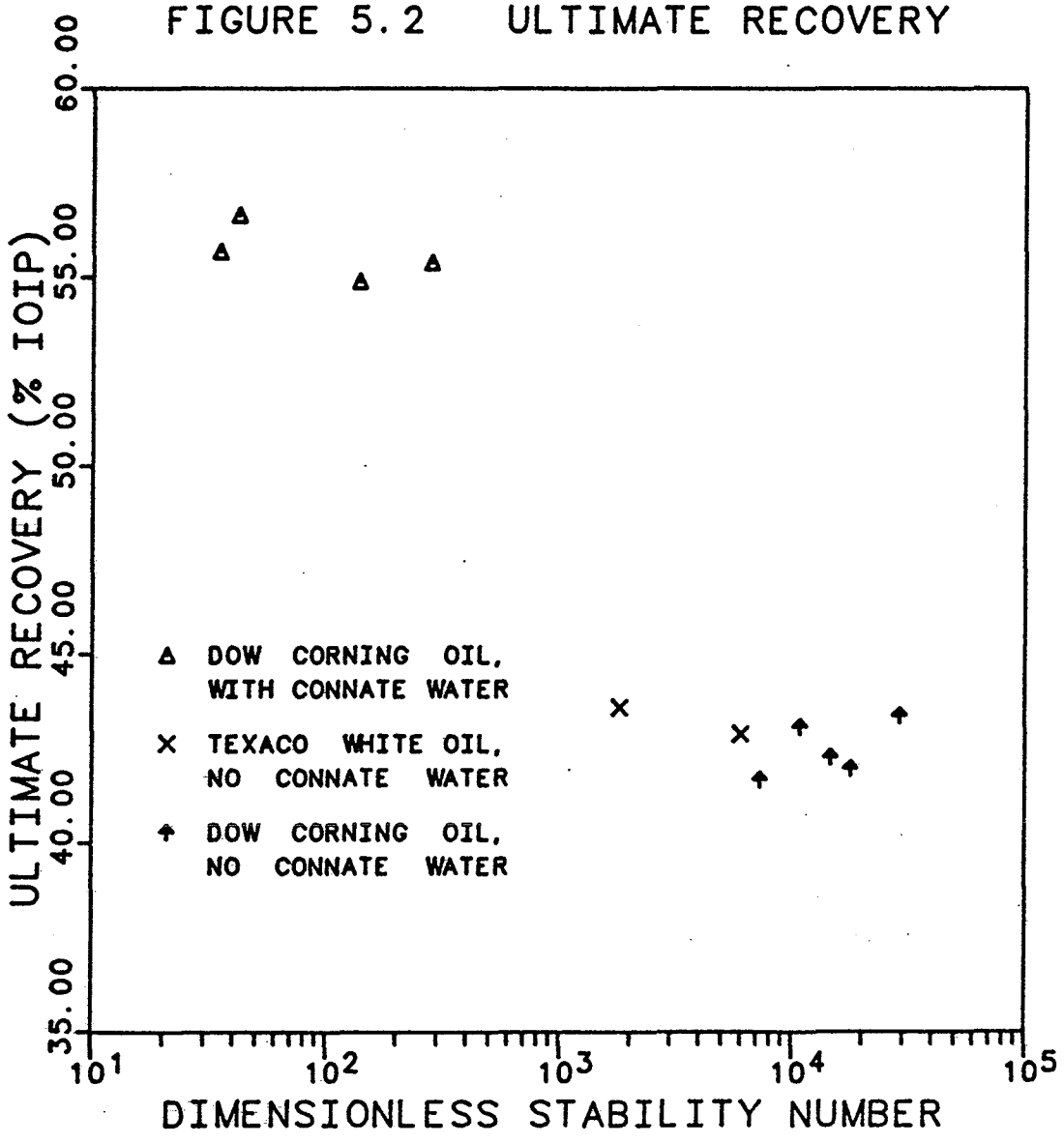

FIGURE 5.3A COMPARISON OF MEASURED OIL AND WATER RELATIVE PERMEABILITY CURVES. N_s = 35 TO 280

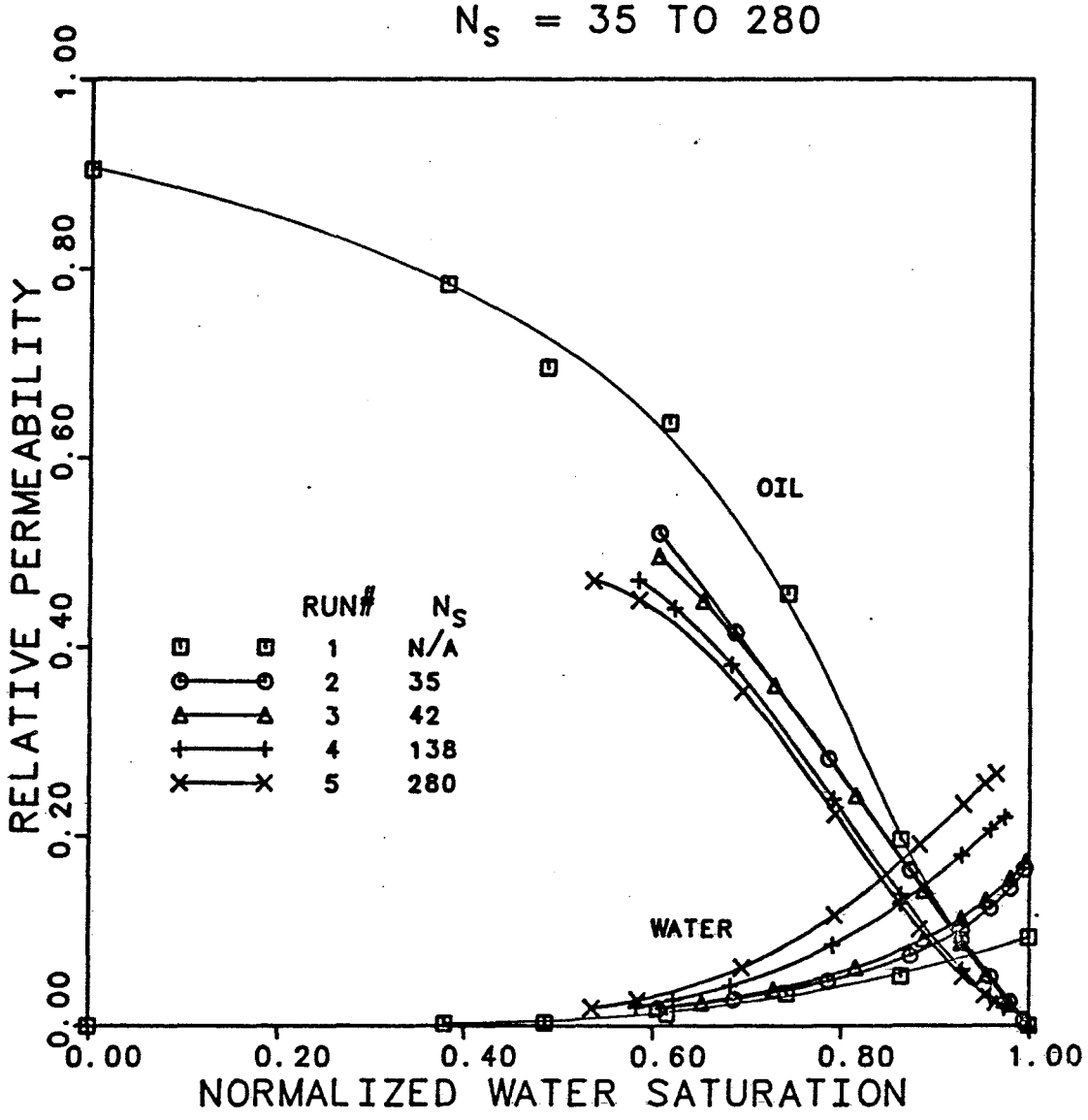

FIGURE 5.3B COMPARISON OF MEASURED OIL AND WATER RELATIVE PERMEABILITY CURVES. N_S = 1815 TO 7275

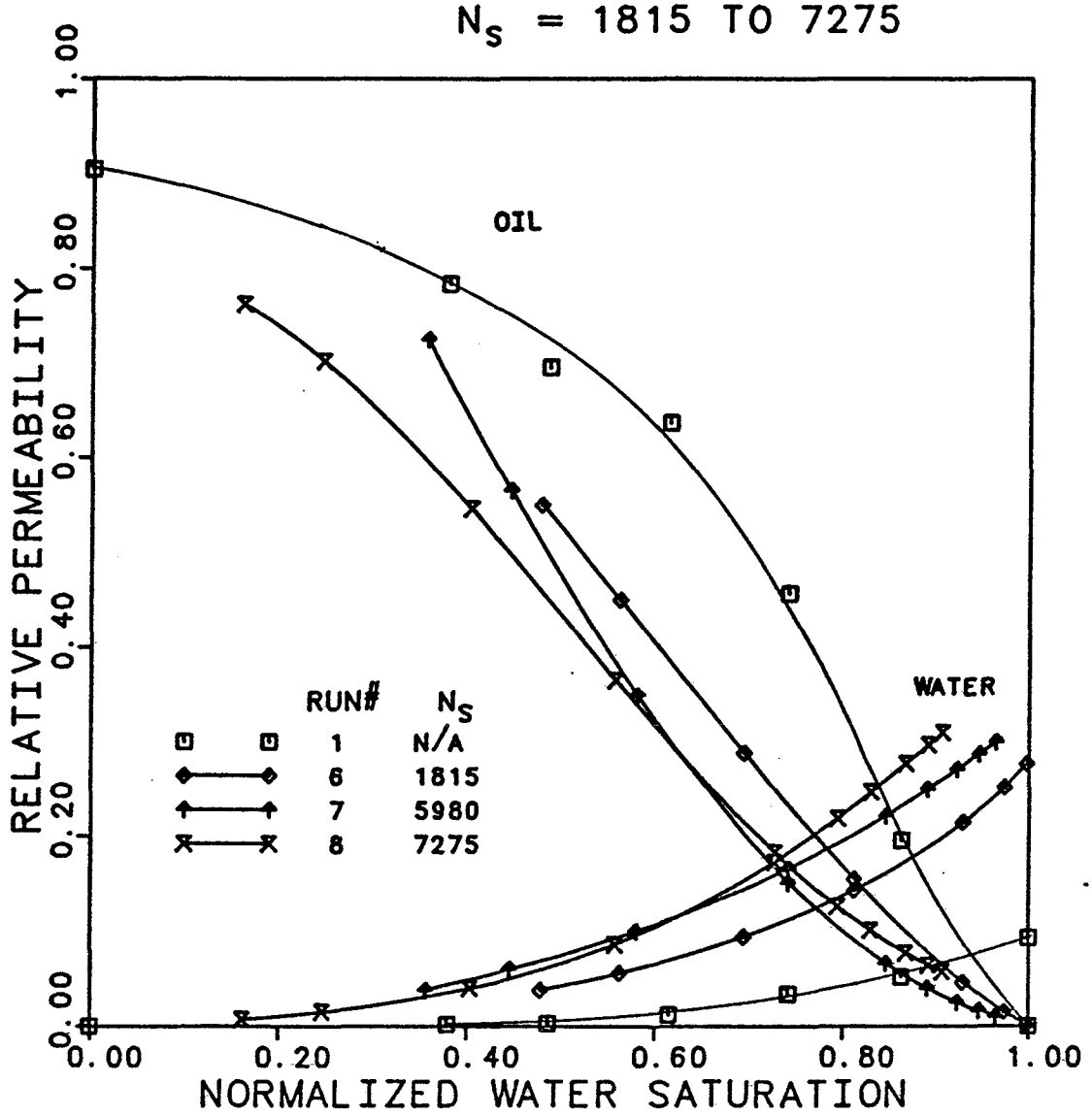

FIGURE 5.3C COMPARISON OF MEASURED OIL AND WATER RELATIVE PERMEABILITY CURVES. N_S = 10850 TO 29170

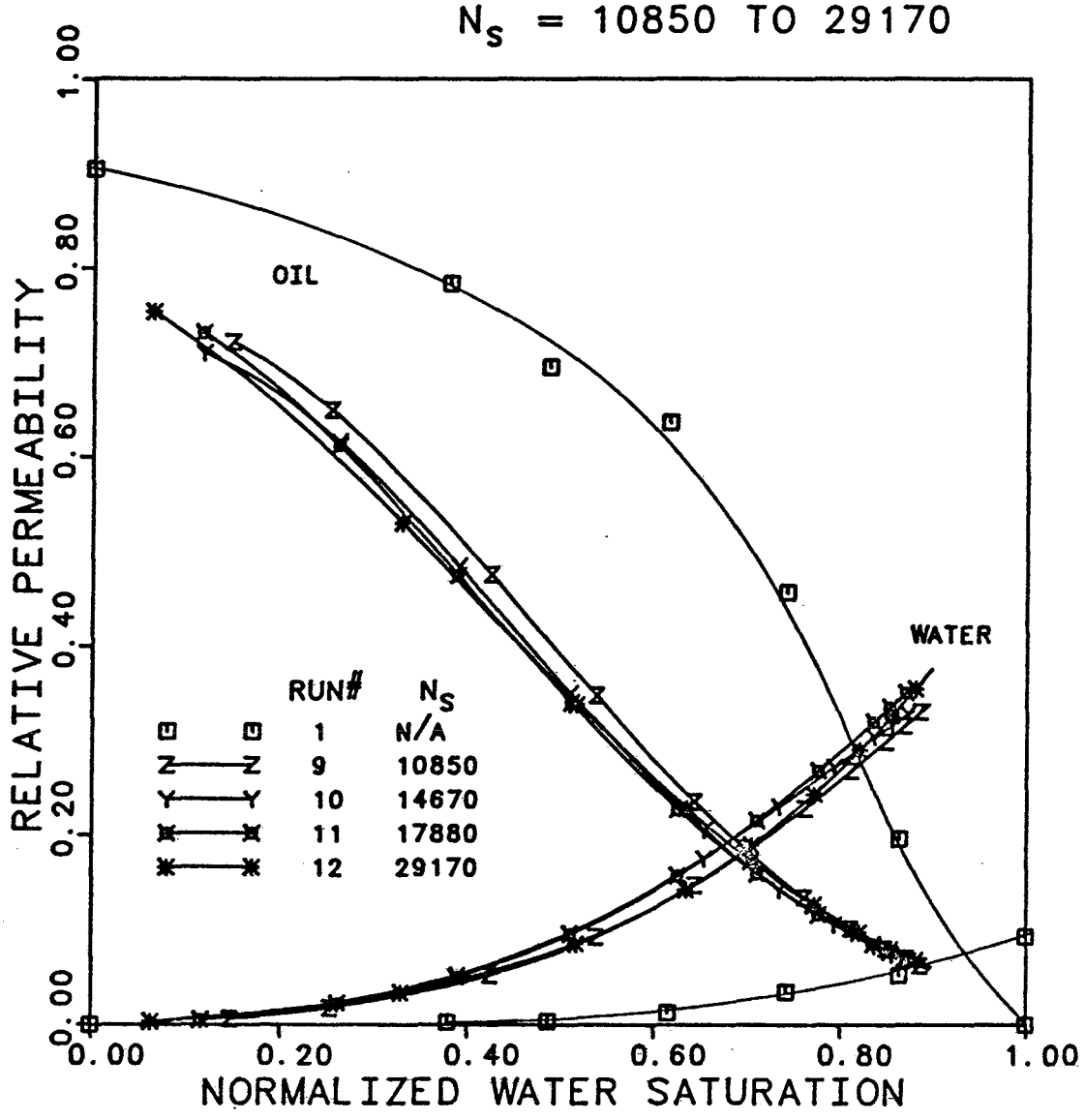

FIGURE 5.3D COMPARISON OF MEASURED OIL AND WATER RELATIVE PERMEABILITY CURVES. N_s = 35 TO 29170

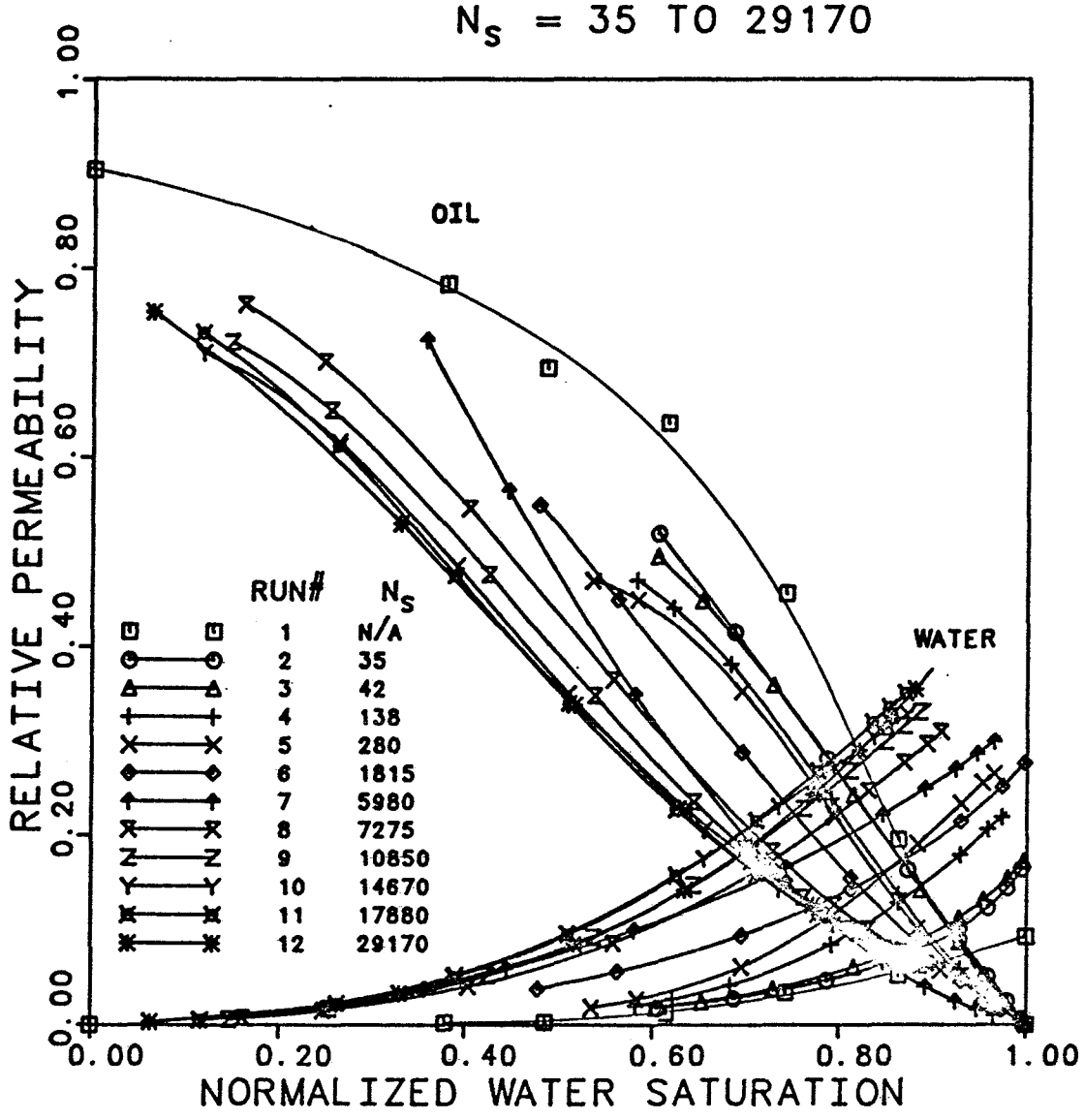

FIGURE 5.3E COMPARISON OF MEASURED OIL AND WATER RELATIVE PERMEABILITY CURVES. N_s = 35 TO 5980

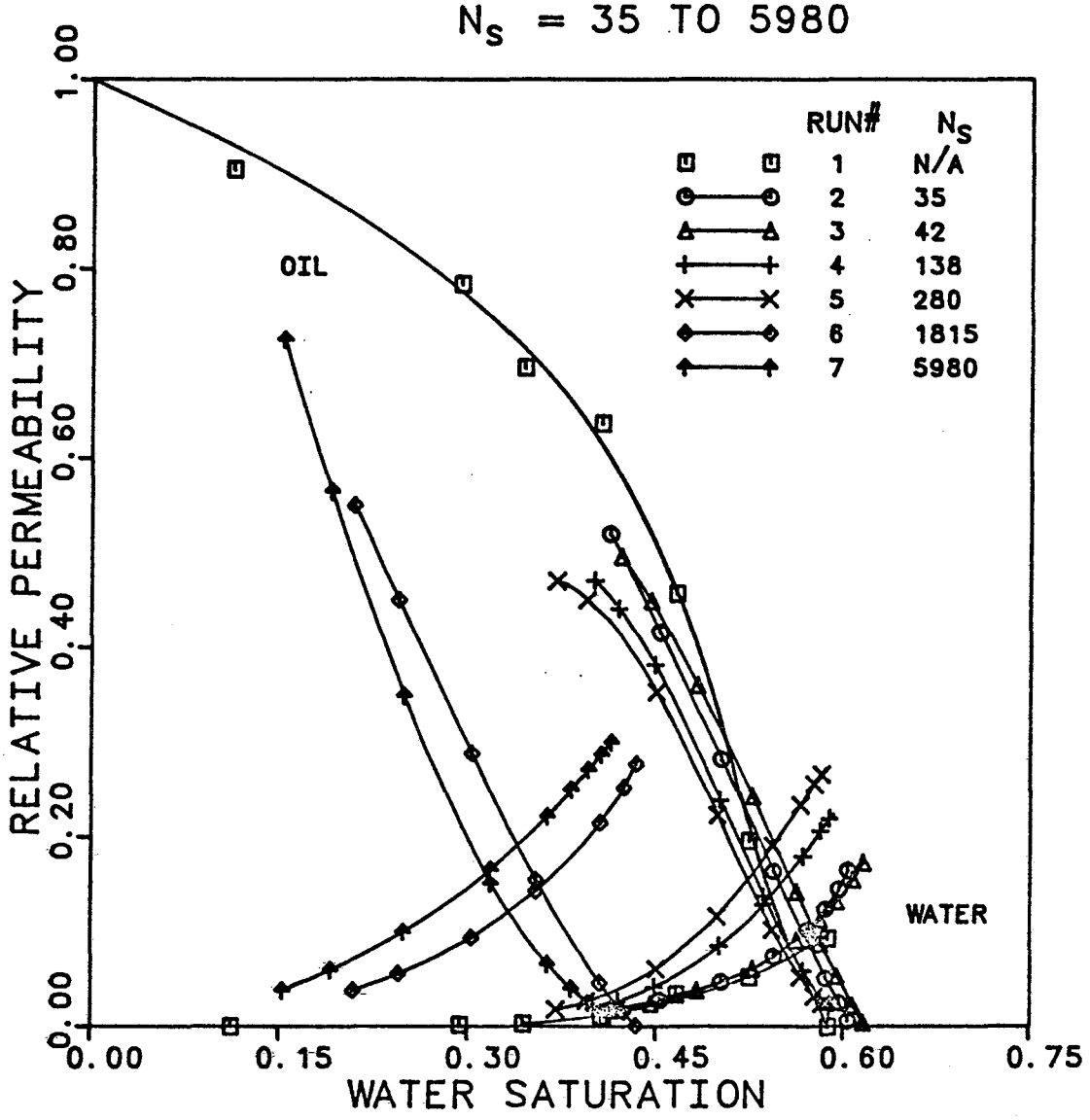

FIGURE 5.3F COMPARISON OF MEASURED OIL AND WATER RELATIVE PERMEABILITY CURVES. N_S = 7275 TO 29170

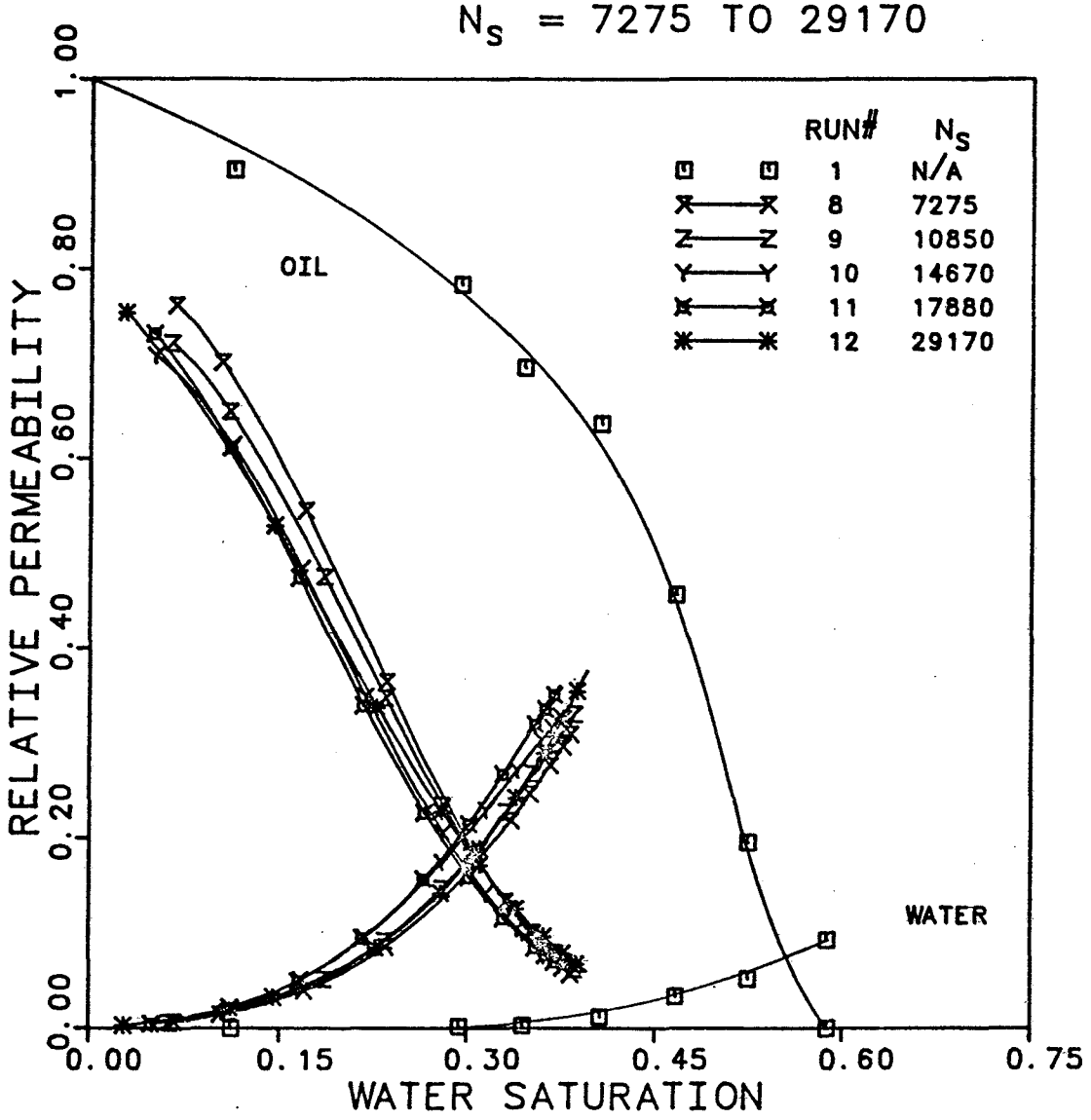

FIGURE 5.3G COMPARISON OF MEASURED OIL AND WATER RELATIVE PERMEABILITY CURVES. N_s = 35 TO 29170

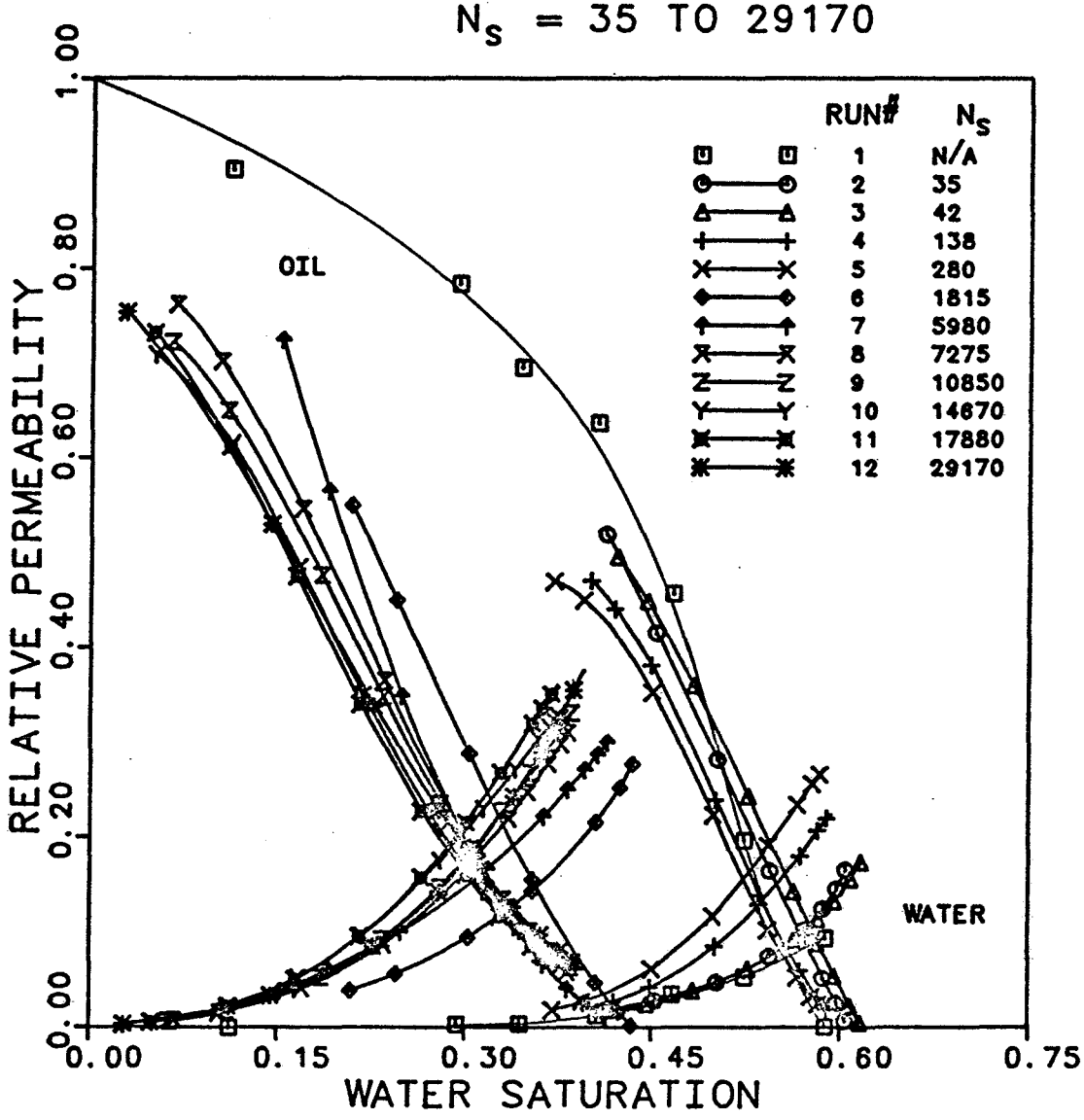

oil. Thus, different stability numbers were achieved by varying the displacement rate, the oil-water viscosity ratio and the sand wettability. It was assumed that the wettability of the sand was determined by the first contacting liquid(13). When the core was initially completely saturated with oil, the sand was assumed to be oil-wet and the corresponding value of the wettability constant was used. Similarly, when the core was initially saturated with water in order to establish a initial water saturation, the sand was assumed to be water-wet and the appropriate value of the wettability constant was used.

All the relative permeabilities presented here are based on the absolute permeability of the core. This is preferred to using the oil permeability at irreducible water saturation as the base(7,8), which was originally proposed by Johnson et al.. Moreover, since some of the runs contained initial water saturation while others did not, it was felt appropriate to express all relative permeabilities with respect to a common base.

5.4 DISCUSSION OF RESULTS

5.4.1 Breakthrough and Ultimate Recoveries

A general decline in the breakthrough recovery with increasing stability number was observed. Displace-

ments made without an initial water saturation and using the more viscous Dow Corning oil exhibited very low breakthrough recoveries. These runs corresponded to very high stability numbers. Relatively high breakthrough recoveries were observed in systems with initial water saturation and with the lower viscosity Texaco oil. These observations are in agreement with those presented earlier by Peters(22) and Broman(31).

The ultimate oil recoveries, in percentage of Initial Oil In Place, were moderately higher for initial water bearing systems than those obtained without initial water saturation. Within the non-initial water system displacements, however, the displacement rate and the oil-water viscosity ratio did not appear to have any significant effect on the ultimate recovery. Similarly, within the initial water bearing systems, the displacement rate did not affect the ultimate oil recovery. For low stability numbers, the breakthrough recovery was high, followed by a relatively small after-production. For high stability numbers, the breakthrough recovery was low, but it was followed by a large after-production. Thus, the rock wettability rather than stability of the displacement appeared to have a significant effect on the final oil recovery. This may be indicative of a time dependent decay of the viscous fingers.

5.4.2 Curve Fitting of Experimental Data

As mentioned in Chapter 4, differentiation of the recovery and the injectivity data was performed by fitting smooth functional relationships through the data and then differentiating the function. Equation 4.1 was used to fit the recovery data of all the runs. The equation fitted the experimental data satisfactorily. The coefficients of correlation for the curve fits were 99.9% or higher with coefficients of variation less than 1.4%. These coefficients were calculated using the MINITAB, a statistical package available on the UT computer system. The coefficient of variation is a relative measure of the scatter in the data. It is defined as the ratio of the standard deviation to the arithmetic mean. The injectivity data were curve-fitted using equation 4.2. The fit obtained was even better than that for recovery data. The coefficients of correlation were 100.0% in most of the cases with coefficients of variation less than 0.6%.

Example curve fits of the recovery and the injectivity data are shown in Figures 5.4 and 5.5, respectively, for Run No. 8. The recovery data curve fit had a coefficient of correlation of 99.9% and a coefficient of variation of 0.83%. The corresponding values

FIGURE 5.4 CURVE FITTING OF RECOVERY DATA USING QUADRATIC POLYNOMIAL.

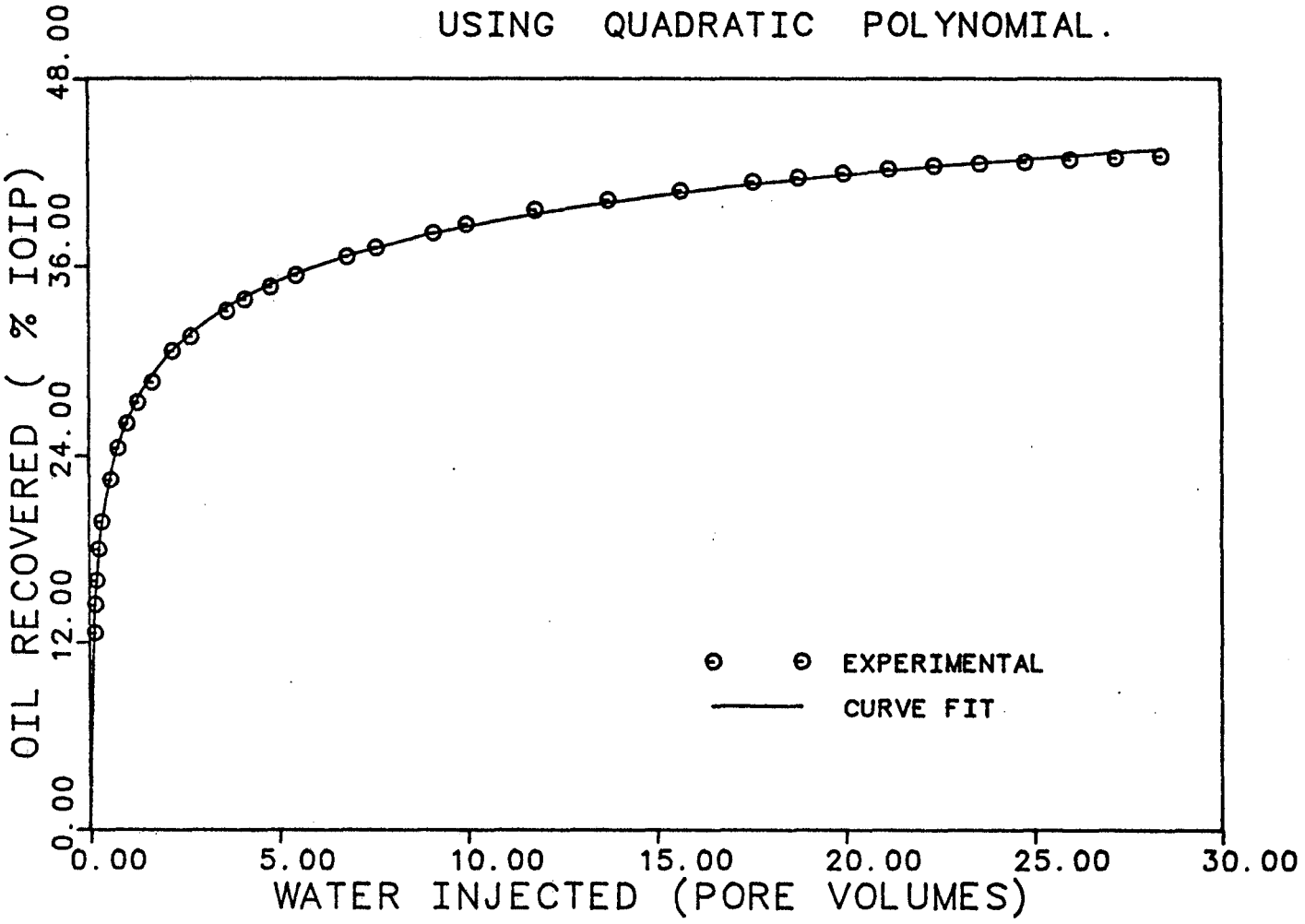

FIGURE 5.5 CURVE FITTING OF INJECTIVITY DATA USING QUADRATIC POLYNOMIAL

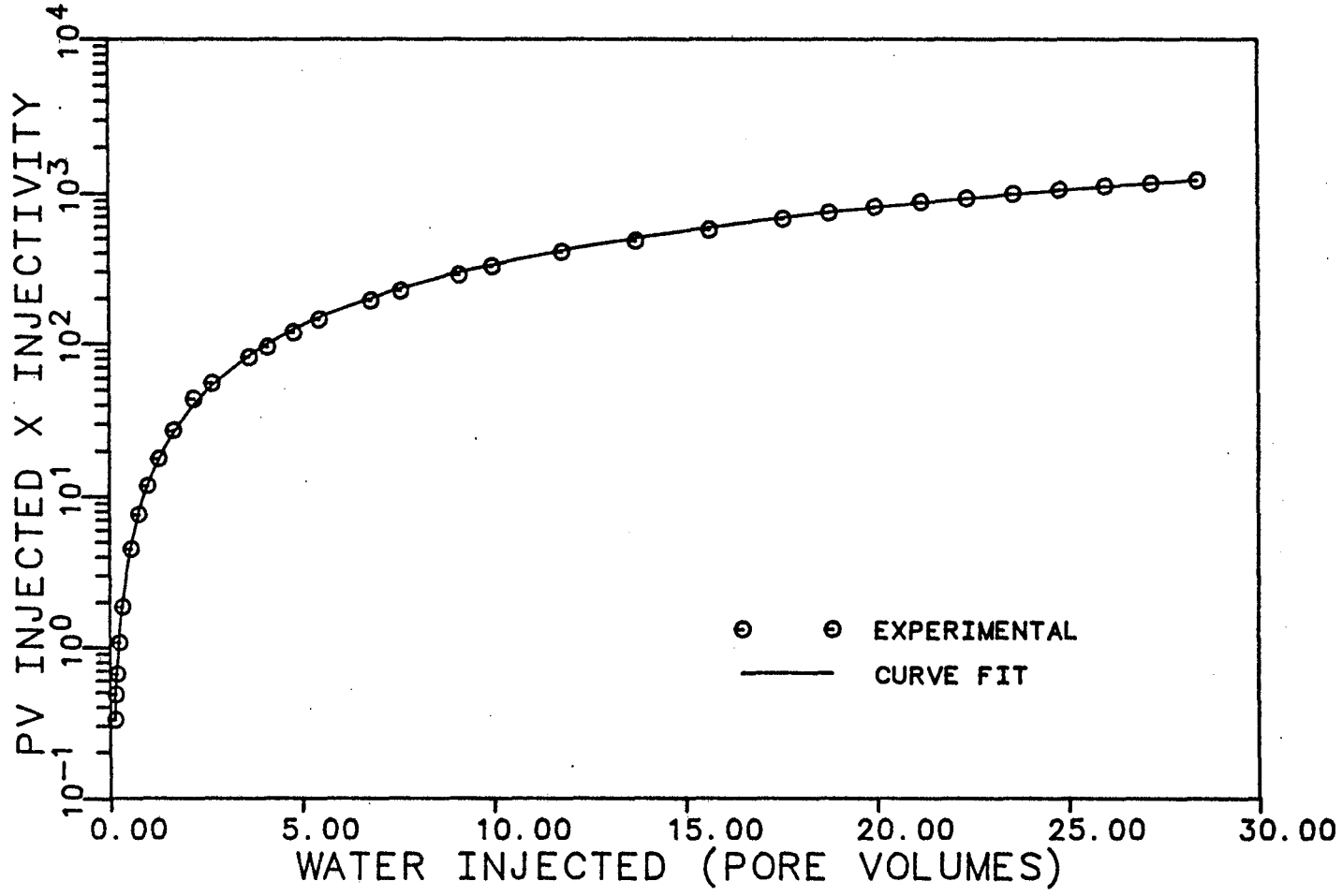

for the injectivity data curve fit were 100.0% and 0.34%, respectively.

An attempt was also made to fit cubic polynomials through the recovery and injectivity data by extending equations 4.1 and 4.2 to include cubic terms on the right hand side. The cubic fits for the previous example case are shown in Figures 5.6 and 5.7. The coefficient of correlation and the coefficient of variation for the recovery curve were 99.9% and 0.84%, respectively, and for the injectivity curve, were 100.0% and 0.30%, respectively. Thus, cubic fits were not better than the quadratic polynomial fits.

5.4.3 Relative Permeability Measurements

The dynamic displacement oil and water relative permeability curves were significantly affected by the stability of the displacement. In general, as the displacement became more unstable, the oil relative permeabilities decreased and the water relative permeabilities increased. For displacements carried out with Dow Corning oil in the presence of initial water, the variation in water relative permeability curves was more pronounced compared to the variation in oil relative permeability curves(Figures 5.3A and 5.3E). These curves corresponded to small values of the stability number.

FIGURE 5.6 CURVE FITTING OF RECOVERY DATA USING CUBIC POLYNOMIAL

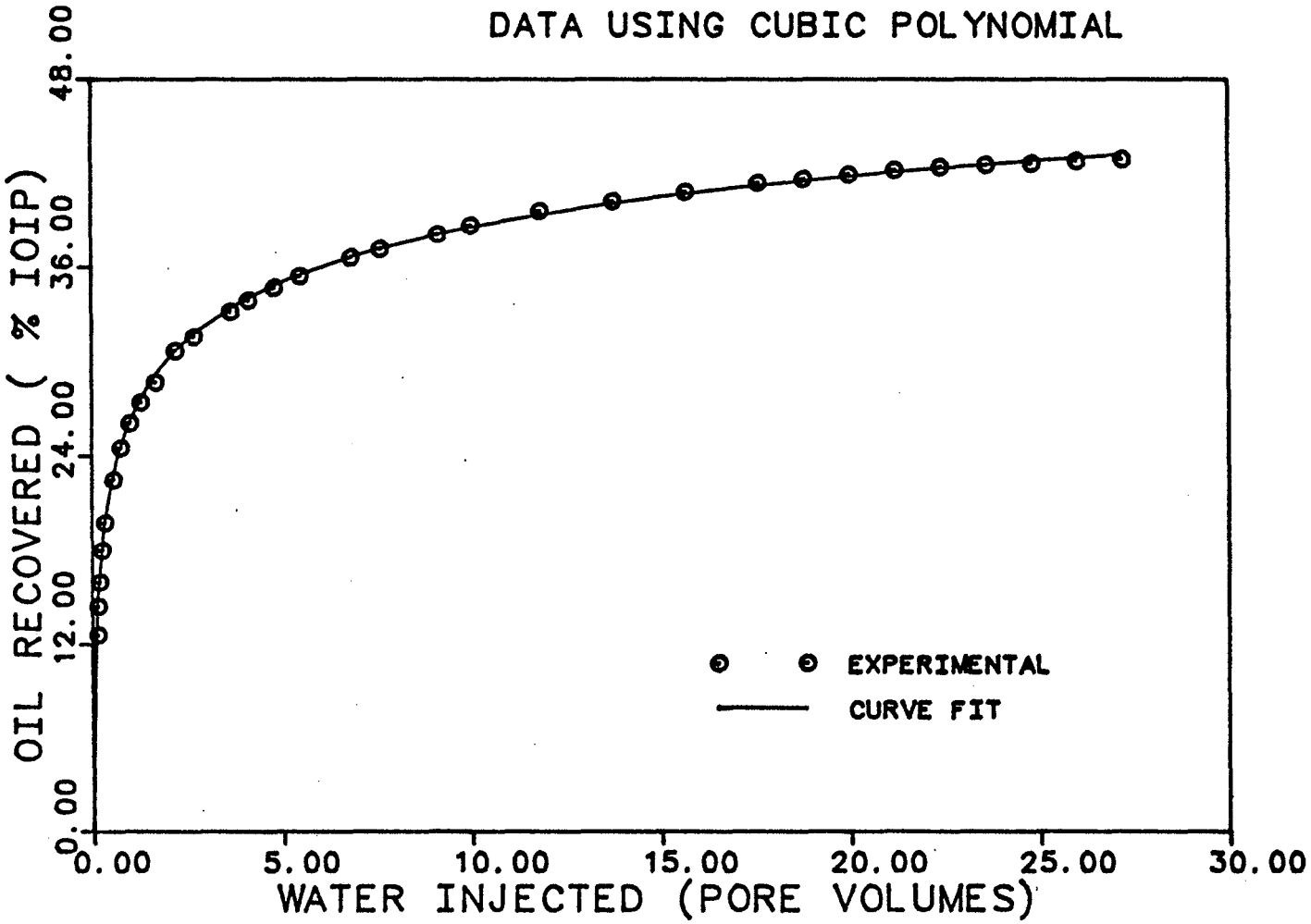

FIGURE 5.7 CURVE FITTING OF INJECTIVITY DATA USING CUBIC POLYNOMIAL

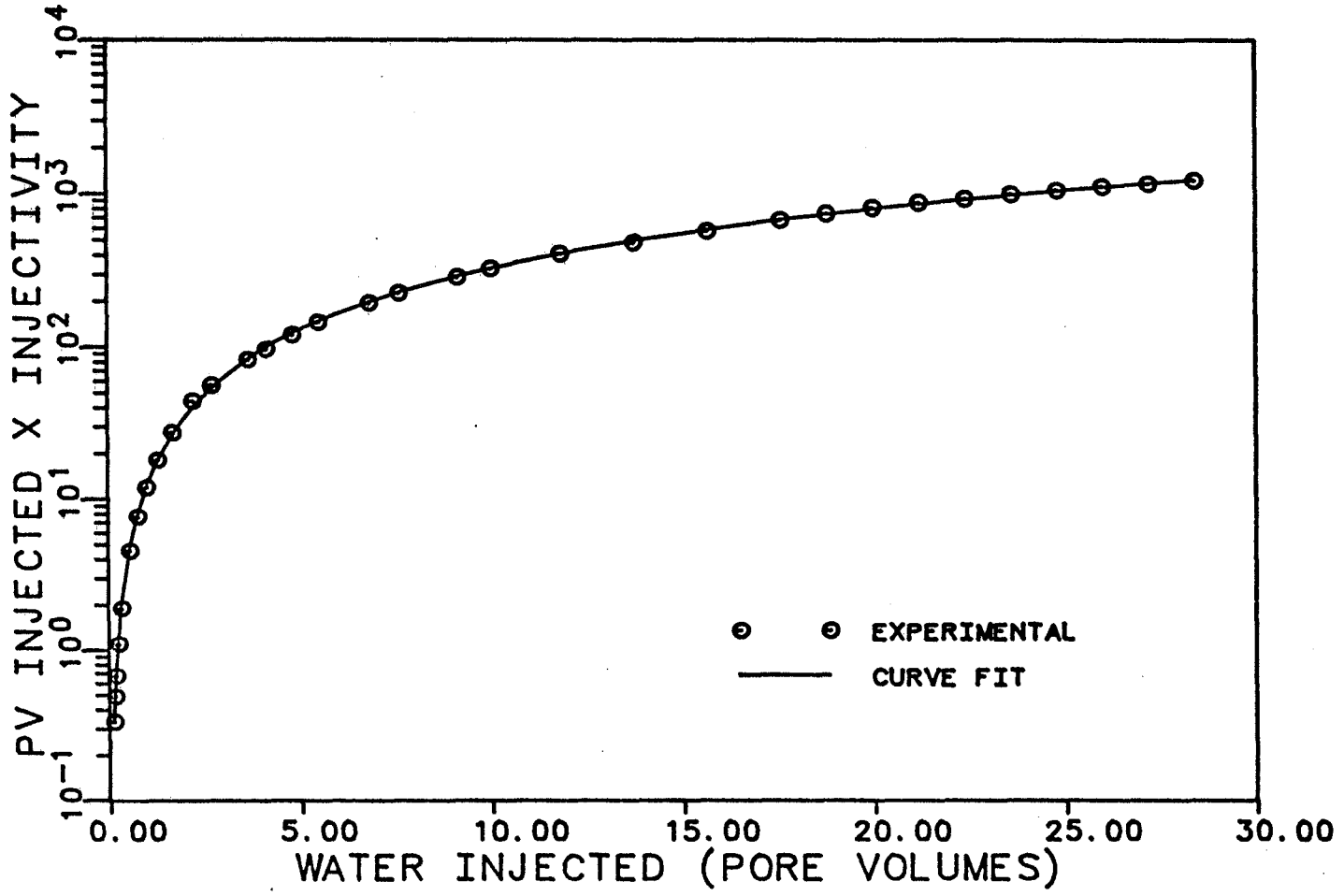

For large values of the stability number, the shift in the oil relative permeability curves was comparable to that of the water relative permeabilities(Figures 5.3C and 5.3F).

When the stability number was increased to about 18000, (displacement rate 200 cc/hr in a non-initial water system with Dow Corning oil), both the oil and water relative permeability curves tended to assume a limiting position. A similar behavior was observed at the lower end of the range of the stability numbers. For stability numbers of about 40, the relative permeability curves again tended to assume another limiting position. Although no displacement was actually conducted at stability numbers below 13.56, that is, in the stable region, the trend of relative permeability curves was clear. Both the oil and the water relative permeability curves computed from dynamic displacement data shifted towards the respective steady state curves as the stability number decreased. Thus, the relative permeabilities were found to stabilize both at very low stability numbers and at very high stability numbers, but the limiting positions were substantially different in the two cases. For low stability numbers the limiting position was close to the steady state curves while the opposite effect was observed for high stability numbers.

It may be noted that the two extreme positions of the relative permeability curves correspond nearly to the stable and the unstable plateau regions of the breakthrough recovery plot. This observation supports the idea that the shift in measured relative permeabilities is due to instability of the displacements.

The trend of water relative permeability curves obtained in this study agreed well with that presented earlier by Sufi et al.(21). The oil relative permeabilities, however, showed a trend opposite to that reported by Sufi et al.. Their oil relative permeabilities showed a slight increase with increasing displacement rate. The trends of both the oil and water relative permeability curves observed in this study, however, agreed with those reported by Amaefule and Handy(29). They found dynamic displacement oil relative permeabilities to decrease and water relative permeabilities to increase with decreasing interfacial tension.

The two displacements made with the lower viscosity Texaco White oil fitted into the overall trend quite satisfactorily. Again, the oil relative permeabilities were lower and the water relative permeablities were higher for the higher stability number. The water relative permeability curves for these two runs were slightly higher than the comparable curves obtained with

the more viscous Dow Corning oil. A similar effect was reported earlier by Lefebvre du Prey. Lefebvre du Prey(28) observed that water relative permeabilities decreased with increasing oil viscosity.

A visual examination of the core cross sections made at the end of Run No. 12 showed evidence of viscous fingering. Only the cross sections near the inlet end were found to be uniformly swept. As the distance from the inlet increased, the water front broke into fingers. This channeling was maximum near the outlet end. Thus, instability seems to affect the displacement process even after several pore volumes of water have been injected.

An attempt was also made to empirically develop a correction factor for minimizing the effect of instability on oil-water relative perrmeability curves obtained from dynamic displacement experiments. Ideally, the correction should be a function of the stability number and should make the dynamic displacement relative permeability curves coincide with the steady state curves. Equations 5.1 and 5.2 describe the corrections for the oil and the water relative permeabilities, respectively, that gave Figure 5.8.

FIGURE 5.8 CORRECTED OIL AND WATER RELATIVE PERMEABILITIES

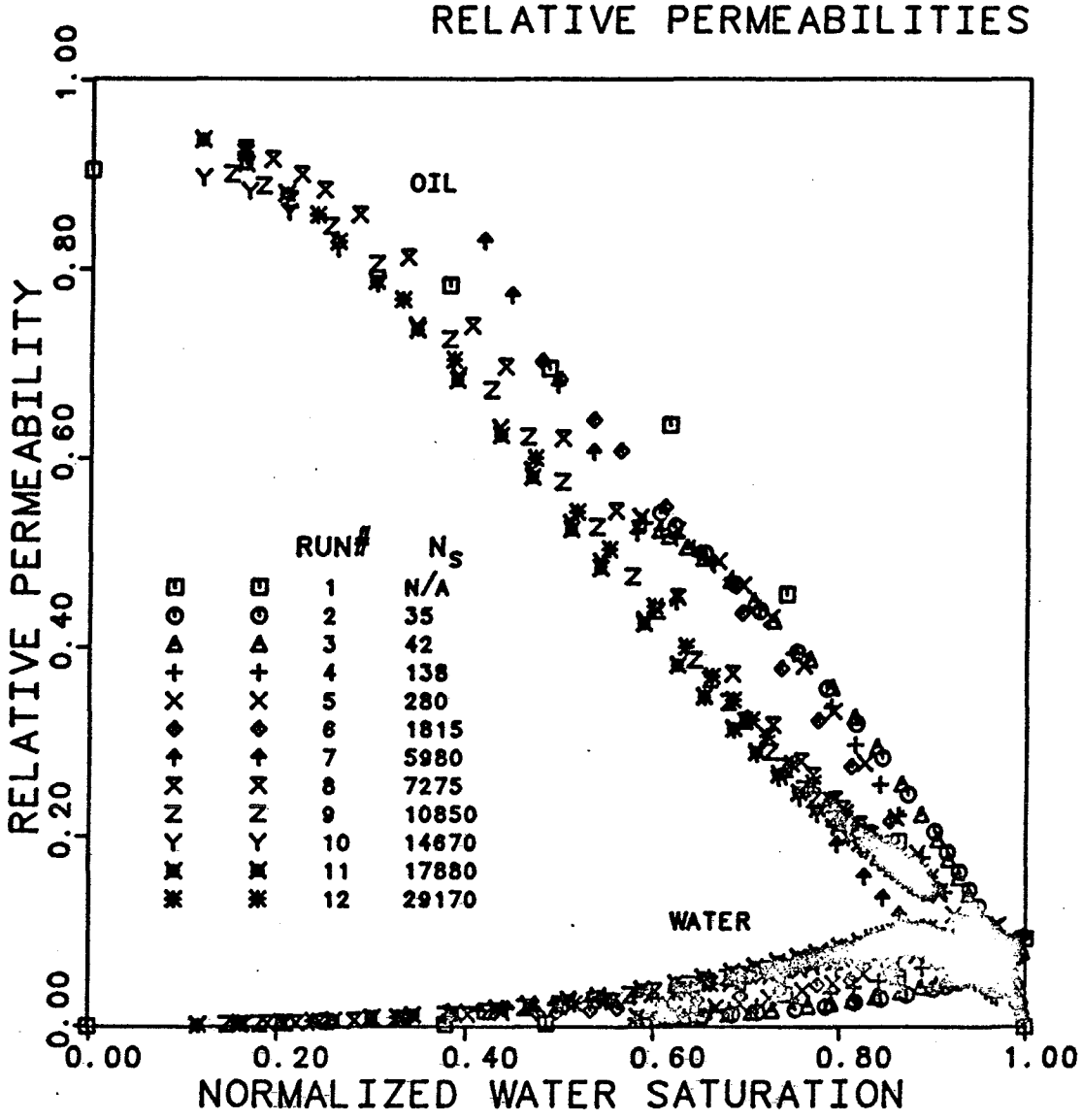

$$(K_{ro})_{corrected} = \frac{K_{ro}(N_s)^{1/13.56}}{C_1(1 - S_{wn})^{1/\pi}} \tag{5.1}$$

$$(K_{rw})_{corrected} = \frac{K_{rw}}{C_1(N_s)^{1/13.56}} \tag{5.2}$$

where

$$C_1 = (13.56\pi)^{13.56/10\pi^2} = 1.6744$$

The correction for water relative permeability curves was fairly satisfactory. While the corrected oil relative permeabilities were better than their uncorrected counterparts, that is, closer to the steady state curve, the improvement was less satisfactory than that achieved with the water relative permeability curves.

CHAPTER 6

CONCLUSIONS AND RECOMMENDATIONS

6.1 CONCLUSIONS

Laboratory displacement experiments were carried out to study the effect of instability on the oil and water relative permeability curves computed by the dynamic displacement technique. The stability numbers for the displacements were varied by varying the displacement rate, the oil-water viscosity ratio and the sand wettability. The following conclusions were drawn from the results of this study :

1) Dynamic displacement oil and water relative permeability measurements are affected by stability of the displacement.
2) In general, oil relative permeabilities decrease and water relative permeabilities increase as the displacement becomes more unstable.
3) The effects of displacement rate, viscosity ratio and wettability on dynamic displacement relative permeability measurements are the manifestations of the single phenomenon of instability.

4) Breakthrough oil recoveries are adversely affected by increasing instability of the displacements. Ultimate recoveries, however, seem to be more affected by sand wettability rather than stability of the displacement.

6.2 RECOMMENDATIONS FOR FURTHER STUDY

The following recommendations are made for future study in this area:

1) The effects of interfacial tension and core diameter and core permeability on dynamic displacement relative permeability measurements should be studied because these parameters also influence the stability of a displacement.
2) Dynamic displacement relative permeability measurements should be conducted under stable displacement conditions to compare the results with those obtained from steady state method and unstable displacements. A stable displacement at sufficiently high displacement rate can be conducted by using a low viscosity oil.
3) The effect of temperature on dynamic displacement relative permeability measurements should be studied in view of the possible effects of temperature on displacement stability.

NOMENCLATURE

C'^{*} = wettability constant, dimensionless

D = core diameter, cm

f_{o2} = oil fractional flow at core outlet, dimensionless

g = acceleration due to gravity, cm/sec^2

K = absolute permeability of the core, darcy

K_{or} = oil permeability at residual water saturation, darcy

K_{ro} = relative permeability to oil, dimensionless

K_{rw} = water relative permeability, dimensionless

L = length of the core, cm

M = oil-water viscosity ratio, dimensionless

N_s = stability number, dimensionless

ΔP = pressure drop across core, psi

q =injection rate, cc/hr

Q_i = cumulative water injected in pore volumes, dimensionless

Q_o = cumulative oil produced in pore volumes, dimensionless

S_{wav}= average water saturation in the core, dimensionless

S_{wi} = initial water saturation in the core, dimensionless

S_{or} = residual oil saturation in the core, dimensionless

S_{wn} = normalized water saturation, dimensionless

S_{w2} = water saturation at core outlet, dimensionless

v = displacement velocity, cm/sec

v_c = critical velocity, cm/sec

α = angle between core axis and the vertical, degrees

μ_w = water viscosity, centipoise

μ_o = oil viscosity, centipoise

ϕ = core porosity, dimensionless

$\Delta\rho$ = density difference, gm/cc

σ = interfacial tension, dynes/cm

APPENDIX A

TABLE A.2

SUMMARY OF DISPLACEMENT DATA FOR RUN NO. 2

Oil Used: Dow Corning 200
Displacement Rate= 25.0 cc/hr
Connate Water Saturation= 11.59 %
Stability Number= 35

Q_i (PORE VOL.)	$\frac{1}{Q_i}$	Q_o (% IOIP) (OBSERVED)	Q_o (% IOIP) (FITTED)	ΔP (PSIA)
.373	2.682	41.95	42.43	2.37
.402	2.486	42.85	43.09	2.08
.472	2.121	44.57	44.41	1.73
.558	1.793	46.07	45.73	1.55
.645	1.550	47.12	46.81	1.42
.813	1.231	48.61	48.38	1.28
.985	1.015	49.81	49.58	1.14
1.203	.831	50.75	50.70	1.01
1.461	.684	51.57	51.68	.90
1.801	.555	52.47	52.61	.79
2.265	.442	53.33	53.48	.68
2.563	.390	53.75	53.88	.61
2.908	.344	54.12	54.25	.55
3.255	.307	54.42	54.54	.52
3.639	.275	54.68	54.78	.50
4.023	.249	54.87	54.97	.47
4.407	.227	55.06	55.12	.44
4.838	.207	55.17	55.24	.43
5.268	.190	55.39	55.34	.42
5.699	.175	55.51	55.40	.42
6.116	.164	55.58	55.45	.41
6.672	.150	55.69	55.48	.40

TABLE A.3

SUMMARY OF DISPLACEMENT DATA FOR RUN NO. 3

Oil Used: Dow Corning 200
Displacement Rate= 30.0 cc/hr
Connate Water Saturation= 12.21 %
Stability Number= 42

Q_i (PORE VOL.)	$\frac{1}{Q_i}$	Q_o (% IOIP) (OBSERVED)	Q_o (% IOIP) (FITTED)	ΔP (PSIA)
.372	2.691	42.14	42.75	2.88
.391	2.557	42.82	43.19	2.50
.433	2.308	44.10	44.04	2.30
.475	2.106	45.00	44.77	2.15
.557	1.794	46.32	46.01	1.86
.640	1.563	47.37	47.02	1.67
.728	1.373	48.19	47.92	1.50
.928	1.078	49.70	49.48	1.31
1.088	.919	50.71	50.42	1.19
1.288	.777	51.43	51.35	1.06
1.529	.654	52.10	52.20	.99
1.894	.528	52.97	53.17	.91
2.274	.440	53.68	53.89	.85
2.644	.378	54.25	54.42	.79
2.967	.337	54.66	54.79	.76
3.333	.300	55.00	55.12	.71
3.739	.267	55.26	55.41	.68
4.106	.244	55.49	55.62	.64
4.472	.224	55.68	55.80	.62
5.132	.195	56.01	56.04	.59
5.752	.174	56.24	56.19	.57
6.373	.157	56.39	56.31	.55
6.993	.143	56.47	56.38	.55
7.733	.129	56.58	56.44	.54
8.472	.118	56.65	56.47	.53

TABLE A.4

SUMMARY OF DISPLACEMENT DATA FOR RUN NO. 4

Oil Used: Dow Corning 200
Displacement Rate= 100.0 cc/hr
Connate Water Saturation= 11.90 %
Stability Number= 138

Q_i (PORE VOL.)	$\frac{1}{Q_i}$	Q_o (% IOIP) (OBSERVED)	Q_o (% IOIP) (FITTED)	ΔP (PSIA)
.339	2.948	38.28	39.00	9.02
.351	2.852	38.95	39.23	8.30
.395	2.531	40.10	40.05	6.91
.439	2.278	40.91	40.76	6.07
.502	1.993	41.92	41.63	5.42
.587	1.705	42.95	42.62	4.87
.670	1.493	43.77	43.42	4.55
.840	1.191	45.11	44.74	4.00
1.137	.880	46.55	46.38	3.32
1.604	.623	47.96	48.08	2.78
2.029	.493	48.96	49.13	2.52
2.624	.381	50.08	50.19	2.30
3.225	.310	50.78	50.97	2.13
4.346	.230	51.78	51.98	1.99
5.719	.175	52.67	52.80	1.90
7.092	.141	53.23	53.35	1.83
8.464	.118	53.67	53.76	1.79
10.516	.095	54.16	54.19	1.75
11.203	.089	54.34	54.31	1.74
12.578	.080	54.60	54.50	1.72
13.271	.075	54.71	54.58	1.70
14.644	.068	54.82	54.72	1.70
16.016	.062	54.90	54.83	1.70

TABLE A.5

SUMMARY OF DISPLACEMENT DATA FOR RUN NO. 5

Oil Used: Dow Corning 200
Displacement Rate= 200.0 cc/hr
Connate Water Saturation= 10.63 %
Stability Number= 280

Q_i (PORE VOL.)	$\frac{1}{Q_i}$	Q_o (% IOIP) (OBSERVED)	Q_o (% IOIP) (FITTED)	ΔP (PSIA)
.324	3.086	36.11	36.87	18.89
.349	2.868	37.10	37.40	16.00
.397	2.519	38.61	38.31	13.35
.446	2.242	39.42	39.11	11.66
.586	1.706	41.22	40.92	9.48
.816	1.225	43.43	42.97	8.43
1.001	.999	44.46	44.16	7.27
1.281	.781	45.57	45.52	5.89
1.741	.574	46.97	47.11	4.96
2.327	.430	48.36	48.49	4.10
3.209	.312	49.65	49.89	3.63
4.592	.218	51.09	51.28	3.42
5.974	.167	52.05	52.20	3.28
8.046	.124	53.00	53.12	3.21
9.888	.101	53.59	53.69	3.17
10.809	.093	53.85	53.92	3.15
12.651	.079	54.29	54.30	3.15
13.572	.074	54.51	54.46	3.13
15.414	.065	54.84	54.73	3.12
16.566	.060	54.99	54.87	3.12
17.717	.056	55.10	55.00	3.11
18.868	.053	55.17	55.11	3.11
20.020	.050	55.25	55.21	3.10
21.178	.047	55.28	55.31	3.10

TABLE A.6

SUMMARY OF DISPLACEMENT DATA FOR RUN NO. 6

Oil Used: Texaco White Oil 22
Displacement Rate= 50.0 cc/hr
Connate Water Saturation= 0 %
Stability Number= 1815

Q_i (PORE VOL.)	$\frac{1}{Q_i}$	Q_o (% IOIP) (OBSERVED)	Q_o (% IOIP) (FITTED)	ΔP (PSIA)
.290	3.449	28.83	29.36	2.22
.312	3.208	29.67	29.97	2.03
.362	2.763	31.34	31.18	1.70
.408	2.451	32.41	32.12	1.52
.504	1.983	33.98	33.68	1.33
.600	1.668	35.15	34.87	1.20
.754	1.327	36.62	36.32	1.08
.941	1.062	37.76	37.60	1.03
1.177	.849	38.70	38.77	.98
1.460	.685	39.57	39.77	.90
1.916	.522	40.67	40.86	.83
2.825	.354	41.87	42.10	.75
3.492	.286	42.41	42.61	.68
4.154	.241	42.84	42.94	.64
4.846	.206	43.04	43.18	.62
5.538	.181	43.34	43.33	.60
6.231	.160	43.51	43.42	.58
7.017	.143	43.65	43.48	.58
7.803	.128	43.71	43.51	.57

TABLE A.7

SUMMARY OF DISPLACEMENT DATA FOR RUN NO. 7

Oil Used: Texaco White Oil 22
Displacement Rate= 160.0 cc/hr
Connate Water Saturation= 0 %
Stability Number= 5980

Q_i (PORE VOL.)	$\frac{1}{Q_i}$	Q_o (% IOIP) (OBSERVED)	Q_o (% IOIP) (FITTED)	ΔP (PSIA)
.228	4.383	22.65	23.29	6.84
.249	4.016	23.68	23.99	6.08
.299	3.348	25.53	25.39	5.42
.344	2.904	26.72	26.45	4.97
.440	2.274	28.51	28.20	4.45
.534	1.872	29.90	29.52	4.01
.686	1.457	31.46	31.14	3.55
.873	1.146	32.78	32.59	3.27
1.386	.721	35.20	35.14	2.80
1.837	.544	36.46	36.51	2.63
2.738	.365	38.05	38.25	2.47
3.421	.292	38.84	39.11	2.32
4.053	.247	39.54	39.72	2.22
4.738	.211	40.07	40.23	2.13
5.424	.184	40.53	40.65	2.06
6.109	.164	40.86	40.98	2.01
6.887	.145	41.16	41.30	1.95
7.666	.130	41.49	41.57	1.93
8.573	.117	41.82	41.83	1.90
9.480	.105	42.09	42.05	1.88
10.387	.096	42.25	42.23	1.87
11.295	.089	42.55	42.38	1.85
12.291	.081	42.68	42.53	1.83
13.288	.075	42.78	42.65	1.83
14.371	.070	42.85	42.76	1.82
15.454	.065	42.91	42.86	1.82

TABLE A.8

SUMMARY OF DISPLACEMENT DATA FOR RUN NO. 8

Oil Used: Dow Corning 200
Displacement Rate= 80.0 cc/hr
Connate Water Saturation= 0 %
Stability Number= 7275

Q_i (PORE VOL.)	$\frac{1}{Q_i}$	Q_o (% IOIP) (OBSERVED)	Q_o (% IOIP) (FITTED)	ΔP (PSIA)
.141	7.109	13.77	14.02	12.51
.165	6.073	15.30	15.15	9.75
.194	5.146	16.53	16.31	7.84
.223	4.478	17.53	17.28	6.78
.275	3.636	19.00	18.70	5.69
.370	2.700	20.63	20.68	4.56
.558	1.793	22.97	23.31	3.40
.695	1.439	24.30	24.68	3.00
1.018	.982	26.70	26.98	2.38
1.477	.677	28.93	29.12	1.94
2.339	.427	31.53	31.65	1.56
3.613	.277	33.83	33.92	1.35
4.967	.201	35.50	35.49	1.24
6.320	.158	36.83	36.64	1.10
7.020	.142	37.33	37.13	1.08
8.420	.119	38.20	37.96	1.03
9.120	.110	38.60	38.32	.99
10.520	.095	39.27	38.95	.94
11.360	.088	39.53	39.28	.89
13.040	.077	40.07	39.87	.87
13.960	.072	40.37	40.16	.84
15.800	.063	40.70	40.67	.82
16.720	.060	40.90	40.90	.78
17.687	.057	41.07	41.13	.76
19.620	.051	41.33	41.54	.75
20.637	.048	41.50	41.74	.75
21.653	.046	41.63	41.92	.74
22.337	.045	41.70	42.04	.74

TABLE A.9

SUMMARY OF DISPLACEMENT DATA FOR RUN NO. 9

Oil Used: Dow Corning 200
Displacement Rate= 120.0 cc/hr
Connate Water Saturation= 0 %
Stability Number= 10850

Q_i (PORE VOL.)	$\frac{1}{Q_i}$	Q_o (% IOIP) (OBSERVED)	Q_o (% IOIP) (FITTED)	ΔP (PSIA)
.129	7.738	12.62	13.17	17.05
.159	6.284	14.45	14.56	14.31
.189	5.290	16.01	15.70	12.41
.249	4.019	18.04	17.49	10.06
.339	2.948	19.77	19.48	7.90
.563	1.776	22.52	22.64	5.46
.764	1.309	24.52	24.49	4.40
.998	1.002	26.08	26.08	3.70
1.287	.777	27.41	27.56	3.15
1.673	.598	28.67	29.06	2.70
2.208	.453	30.66	30.62	2.20
2.689	.372	31.56	31.71	2.12
3.653	.274	33.19	33.37	1.96
4.136	.242	33.92	34.03	1.90
4.811	.208	34.72	34.83	1.78
5.485	.182	35.45	35.51	1.68
6.834	.146	36.64	36.64	1.54
7.601	.132	37.24	37.18	1.48
9.136	.109	38.17	38.10	1.40
10.000	.100	38.74	38.55	1.35
11.827	.085	39.67	39.38	1.28
13.748	.073	40.30	40.10	1.27
15.668	.064	40.90	40.72	1.22
17.588	.057	41.46	41.27	1.15
18.791	.053	41.73	41.58	1.12
19.993	.050	41.99	41.87	1.09
21.196	.047	42.29	42.14	1.07

22.399	.045	42.49	42.40	1.07
23.601	.042	42.62	42.63	1.06
24.804	.040	42.72	42.86	1.05
26.003	.038	42.89	43.08	1.03
27.203	.037	42.99	43.28	1.04
28.402	.035	43.12	43.48	1.03

TABLE A.10

SUMMARY OF DISPLACEMENT DATA FOR RUN NO. 10

Oil Used: Dow Corning 200
Displacement Rate= 160.0 cc/hr
Connate Water Saturation= 0 %
Stability Number= 14670

Q_i (PORE VOL.)	$\frac{1}{Q_i}$	Q_o (% IOIP) (OBSERVED)	Q_o (% IOIP) (FITTED)	ΔP (PSIA)
.108	9.233	10.56	11.18	24.20
.151	6.615	13.12	13.21	19.00
.202	4.959	15.08	14.95	15.28
.292	3.428	17.38	17.16	11.49
.389	2.568	19.44	18.87	9.54
.526	1.900	21.26	20.65	7.71
.723	1.384	22.89	22.50	6.22
.992	1.008	24.35	24.33	4.98
1.271	.787	25.68	25.76	4.24
1.730	.578	27.01	27.51	3.51
2.185	.458	28.17	28.83	3.12
3.096	.323	30.40	30.78	2.70
5.083	.197	33.22	33.53	2.33
6.458	.155	34.65	34.84	2.10
7.824	.128	35.75	35.89	2.00
9.392	.106	36.94	36.87	1.88
11.219	.089	38.04	37.83	1.82
13.027	.077	38.87	38.63	1.75
14.841	.067	39.67	39.33	1.68
16.744	.060	40.30	39.97	1.61
18.757	.053	40.83	40.57	1.56
20.847	.048	41.33	41.13	1.53
21.957	.046	41.59	41.41	1.51
23.063	.043	41.79	41.66	1.50
24.166	.041	41.96	41.91	1.49
25.262	.040	42.09	42.14	1.47
26.432	.038	42.23	42.38	1.46
27.661	.036	42.33	42.61	1.46
28.777	.035	42.43	42.81	1.46

TABLE A.11
SUMMARY OF DISPLACEMENT DATA FOR RUN NO. 11

Oil Used: Dow Corning 200
Displacement Rate= 200.0 cc/hr
Connate Water Saturation= 0 %
Stability Number= 17880

Q_i (PORE VOL.)	$\frac{1}{Q_i}$	Q_o (% IOIP) (OBSERVED)	Q_o (% IOIP) (FITTED)	ΔP (PSIA)
.107	9.323	10.50	11.04	30.10
.147	6.824	12.81	12.93	23.60
.196	5.092	14.79	14.69	19.05
.289	3.459	17.19	16.99	14.17
.383	2.612	19.17	18.64	11.59
.523	1.913	21.06	20.45	9.25
.709	1.411	22.61	22.21	7.75
.986	1.014	24.13	24.09	6.33
1.263	.792	25.45	25.49	5.28
1.716	.583	26.77	27.21	4.35
2.168	.461	27.89	28.51	3.93
3.073	.325	30.03	30.43	3.44
4.066	.246	31.62	31.95	3.06
5.056	.198	32.87	33.13	2.84
6.409	.156	34.22	34.40	2.57
7.762	.129	35.45	35.41	2.32
9.330	.107	36.67	36.38	2.06
11.132	.090	37.52	37.31	1.97
12.934	.077	38.38	38.09	1.87
15.640	.064	39.37	39.08	1.75
18.624	.054	40.23	39.98	1.69
20.710	.048	40.73	40.52	1.66
21.802	.046	40.96	40.78	1.66
22.894	.044	41.16	41.03	1.65
23.987	.042	41.32	41.27	1.63
25.079	.040	41.42	41.50	1.62
26.234	.038	41.62	41.73	1.61
27.396	.037	41.82	41.94	1.60
28.551	.035	41.98	42.15	1.60
29.360	.034	42.05	42.32	1.59

TABLE A.12

SUMMARY OF DISPLACEMENT DATA FOR RUN NO. 12

Oil Used: Dow Corning 200
Displacement Rate= 320.0 cc/hr
Connate Water Saturation= 0 %
Stability Number= 29170

Q_i (PORE VOL.)	$\frac{1}{Q_i}$	Q_o (% IOIP) (OBSERVED)	Q_o (% IOIP) (FITTED)	ΔP (PSIA)
.109	9.172	10.56	10.44	24.60
.185	5.393	14.72	14.40	18.57
.290	3.453	17.64	17.60	14.13
.490	2.040	21.04	21.24	9.36
.687	1.456	23.26	23.49	7.00
1.188	.842	26.67	27.00	4.52
1.593	.628	28.54	28.81	3.85
1.993	.502	29.93	30.17	3.50
2.778	.360	31.81	32.11	3.02
3.563	.281	33.40	33.53	2.71
4.347	.230	34.79	34.64	2.51
5.132	.195	35.76	35.55	2.24
5.917	.169	36.60	36.32	2.01
6.701	.149	37.29	36.98	1.85
8.271	.121	38.40	38.08	1.66
9.840	.102	39.17	38.97	1.57
11.410	.088	39.93	39.71	1.50
12.979	.077	40.56	40.34	1.45
14.549	.069	41.11	40.90	1.40
16.118	.062	41.60	41.39	1.36
17.688	.057	42.01	41.83	1.34
19.257	.052	42.22	42.23	1.32
20.826	.048	42.50	42.60	1.29
22.396	.045	42.71	42.93	1.27
23.965	.042	43.06	43.24	1.25
25.535	.039	43.26	43.53	1.25
27.319	.037	43.40	43.81	1.25

APPENDIX B

TABLE B.2

SUMMARY OF INJECTIVITY DATA FOR RUN NO. 2

Oil Used: Dow Corning 200
Displacement Rate= 25.0 cc/hr
Connate Water Saturation= 11.59 %
Stability Number= 35

Q_i (PORE VOL.)	$\frac{1}{Q_i}$	$\ln(Q_i I_r)$ (OBSERVED)	$\ln(Q_i I_r)$ (FITTED)
.373	2.682	.186	.216
.402	2.486	.276	.274
.472	2.121	.425	.395
.558	1.793	.545	.521
.645	1.550	.646	.630
.813	1.231	.792	.800
.985	1.015	.926	.940
1.203	.831	1.065	1.083
1.461	.684	1.199	1.221
1.801	.555	1.347	1.367
2.265	.442	1.512	1.524
2.563	.390	1.612	1.608
2.908	.344	1.712	1.693
3.255	.307	1.786	1.768
3.639	.275	1.851	1.842
4.023	.249	1.919	1.906
4.407	.227	1.989	1.967
4.838	.207	2.041	2.028
5.268	.190	2.089	2.084
5.699	.175	2.124	2.132
6.116	.164	2.163	2.180
6.672	.150	2.210	2.232

TABLE B.3

SUMMARY OF INJECTIVITY DATA FOR RUN NO. 3

Oil Used: Dow Corning 200
Displacement Rate= 30.0 cc/hr
Connate Water Saturation= 12.21 %
Stability Number= 42

Q_i (PORE VOL.)	$\frac{1}{Q_i}$	$\ln(Q_i I_r)$ (OBSERVED)	$\ln(Q_i I_r)$ (FITTED)
.372	2.691	.181	.221
.391	2.557	.264	.262
.433	2.308	.345	.342
.475	2.106	.414	.413
.557	1.794	.547	.536
.640	1.563	.653	.640
.728	1.373	.756	.736
.928	1.078	.920	.911
1.088	.919	1.031	1.023
1.288	.777	1.154	1.140
1.529	.654	1.259	1.257
1.894	.528	1.388	1.398
2.274	.440	1.498	1.515
2.644	.378	1.594	1.610
2.967	.337	1.662	1.681
3.333	.300	1.742	1.752
3.739	.267	1.810	1.820
4.106	.244	1.879	1.875
4.472	.224	1.927	1.922
5.132	.195	2.009	2.000
5.752	.174	2.074	2.066
6.373	.157	2.135	2.122
6.993	.143	2.174	2.174
7.733	.129	2.226	2.226
8.472	.118	2.274	2.274

TABLE B.4

SUMMARY OF INJECTIVITY DATA FOR RUN NO. 4

Oil Used: Dow Corning 200
Displacement Rate= 100.0 cc/hr
Connate Water Saturation= 11.90 %
Stability Number= 138

Q_i (PORE VOL.)	$\frac{1}{Q_i}$	$\ln(Q_i I_r)$ (OBSERVED)	$\ln(Q_i I_r)$ (FITTED)
.339	2.948	.163	.215
.351	2.852	.213	.242
.395	2.531	.345	.337
.439	2.278	.447	.420
.502	1.993	.554	.524
.587	1.705	.668	.643
.670	1.493	.755	.742
.840	1.191	.909	.906
1.137	.880	1.122	1.118
1.604	.623	1.349	1.346
2.029	.493	1.493	1.495
2.624	.381	1.644	1.651
3.225	.310	1.767	1.771
4.346	.230	1.927	1.935
5.719	.175	2.066	2.079
7.092	.141	2.174	2.187
8.464	.118	2.261	2.270
10.516	.095	2.365	2.370
11.203	.089	2.396	2.400
12.578	.080	2.452	2.448
13.271	.075	2.478	2.470
14.644	.068	2.522	2.513
16.016	.062	2.561	2.548

TABLE B.5

SUMMARY OF INJECTIVITY DATA FOR RUN NO. 5

Oil Used: Dow Corning 200
Displacement Rate= 200.0 cc/hr
Connate Water Saturation= 10.63 %
Stability Number= 280

Q_i (PORE VOL.)	$\frac{1}{Q_i}$	$\ln(Q_i I_r)$ (OBSERVED)	$\ln(Q_i I_r)$ (FITTED)
.324	3.086	.130	.176
.349	2.868	.234	.238
.397	2.519	.369	.346
.446	2.242	.479	.442
.586	1.706	.687	.659
.816	1.225	.882	.912
1.001	.999	1.035	1.061
1.281	.781	1.233	1.234
1.741	.574	1.441	1.441
2.327	.430	1.650	1.626
3.209	.312	1.842	1.820
4.592	.218	2.025	2.021
5.974	.167	2.155	2.160
8.046	.124	2.294	2.307
9.888	.101	2.390	2.403
10.809	.093	2.433	2.442
12.651	.079	2.498	2.512
13.572	.074	2.533	2.542
15.414	.065	2.590	2.594
16.566	.060	2.620	2.620
17.717	.056	2.650	2.646
18.868	.053	2.681	2.672
20.020	.050	2.707	2.694
21.178	.047	2.729	2.716

TABLE B.6

SUMMARY OF INJECTIVITY DATA FOR RUN NO. 6

Oil Used: Texaco White Oil 22
Displacement Rate= 50.0 cc/hr
Connate Water Saturation= 0 %
Stability Number= 1815

Q_i (PORE VOL.)	$\frac{1}{Q_i}$	$\ln(Q_i I_r)$ (OBSERVED)	$\ln(Q_i I_r)$ (FITTED)
.290	3.449	-.093	-.047
.312	3.208	-.022	.005
.362	2.763	.120	.111
.408	2.451	.220	.194
.504	1.983	.370	.339
.600	1.668	.490	.455
.754	1.327	.635	.605
.941	1.062	.752	.747
1.177	.849	.871	.887
1.460	.685	1.002	1.017
1.916	.522	1.155	1.178
2.825	.354	1.367	1.397
3.492	.286	1.502	1.512
4.154	.241	1.604	1.604
4.846	.206	1.684	1.684
5.538	.181	1.757	1.752
6.231	.160	1.823	1.810
7.017	.143	1.876	1.867
7.803	.128	1.928	1.919

TABLE B.7

SUMMARY OF INJECTIVITY DATA FOR RUN NO. 7

Oil Used: Texaco White Oil 22
Displacement Rate= 160.0 cc/hr
Connate Water Saturation= 0 %
Stability Number= 5980

Q_i (PORE VOL.)	$\frac{1}{Q_i}$	$\ln(Q_i I_r)$ (OBSERVED)	$\ln(Q_i I_r)$ (FITTED)
.228	4.383	-.171	-.137
.249	4.016	-.082	-.078
.299	3.348	.047	.042
.344	2.904	.146	.135
.440	2.274	.300	.293
.534	1.872	.430	.416
.686	1.457	.592	.572
.873	1.146	.732	.718
1.386	.721	1.000	.990
1.837	.544	1.149	1.151
2.738	.365	1.350	1.372
3.421	.292	1.474	1.491
4.053	.247	1.567	1.581
4.738	.211	1.653	1.661
5.424	.184	1.726	1.730
6.109	.164	1.788	1.790
6.887	.145	1.853	1.850
7.666	.130	1.906	1.902
8.573	.117	1.958	1.958
9.480	.105	2.006	2.006
10.387	.096	2.050	2.050
11.295	.089	2.093	2.089
12.291	.081	2.132	2.128
13.288	.075	2.167	2.163
14.371	.070	2.202	2.197
15.454	.065	2.236	2.232

TABLE B.8

SUMMARY OF INJECTIVITY DATA FOR RUN NO. 8

Oil Used: Dow Corning 200
Displacement Rate= 80.0 cc/hr
Connate Water Saturation= 0 %
Stability Number= 7275

Q_i (PORE VOL.)	$\frac{1}{Q_i}$	$\ln(Q_i I_r)$ (OBSERVED)	$\ln(Q_i I_r)$ (FITTED)
.141	7.109	-.479	-.406
.165	6.073	-.303	-.279
.194	5.146	-.136	-.147
.223	4.478	-.013	-.037
.275	3.636	.154	.125
.370	2.700	.379	.352
.558	1.793	.685	.656
.695	1.439	.835	.815
1.018	.982	1.101	1.084
1.477	.677	1.351	1.338
2.339	.427	1.646	1.640
3.613	.277	1.896	1.914
4.967	.201	2.074	2.105
6.320	.158	2.231	2.248
7.020	.142	2.283	2.309
8.420	.119	2.383	2.413
9.120	.110	2.435	2.456
10.520	.095	2.517	2.539
11.360	.088	2.574	2.578
13.040	.077	2.648	2.652
13.960	.072	2.691	2.691
15.800	.063	2.756	2.756
16.720	.060	2.800	2.787
17.687	.057	2.839	2.817
19.620	.051	2.886	2.869
20.637	.048	2.908	2.895
21.653	.046	2.934	2.921
22.337	.045	2.952	2.939

TABLE B.9

SUMMARY OF INJECTIVITY DATA FOR RUN NO. 9

Oil Used: Dow Corning 200
Displacement Rate= 120.0 cc/hr
Connate Water Saturation= 0 %
Stability Number= 10850

Q_i (PORE VOL.)	$\frac{1}{Q_i}$	$\ln(Q_i I_r)$ (OBSERVED)	$\ln(Q_i I_r)$ (FITTED)
.129	7.738	-.476	-.475
.159	6.284	-.309	-.307
.189	5.290	-.173	-.170
.249	4.019	.038	.046
.339	2.948	.277	.283
.563	1.776	.658	.660
.764	1.309	.884	.880
.998	1.002	1.076	1.068
1.287	.777	1.256	1.243
1.673	.598	1.437	1.420
2.208	.453	1.646	1.603
2.689	.372	1.748	1.730
3.654	.274	1.916	1.925
4.136	.242	1.982	1.999
4.811	.208	2.077	2.095
5.485	.182	2.160	2.173
6.834	.146	2.290	2.303
7.601	.132	2.355	2.364
9.136	.109	2.459	2.472
10.000	.100	2.516	2.520
11.827	.085	2.611	2.616
13.748	.073	2.681	2.698
15.668	.064	2.755	2.768
17.588	.057	2.829	2.833
18.791	.053	2.868	2.868
19.993	.050	2.907	2.898
21.196	.047	2.941	2.928

22.399	.045	2.963	2.959
23.601	.042	2.994	2.985
24.804	.040	3.020	3.011
26.003	.038	3.046	3.037
27.203	.037	3.063	3.059
28.402	.035	3.085	3.080

TABLE B.10

SUMMARY OF INJECTIVITY DATA FOR RUN NO. 10

Oil Used: Dow Corning 200
Displacement Rate= 160.0 cc/hr
Connate Water Saturation= 0 %
Stability Number= 14670

Q_i (PORE VOL.)	$\frac{1}{Q_i}$	$\ln(Q_i I_r)$ (OBSERVED)	$\ln(Q_i I_r)$ (FITTED)
.108	9.233	-.574	-.592
.151	6.615	-.324	-.324
.202	4.959	-.104	-.097
.292	3.428	.180	.187
.389	2.568	.386	.403
.526	1.900	.609	.624
.723	1.384	.840	.851
.992	1.008	1.075	1.073
1.271	.787	1.252	1.242
1.730	.578	1.468	1.447
2.185	.458	1.620	1.599
3.096	.323	1.835	1.820
5.083	.197	2.112	2.121
6.458	.155	2.264	2.264
7.824	.128	2.368	2.373
9.392	.106	2.472	2.477
11.219	.089	2.564	2.577
13.027	.077	2.646	2.659
14.841	.067	2.720	2.729
16.744	.060	2.794	2.794
18.757	.053	2.855	2.855
20.847	.048	2.911	2.907
21.957	.046	2.937	2.933
23.063	.043	2.963	2.959
24.166	.041	2.985	2.985
25.262	.040	3.011	3.007
26.432	.038	3.033	3.028
27.661	.036	3.054	3.050
28.741	.035	3.072	3.072

TABLE B.11

SUMMARY OF INJECTIVITY DATA FOR RUN NO. 11

Oil Used: Dow Corning 200
Displacement Rate= 200.0 cc/hr
Connate Water Saturation= 0 %
Stability Number= 17880

Q_i (PORE VOL.)	$\frac{1}{Q_i}$	$\ln(Q_i I_r)$ (OBSERVED)	$\ln(Q_i I_r)$ (FITTED)
.107	9.323	-.585	-.593
.147	6.824	-.344	-.346
.196	5.092	-.124	-.118
.289	3.459	.173	.177
.383	2.612	.382	.386
.523	1.913	.616	.614
.709	1.411	.824	.832
.986	1.014	1.056	1.064
1.263	.792	1.242	1.234
1.716	.583	1.459	1.441
2.168	.461	1.605	1.595
3.073	.325	1.814	1.821
4.066	.246	1.987	1.996
5.056	.198	2.113	2.135
6.409	.156	2.261	2.278
7.762	.129	2.387	2.391
9.330	.107	2.517	2.500
11.132	.090	2.617	2.604
12.934	.077	2.704	2.691
15.640	.064	2.813	2.795
18.624	.054	2.904	2.895
20.710	.048	2.960	2.952
21.802	.046	2.982	2.982
22.894	.044	3.004	3.008
23.987	.042	3.030	3.034
25.079	.040	3.051	3.056
26.234	.038	3.078	3.082
27.396	.037	3.095	3.104
28.551	.035	3.117	3.125
29.360	.034	3.130	3.143

TABLE B.12

SUMMARY OF INJECTIVITY DATA FOR RUN NO. 12

Oil Used: Dow Corning 200
Displacement Rate= 320.0 cc/hr
Connate Water Saturation= 0 %
Stability Number= 29170

Q_i (PORE VOL.)	$\frac{1}{Q_i}$	$\ln(Q_i I_r)$ (OBSERVED)	$\ln(Q_i I_r)$ (FITTED)
.109	9.172	-.602	-.658
.185	5.393	-.249	-.235
.290	3.453	.063	.111
.490	2.040	.470	.507
.687	1.456	.743	.754
1.188	.842	1.171	1.145
1.593	.628	1.368	1.349
1.993	.502	1.507	1.501
2.778	.360	1.715	1.724
3.563	.281	1.870	1.887
4.347	.230	1.990	2.016
5.132	.195	2.111	2.122
5.917	.169	2.219	2.211
6.701	.149	2.311	2.289
8.271	.121	2.450	2.419
9.840	.102	2.549	2.523
11.410	.088	2.632	2.615
12.979	.077	2.701	2.688
14.549	.069	2.767	2.758
16.118	.062	2.823	2.819
17.688	.057	2.871	2.871
19.257	.052	2.914	2.919
20.826	.048	2.958	2.966
22.396	.045	2.997	3.005
23.965	.042	3.036	3.044
25.535	.039	3.062	3.079
27.319	.037	3.092	3.110

APPENDIX C

TABLE C.1

STEADY STATE RELATIVE PERMEABILITIES: RUN NO. 1

S_{wn}	K_{ro}	K_{rw}
0	.905	0
.380	.784	.002
.487	.696	.003
.616	.637	.012
.743	.457	.034
.864	.196	.052
1.000	0	.093

TABLE C.2

DYNAMIC DISPLACEMENT RELATIVE PERMEABILITIES: RUN NO. 2

Oil Used: Dow Corning 200
Displacement Rate= 25.0 cc/hr
Connate Water Saturation= 11.59 %
Stability Number= 35

S_{wn}	K_{ro}	K_{rw}
.606	.520	.018
.622	.500	.020
.655	.459	.024
.687	.416	.028
.714	.380	.033
.755	.326	.040
.787	.282	.047
.818	.240	.055
.846	.202	.064
.874	.164	.074
.902	.127	.087
.916	.108	.094
.929	.091	.102
.940	.076	.109
.950	.063	.117
.959	.051	.124
.967	.042	.131
.974	.033	.138
.980	.025	.145
.986	.018	.151
.990	.013	.157
.995	.006	.165

TABLE C.3

DYNAMIC DISPLACEMENT RELATIVE PERMEABILITIES: RUN NO. 3

Oil Used: Dow Corning 200
Displacement Rate= 30.0 cc/hr
Connate Water Saturation= 12.21 %
Stability Number= 42

S_{wn}	K_{ro}	K_{rw}
.605	.496	.018
.615	.486	.019
.635	.467	.022
.653	.449	.024
.682	.416	.029
.707	.387	.033
.729	.360	.038
.768	.310	.047
.792	.277	.054
.816	.243	.061
.840	.210	.069
.867	.172	.081
.888	.142	.091
.905	.119	.099
.917	.102	.106
.928	.087	.113
.939	.073	.121
.947	.062	.126
.954	.053	.132
.965	.040	.141
.973	.030	.148
.980	.022	.155
.986	.015	.161
.992	.009	.167
.997	.004	.173

TABLE C.4

DYNAMIC DISPLACEMENT RELATIVE PERMEABILITIES: RUN NO. 4

Oil Used: Dow Corning 200
Displacement Rate= 100.0 cc/hr
Connate Water Saturation= 11.90 %
Stability Number= 138

S_{wn}	K_{ro}	K_{rw}
.583	.471	.020
.589	.467	.021
.607	.454	.024
.623	.441	.027
.642	.424	.031
.664	.402	.037
.683	.382	.042
.713	.346	.051
.751	.295	.066
.792	.239	.085
.817	.202	.099
.844	.165	.115
.864	.138	.129
.890	.103	.149
.913	.076	.167
.929	.059	.180
.941	.046	.191
.955	.034	.203
.959	.030	.207
.965	.025	.213
.968	.023	.215
.974	.019	.220
.978	.016	.224

TABLE C.5

DYNAMIC DISPLACEMENT RELATIVE PERMEABILITIES: RUN NO. 5

Oil Used: Dow Corning 200
Displacement Rate= 200.0 cc/hr
Connate Water Saturation= 10.63 %
Stability Number= 280

S_{wn}	K_{ro}	K_{rw}
.536	.470	.018
.548	.467	.020
.567	.459	.023
.584	.450	.027
.624	.424	.036
.669	.382	.051
.695	.353	.061
.726	.316	.076
.762	.267	.096
.794	.223	.116
.827	.176	.141
.861	.130	.170
.884	.102	.191
.908	.074	.213
.923	.058	.228
.930	.052	.234
.940	.043	.244
.945	.039	.249
.953	.032	.256
.957	.029	.260
.961	.026	.263
.965	.024	.266
.968	.022	.269
.971	.020	.272

TABLE C.6

DYNAMIC DISPLACEMENT RELATIVE PERMEABILITIES: RUN NO. 6

Oil Used: Texaco White Oil 22
Displacement Rate= 50.0 cc/hr
Connate Water Saturation= 0 %
Stability Number= 1815

S_{wn}	K_{ro}	K_{rw}
.479	.550	.038
.498	.529	.042
.534	.484	.049
.563	.450	.056
.611	.391	.068
.649	.345	.079
.695	.288	.094
.738	.238	.110
.778	.193	.127
.813	.155	.143
.855	.113	.165
.906	.066	.197
.930	.046	.215
.948	.033	.229
.962	.023	.241
.974	.015	.252
.983	.010	.261
.991	.005	.270
.998	.001	.277

TABLE C.7

DYNAMIC DISPLACEMENT RELATIVE PERMEABILITIES: RUN NO. 7

Oil Used: Texaco White Oil 22
Displacement Rate= 160.0 cc/hr
Connate Water Saturation= 0 %
Stability Number= 5980

S_{wn}	K_{ro}	K_{rw}
.357	.725	.038
.376	.689	.043
.416	.617	.052
.446	.565	.060
.496	.481	.073
.534	.420	.085
.581	.349	.100
.624	.290	.115
.700	.196	.146
.743	.151	.166
.798	.102	.194
.827	.080	.210
.847	.066	.222
.865	.055	.233
.879	.046	.242
.892	.040	.250
.904	.034	.258
.914	.029	.264
.924	.025	.271
.933	.021	.277
.940	.018	.283
.947	.016	.287
.954	.014	.292
.959	.012	.296
.965	.010	.300
.970	.009	.304

TABLE C.8

DYNAMIC DISPLACEMENT RELATIVE PERMEABILITIES: RUN NO. 8

Oil Used: Dow Corning 200
Displacement Rate= 80.0 cc/hr
Connate Water Saturation= 0 %
Stability Number= 7275

S_{wn}	K_{ro}	K_{rw}
.162	.762	.007
.191	.744	.009
.222	.722	.012
.247	.702	.015
.284	.670	.019
.335	.620	.027
.404	.546	.040
.440	.504	.048
.501	.433	.066
.558	.365	.086
.625	.288	.115
.685	.224	.147
.728	.183	.173
.759	.155	.194
.772	.144	.203
.795	.126	.219
.804	.119	.227
.822	.107	.240
.831	.101	.247
.847	.090	.259
.855	.085	.266
.869	.077	.277
.875	.074	.282
.881	.070	.287
.893	.064	.297
.898	.061	.301
.904	.059	.306
.908	.057	.310

TABLE C.9
DYNAMIC DISPLACEMENT RELATIVE PERMEABILITIES: RUN NO. 9

Oil Used: Dow Corning 200
Displacement Rate= 120.0 cc/hr
Connate Water Saturation= 0 %
Stability Number= 10850

S_{wn}	K_{ro}	K_{rw}
.148	.722	.006
.182	.703	.009
.210	.684	.012
.254	.650	.017
.302	.606	.025
.380	.526	.040
.425	.476	.052
.464	.431	.064
.501	.389	.077
.538	.348	.092
.576	.305	.110
.603	.276	.124
.644	.235	.147
.661	.219	.157
.681	.201	.170
.698	.186	.181
.726	.162	.201
.739	.151	.211
.762	.134	.228
.773	.126	.237
.794	.112	.253
.812	.101	.268
.828	.092	.281
.841	.084	.293
.849	.080	.299
.856	.076	.305
.863	.073	.311
.869	.070	.316
.875	.067	.321
.881	.064	.326
.886	.062	.331
.892	.060	.335
.896	.058	.339

TABLE C.10

DYNAMIC DISPLACEMENT RELATIVE PERMEABILITIES: RUN NO. 10

Oil Used: Dow Corning 200
Displacement Rate= 160.0 cc/hr
Connate Water Saturation= 0 %
Stability Number= 14670

S_{wn}	K_{ro}	K_{rw}
.118	.711	.005
.167	.687	.010
.209	.659	.014
.262	.616	.022
.303	.577	.030
.345	.534	.040
.390	.485	.052
.434	.436	.066
.468	.397	.079
.510	.350	.096
.542	.316	.111
.589	.267	.136
.655	.205	.175
.686	.179	.196
.711	.160	.213
.735	.142	.230
.758	.127	.246
.777	.115	.260
.794	.105	.272
.810	.097	.283
.824	.089	.294
.837	.083	.304
.844	.079	.308
.850	.077	.313
.856	.074	.317
.862	.072	.321
.868	.069	.325
.873	.067	.329
.878	.065	.332

TABLE C.11

DYNAMIC DISPLACEMENT RELATIVE PERMEABILITIES: RUN NO. 11

Oil Used: Dow Corning 200
Displacement Rate= 200.0 cc/hr
Connate Water Saturation= 0 %
Stability Number= 17880

S_{wn}	K_{ro}	K_{rw}
.117	.732	.005
.163	.700	.009
.206	.665	.014
.262	.612	.022
.302	.571	.030
.346	.523	.039
.389	.475	.050
.435	.424	.065
.469	.386	.077
.511	.340	.095
.542	.307	.109
.589	.261	.134
.626	.227	.157
.655	.202	.175
.686	.177	.197
.711	.159	.215
.735	.142	.234
.757	.128	.252
.777	.116	.268
.801	.103	.289
.823	.091	.308
.836	.085	.320
.842	.082	.326
.848	.079	.331
.854	.077	.336
.860	.074	.341
.865	.072	.346
.871	.070	.351
.876	.068	.356
.881	.066	.360

TABLE C.12

DYNAMIC DISPLACEMENT RELATIVE PERMEABILITIES: RUN NO. 12

Oil Used: Dow Corning 200
Displacement Rate= 320.0 cc/hr
Connate Water Saturation= 0 %
Stability Number= 29170

S_{wn}	K_{ro}	K_{rw}
.064	.754	.003
.162	.684	.011
.240	.616	.019
.330	.530	.033
.385	.473	.045
.472	.384	.069
.517	.338	.085
.551	.306	.099
.600	.260	.122
.635	.228	.142
.663	.205	.159
.686	.187	.175
.705	.172	.189
.722	.160	.201
.749	.140	.224
.772	.126	.243
.791	.114	.260
.807	.105	.276
.821	.097	.290
.834	.090	.303
.845	.084	.315
.855	.079	.326
.864	.075	.336
.873	.071	.346
.881	.068	.355
.888	.064	.364
.898	.060	.376

APPENDIX D

FIGURE D.2. A RECOVERY PLOT FOR RUN 2

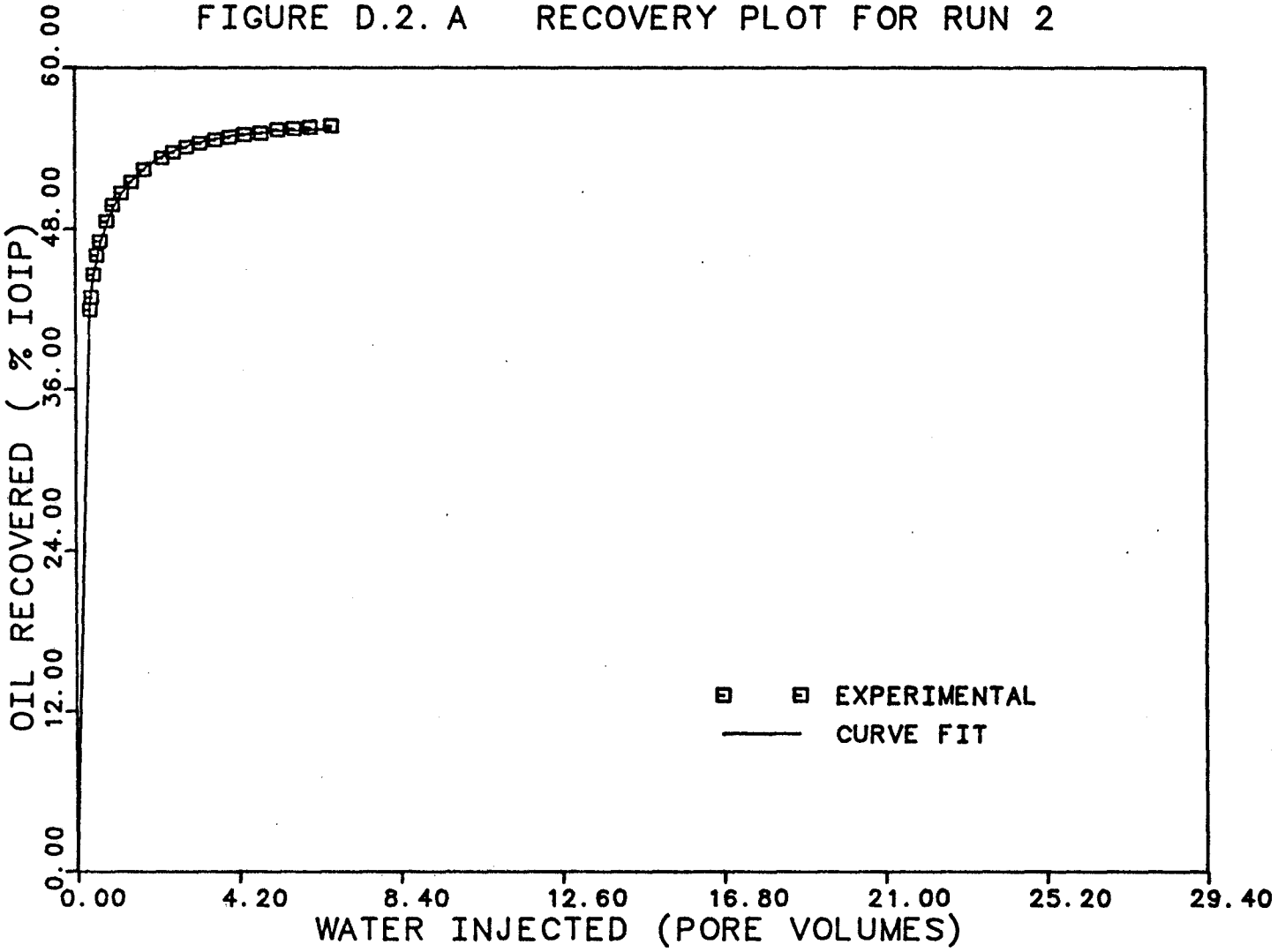

FIGURE D.2. B RECOVERY PLOT FOR RUN 2

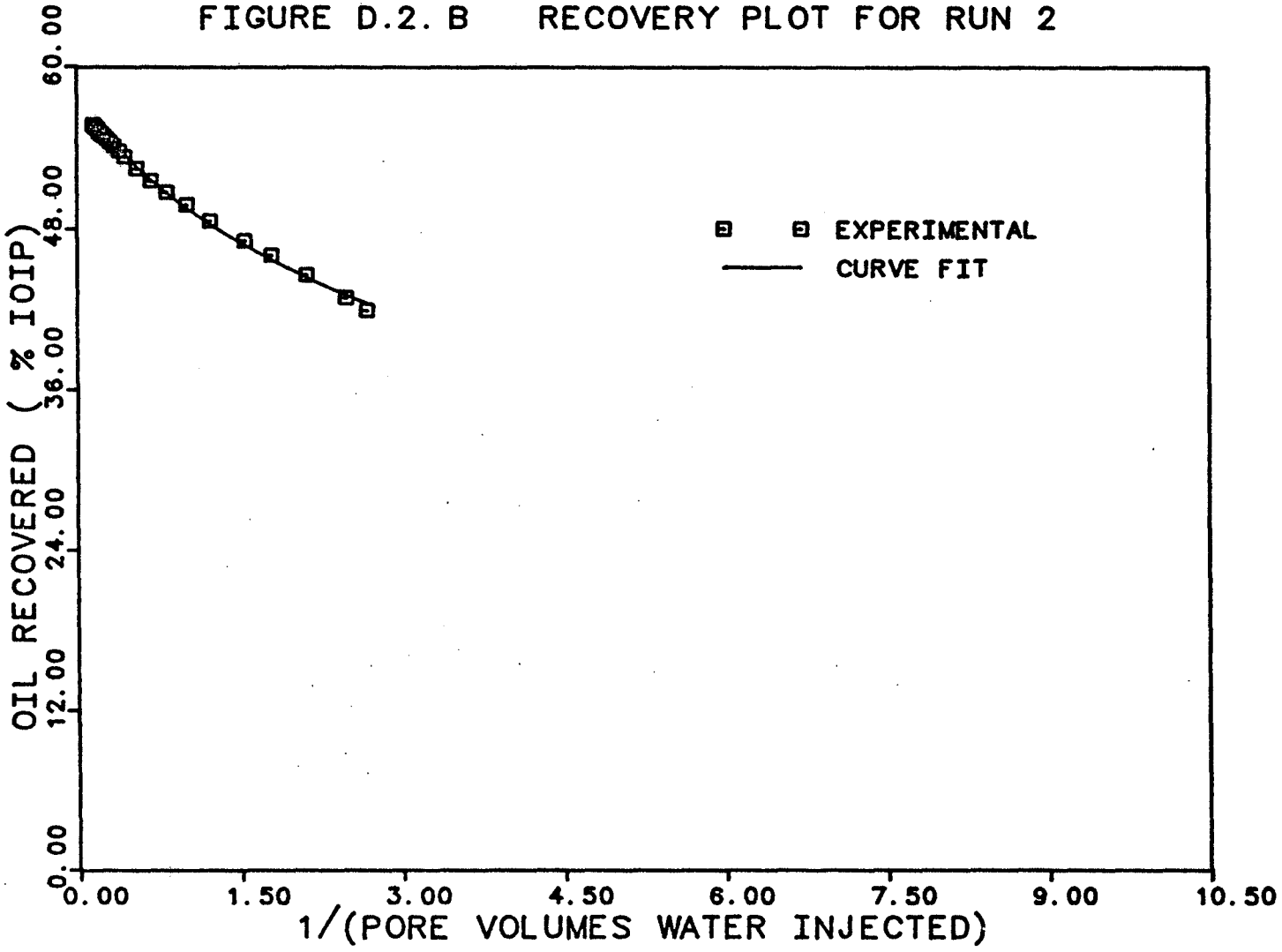

FIGURE D.3. A RECOVERY PLOT FOR RUN 3

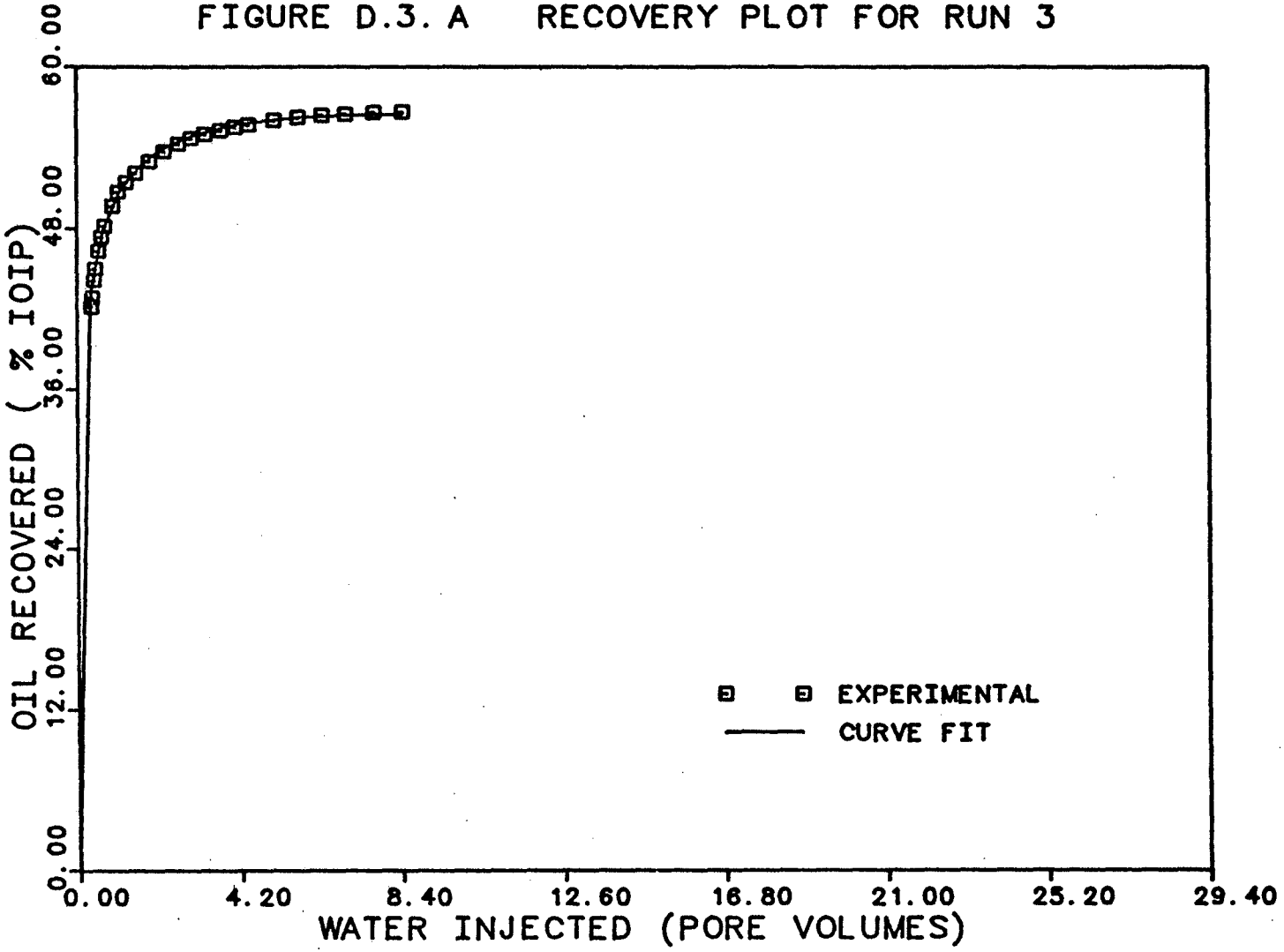

FIGURE D.3. B RECOVERY PLOT FOR RUN 3

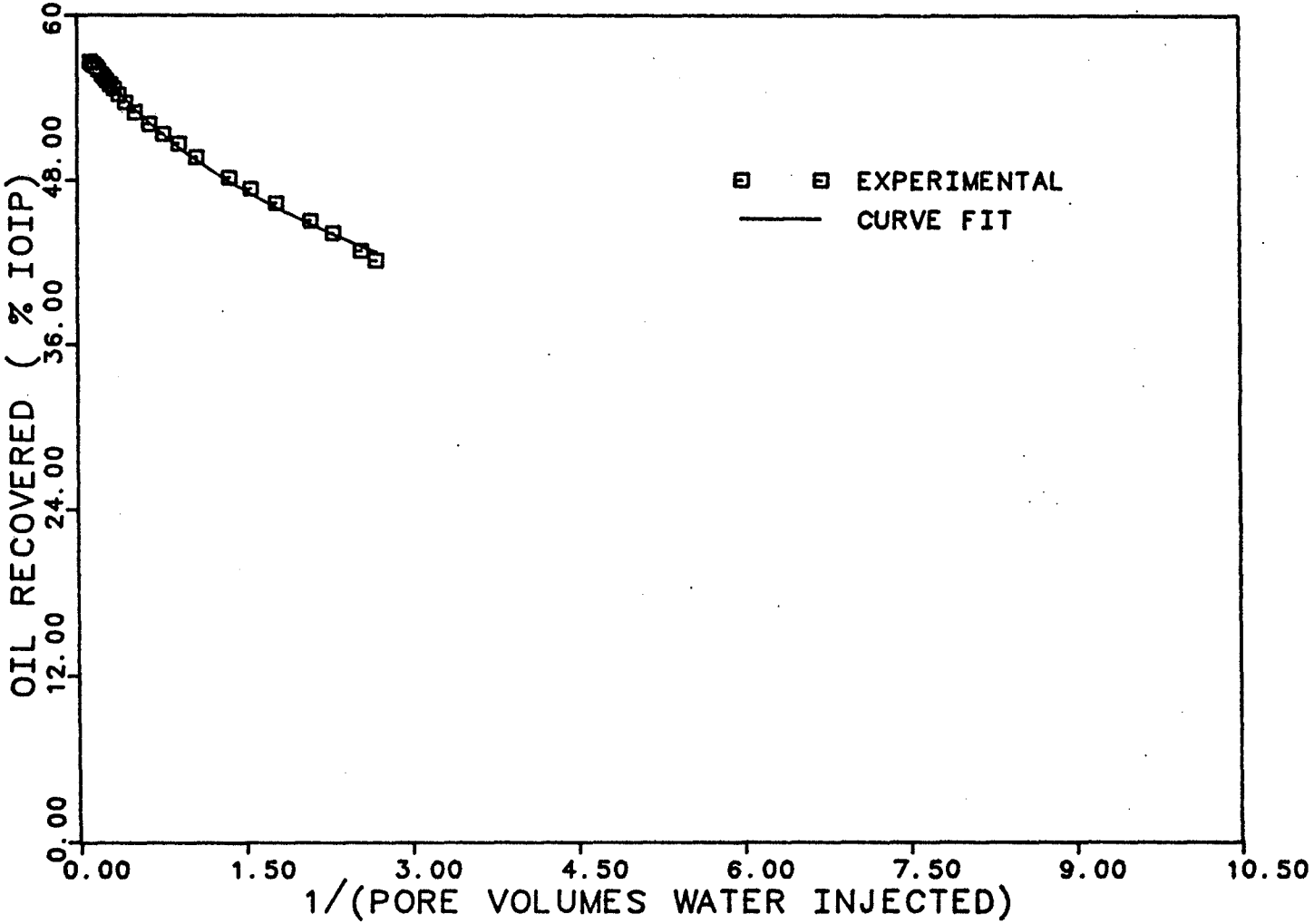

FIGURE D.4. A RECOVERY PLOT FOR RUN 4

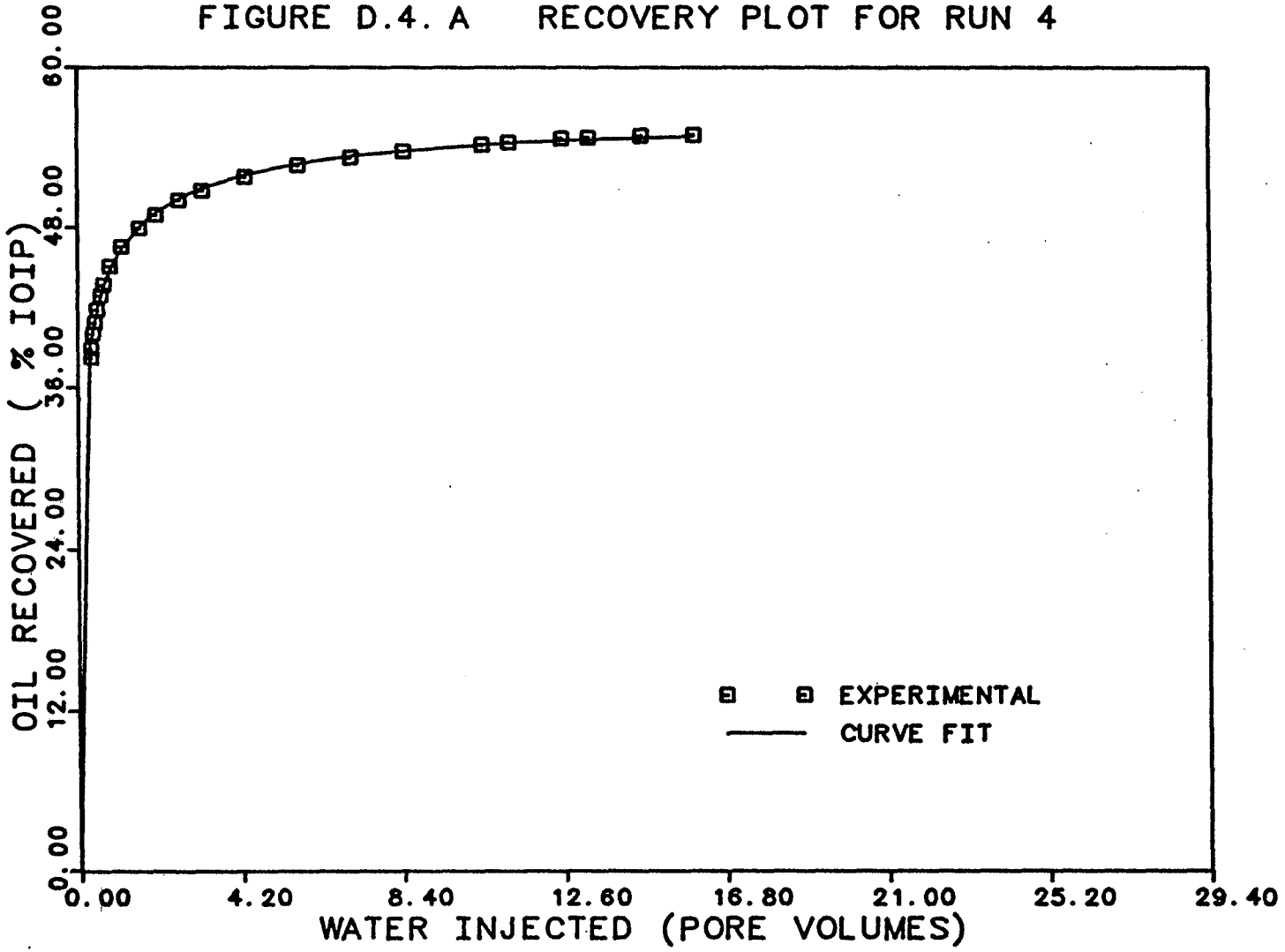

FIGURE D.4. B RECOVERY PLOT FOR RUN 4

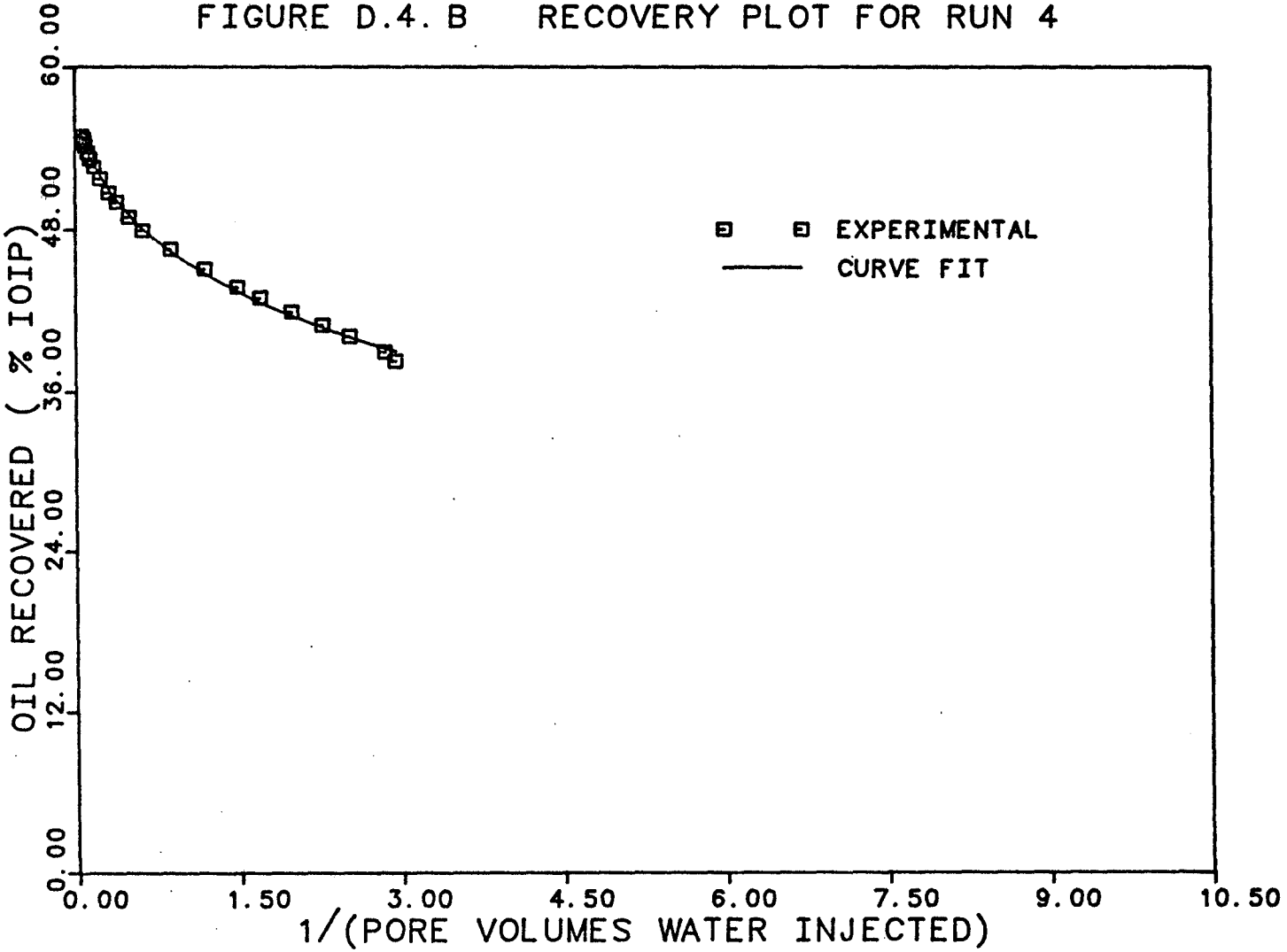

FIGURE D.5. A RECOVERY PLOT FOR RUN 5

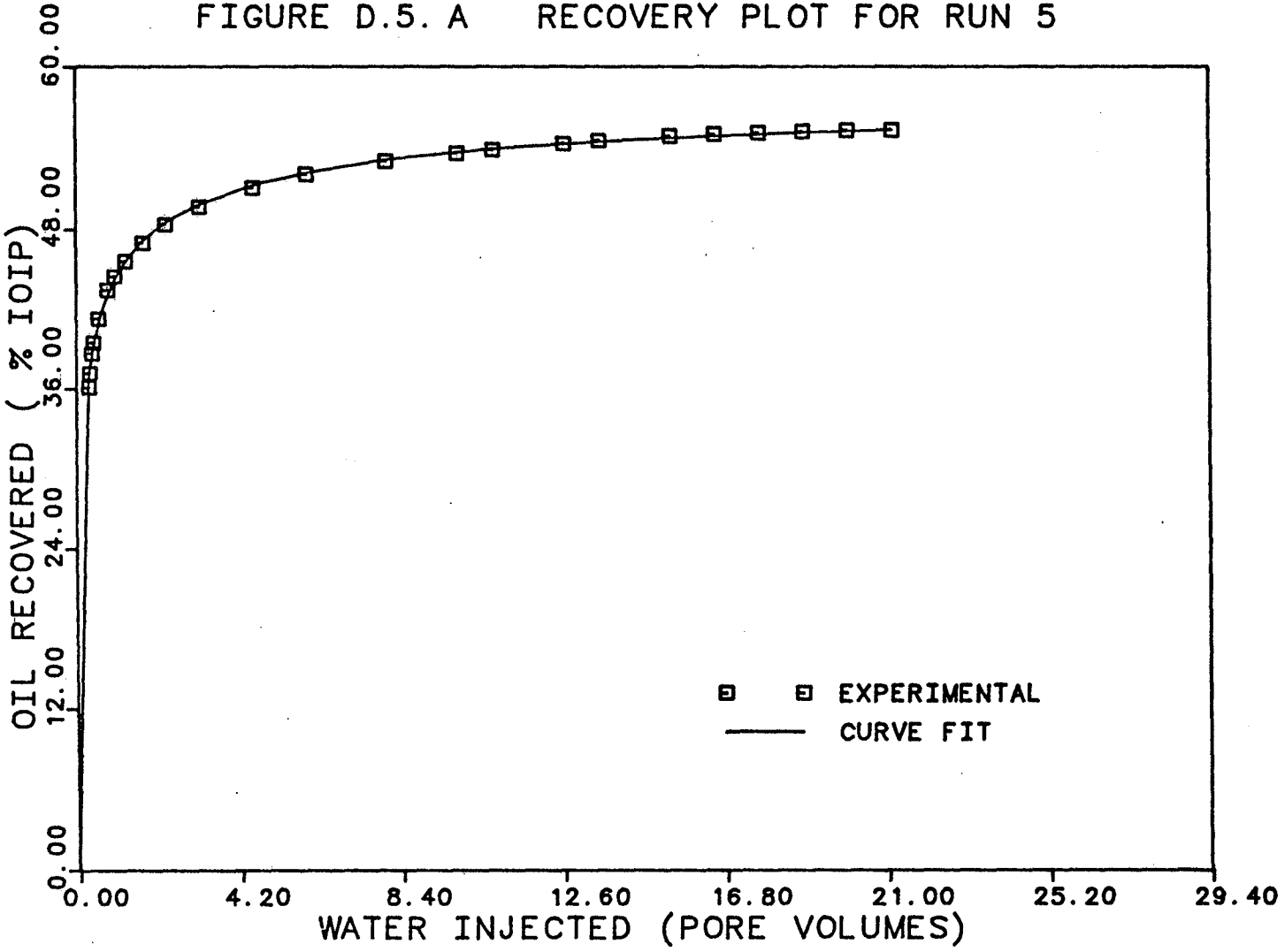

FIGURE D.5. B RECOVERY PLOT FOR RUN 5

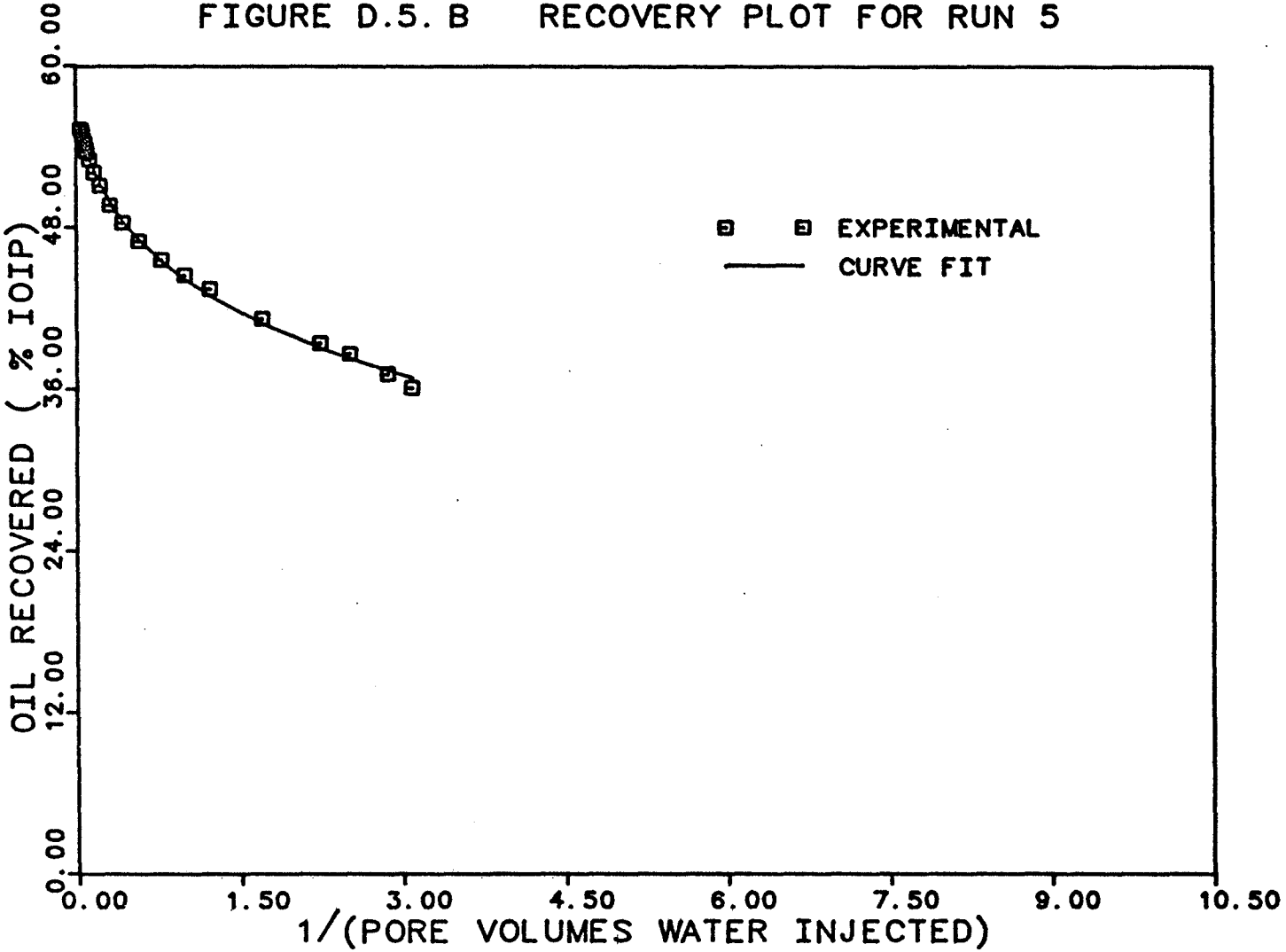

FIGURE D.6. A RECOVERY PLOT FOR RUN 6

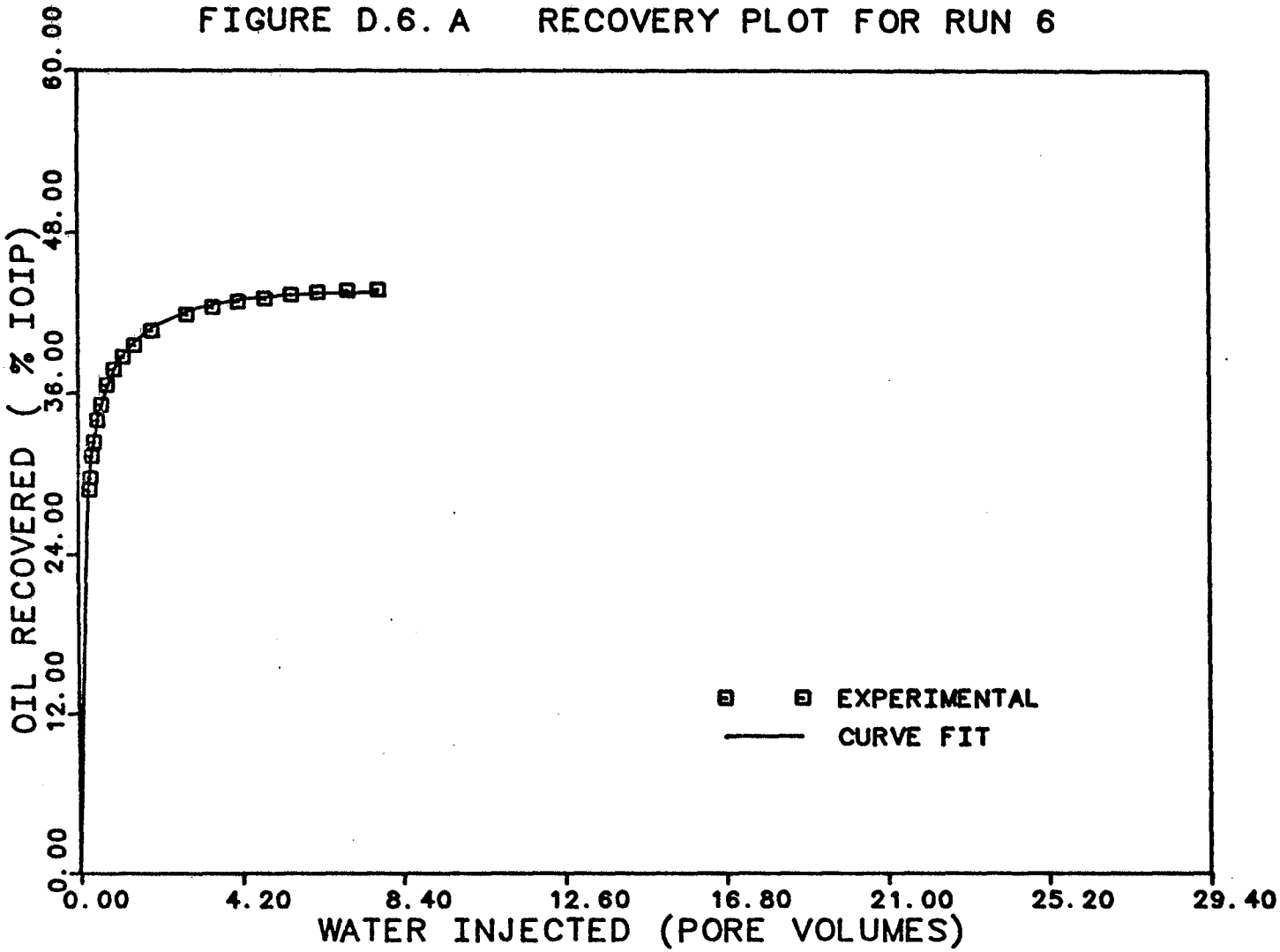

FIGURE D.6. B RECOVERY PLOT FOR RUN 6

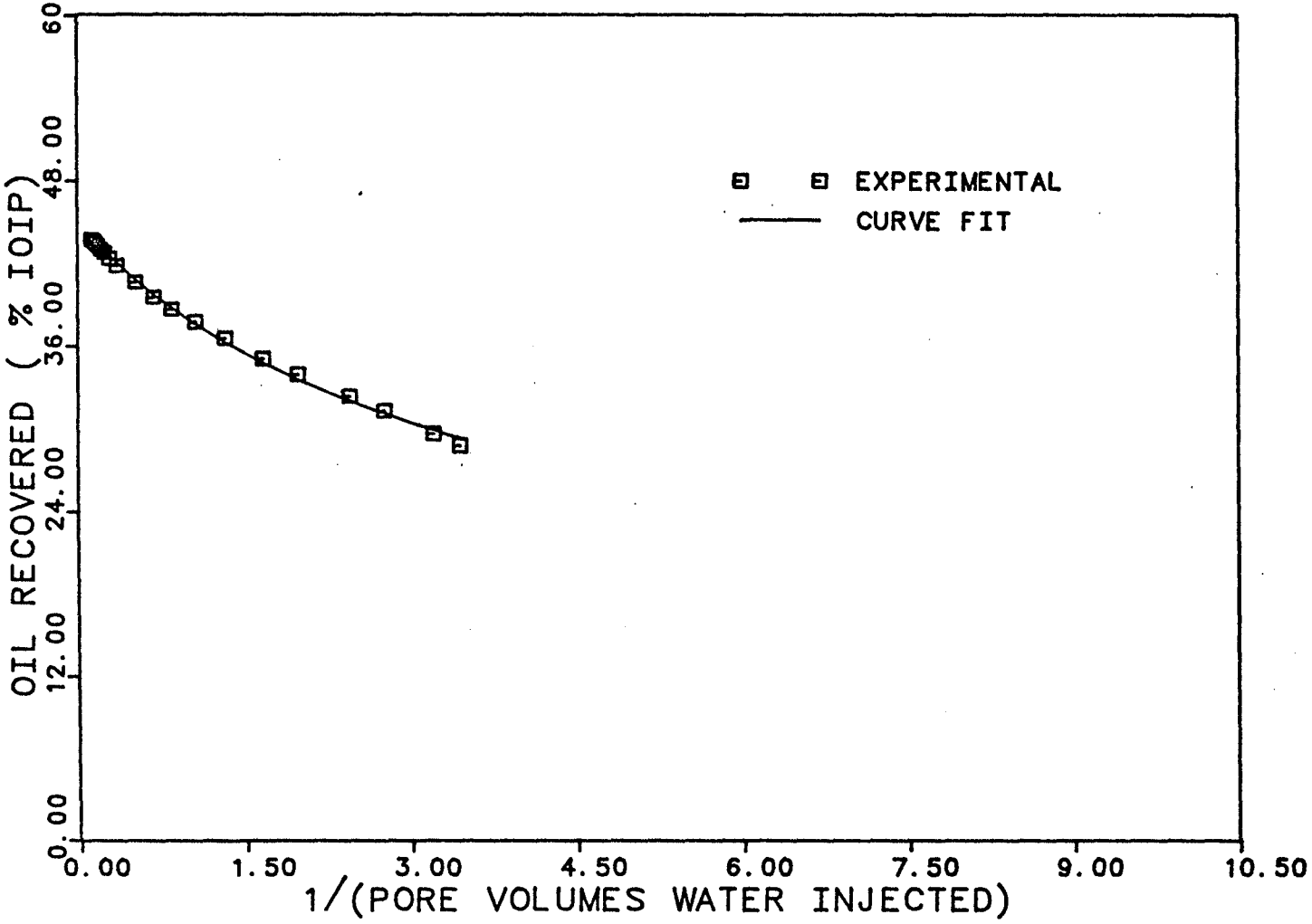

FIGURE D.7. A RECOVERY PLOT FOR RUN 7

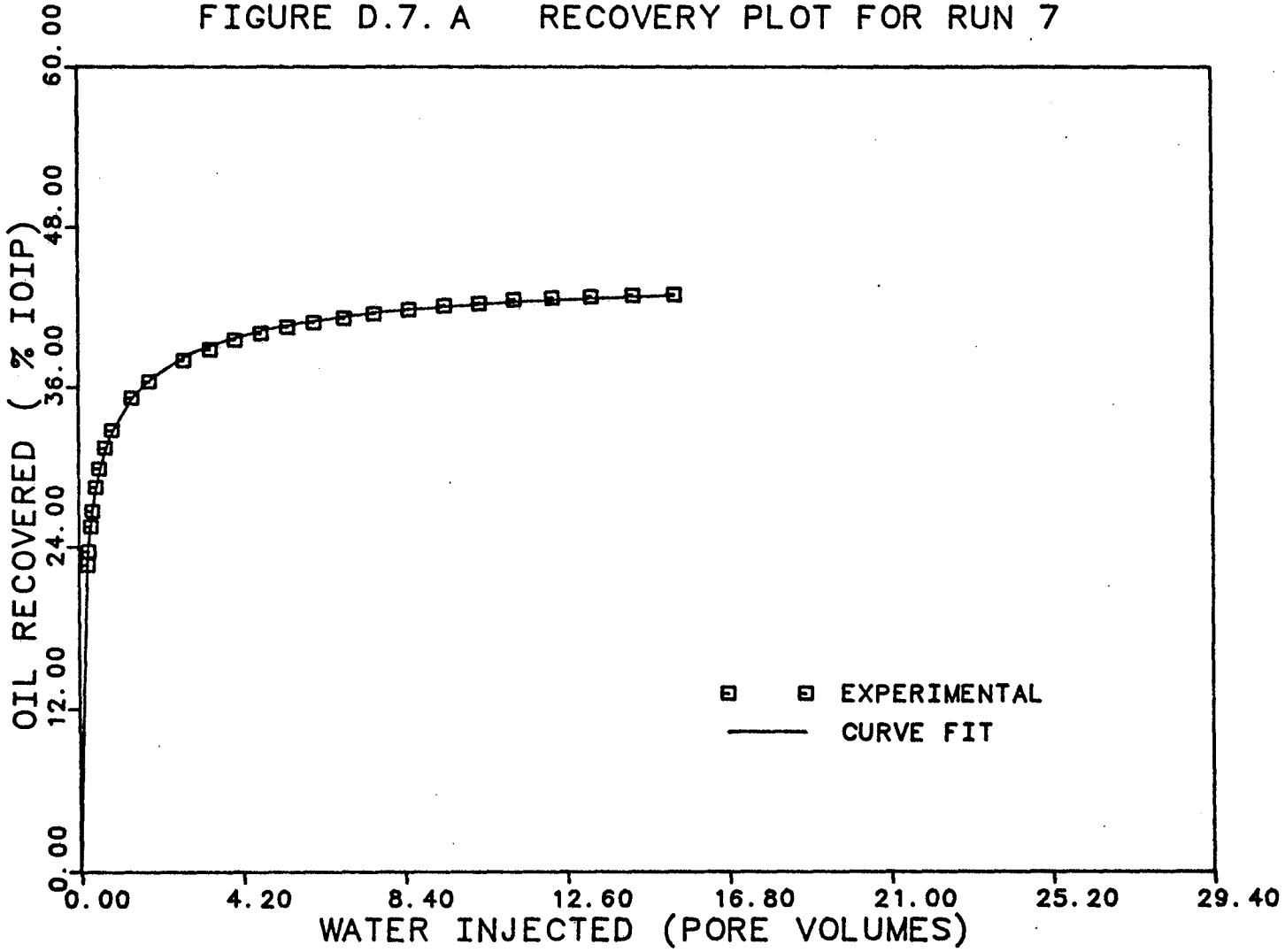

FIGURE D.7. B RECOVERY PLOT FOR RUN 7

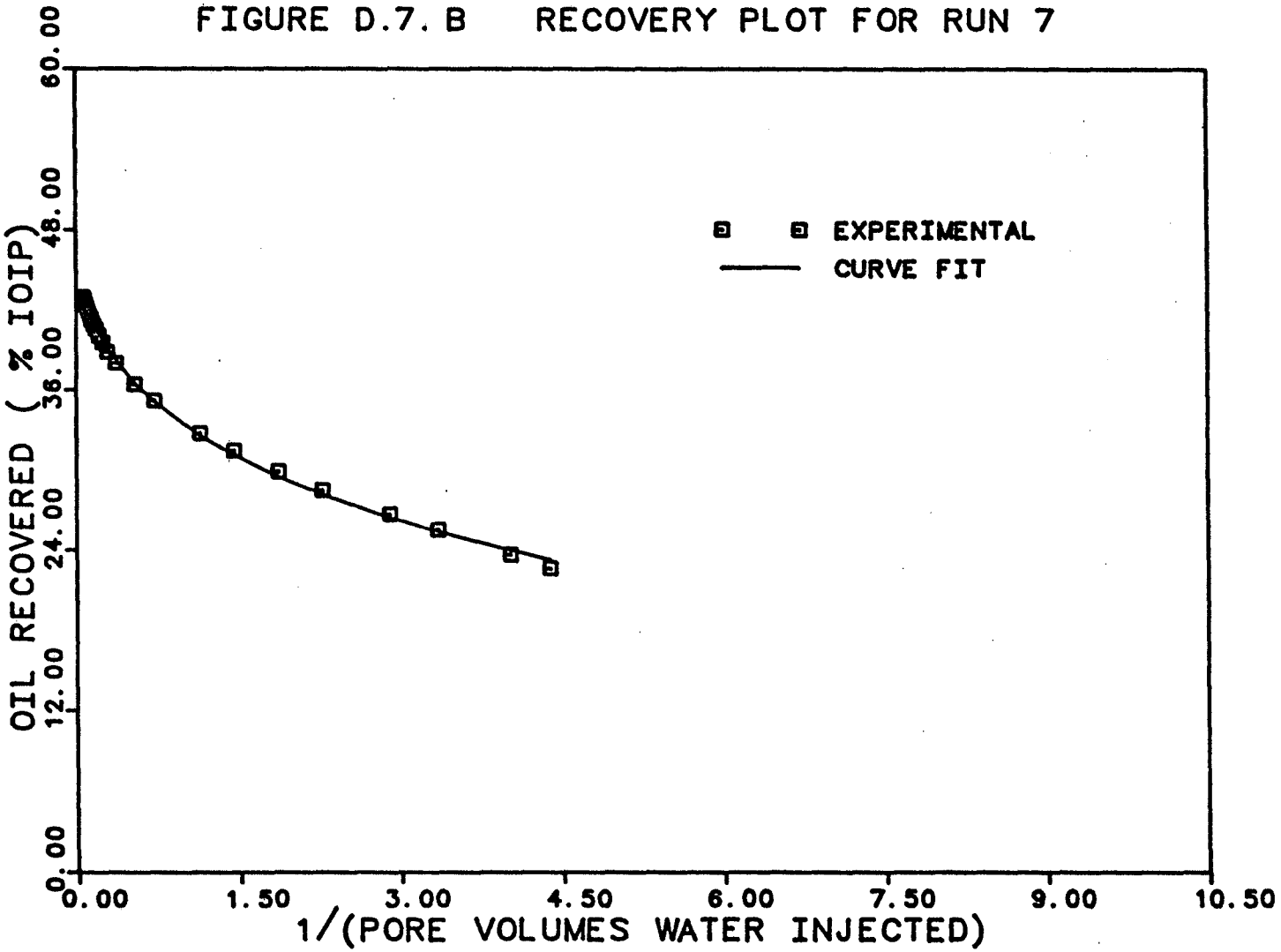

FIGURE D.8. A RECOVERY PLOT FOR RUN 8

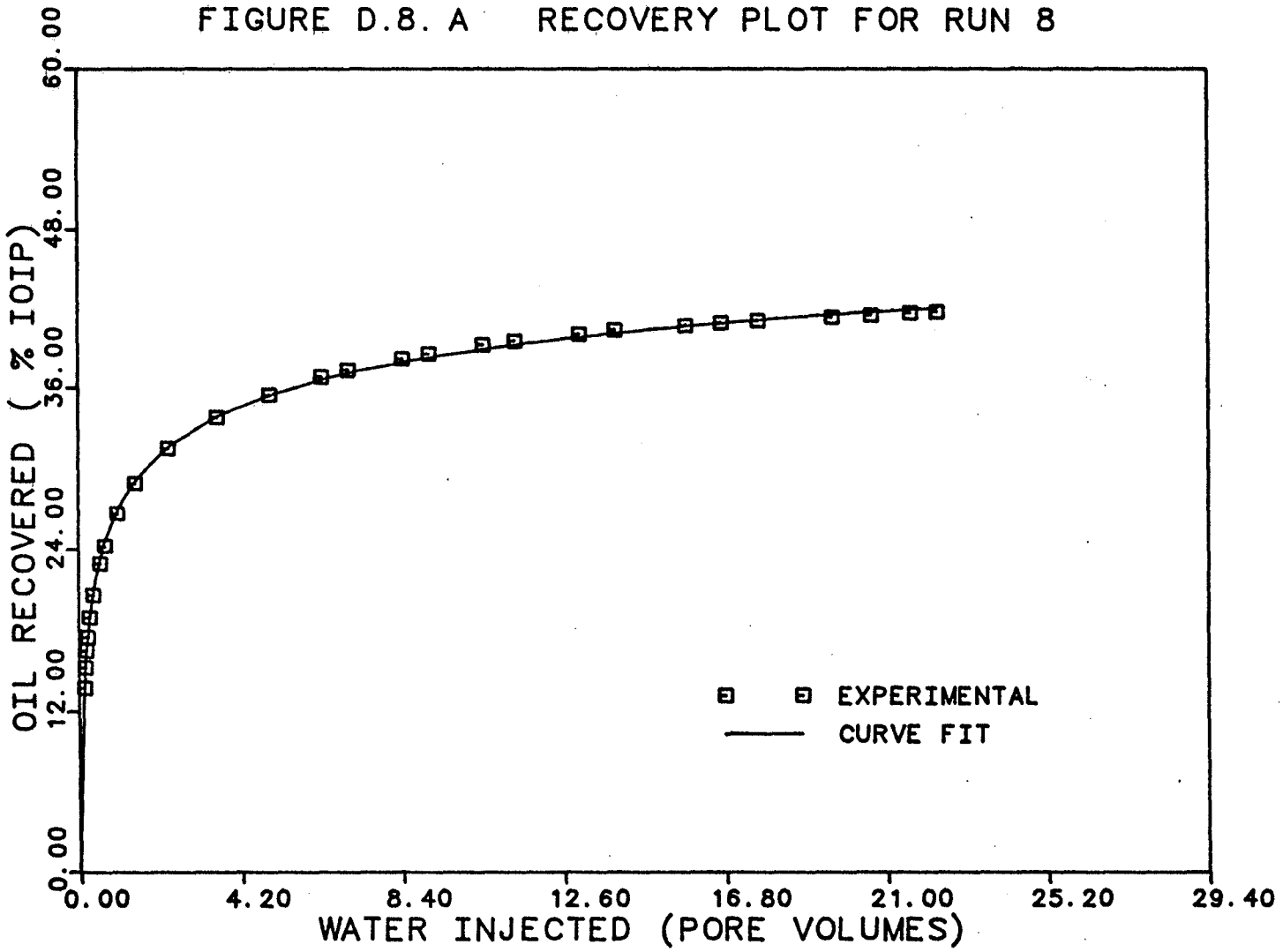

FIGURE D.8. B RECOVERY PLOT FOR RUN 8

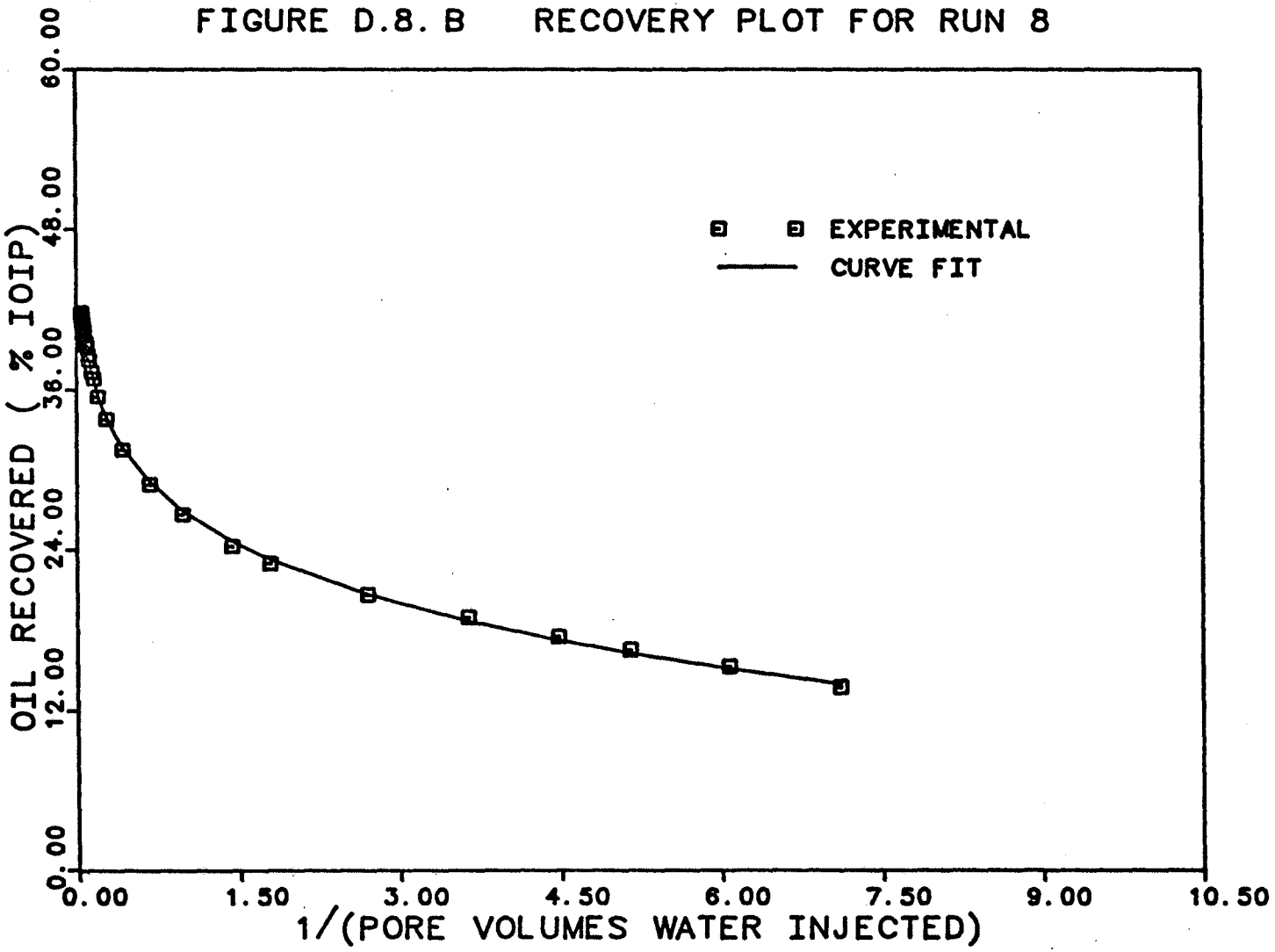

FIGURE D.9. A RECOVERY PLOT FOR RUN 9

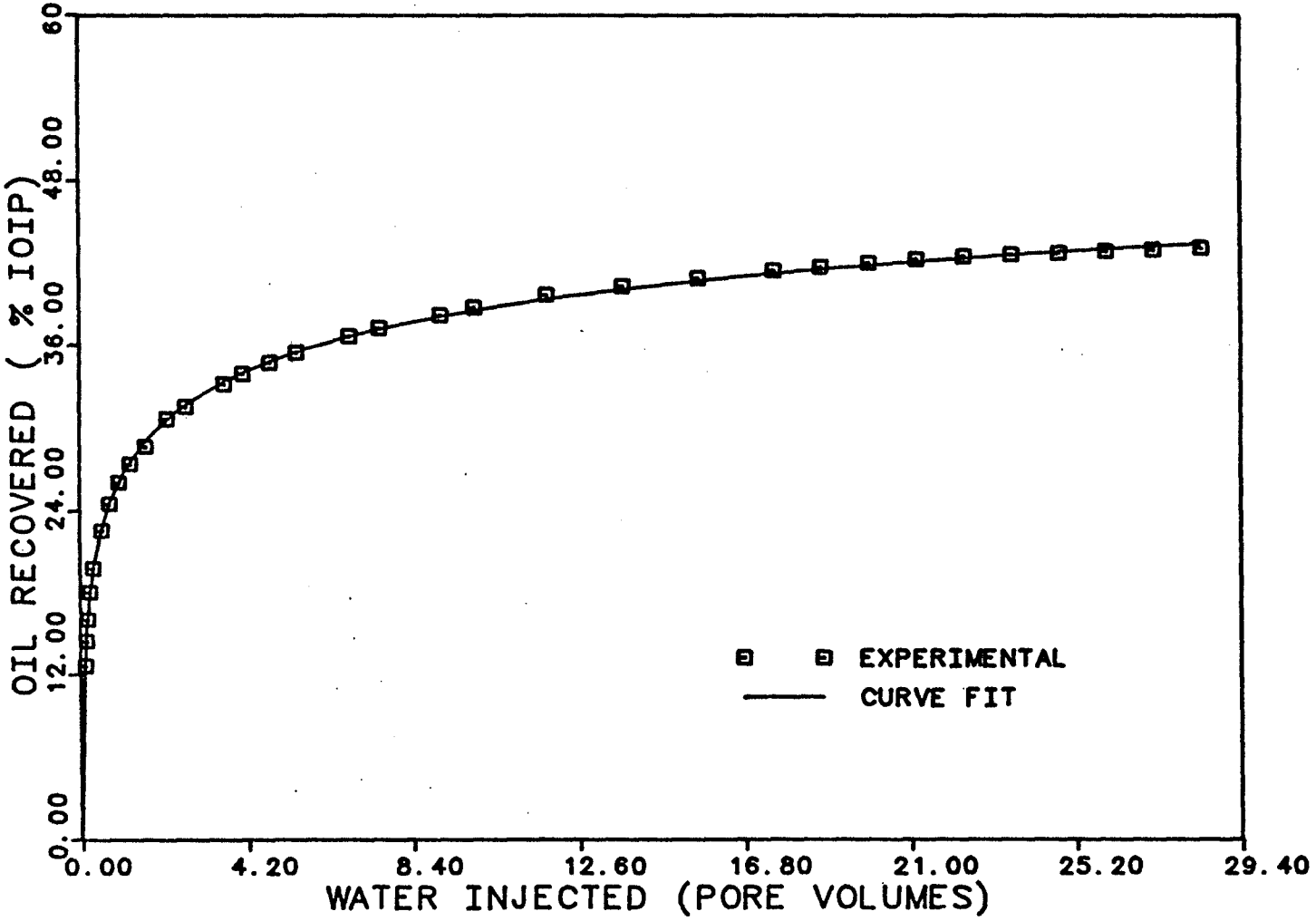

FIGURE D.9. B RECOVERY PLOT FOR RUN 9

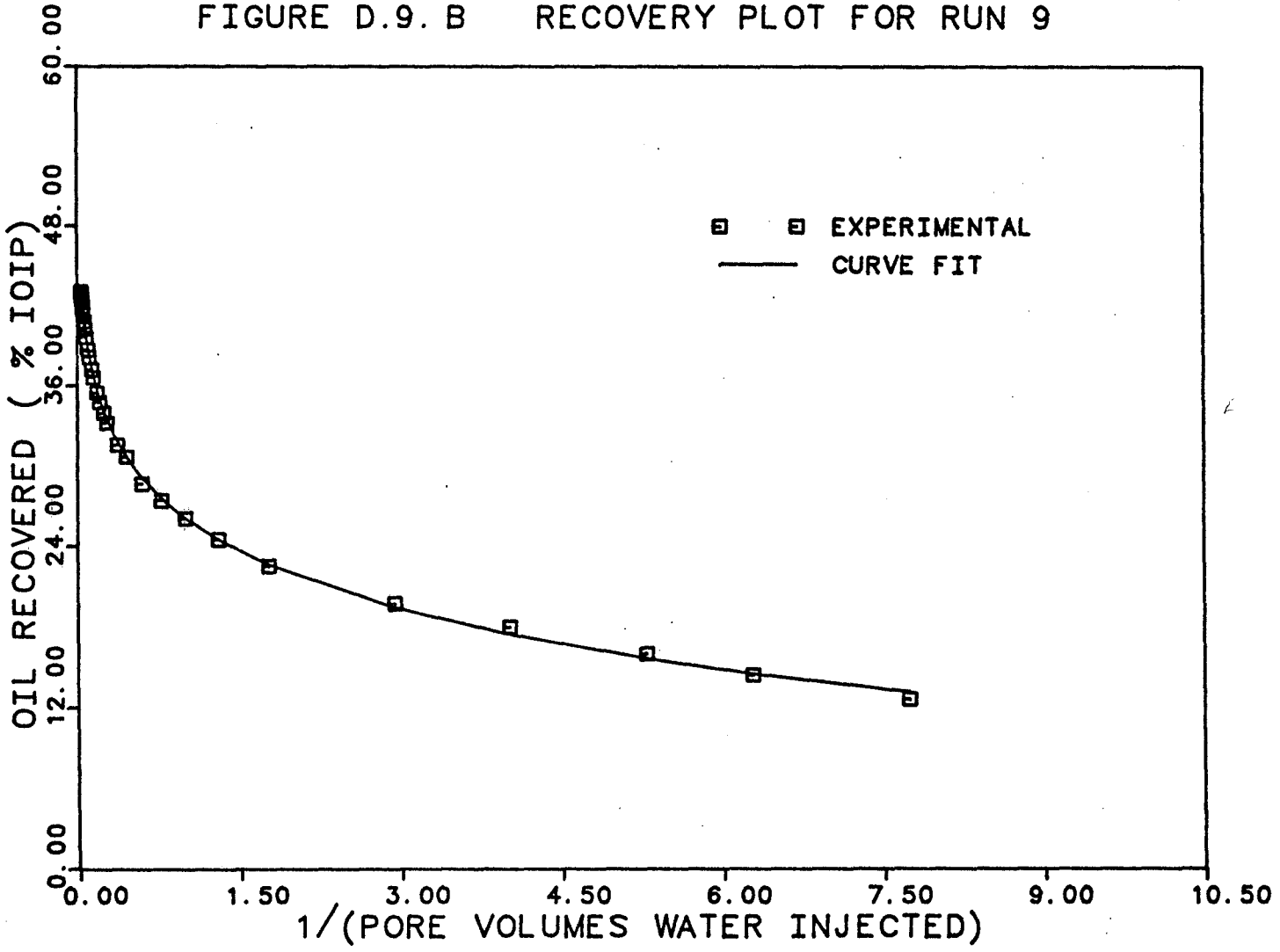

FIGURE D.10.A RECOVERY PLOT FOR RUN 10

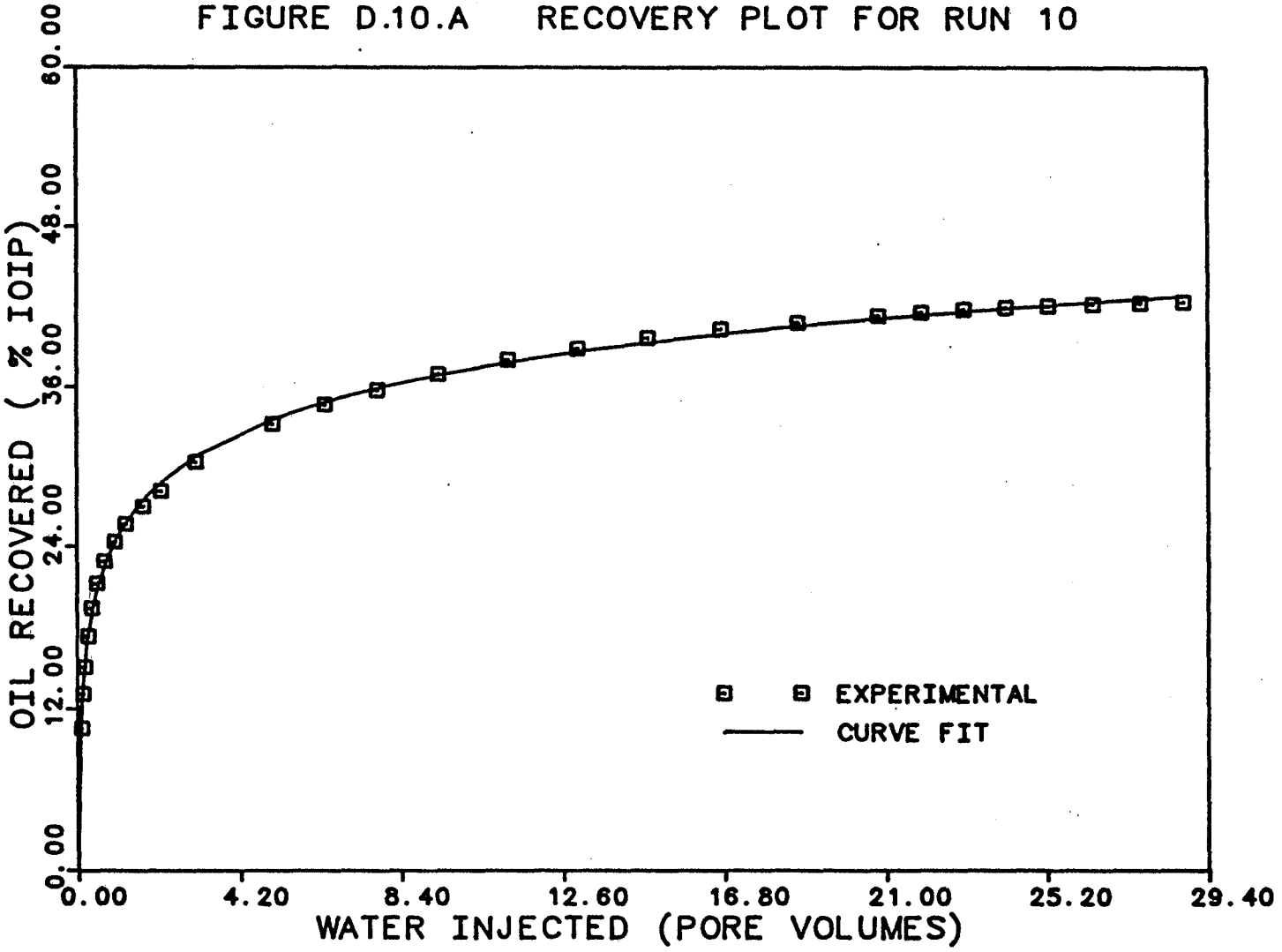

FIGURE D.10.B RECOVERY PLOT FOR RUN 10

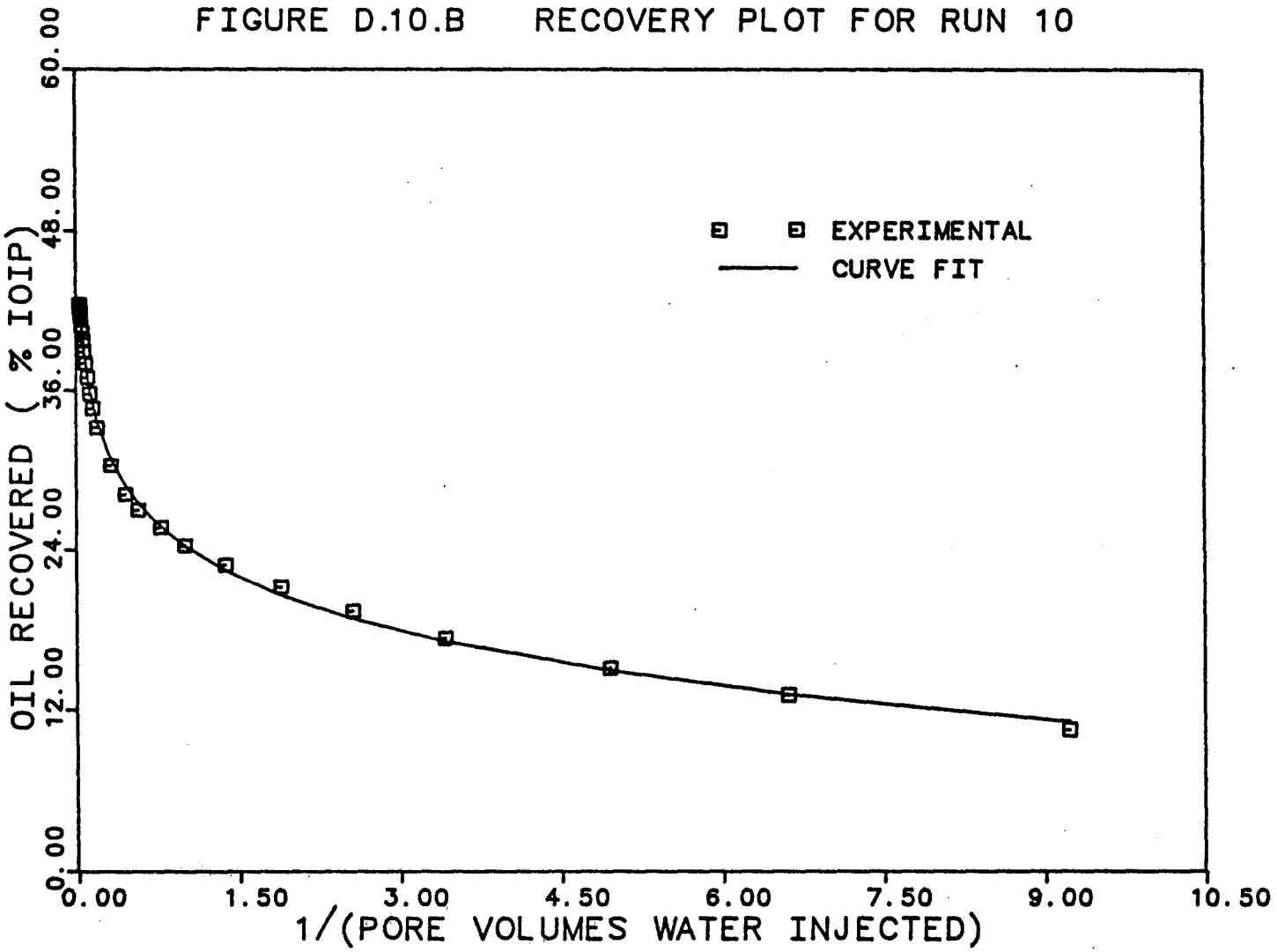

FIGURE D.11.A RECOVERY PLOT FOR RUN 11

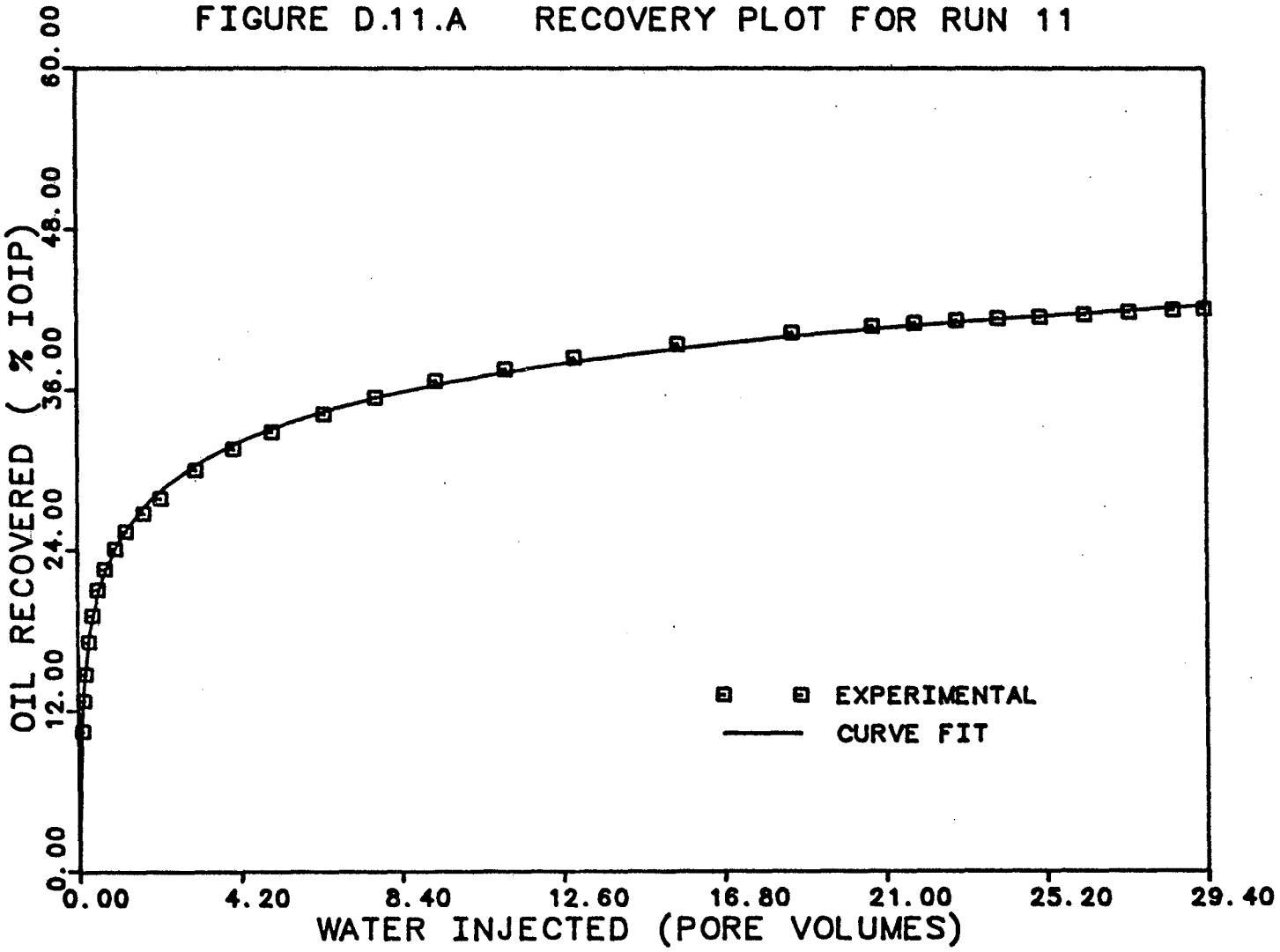

FIGURE D.11.B RECOVERY PLOT FOR RUN 11

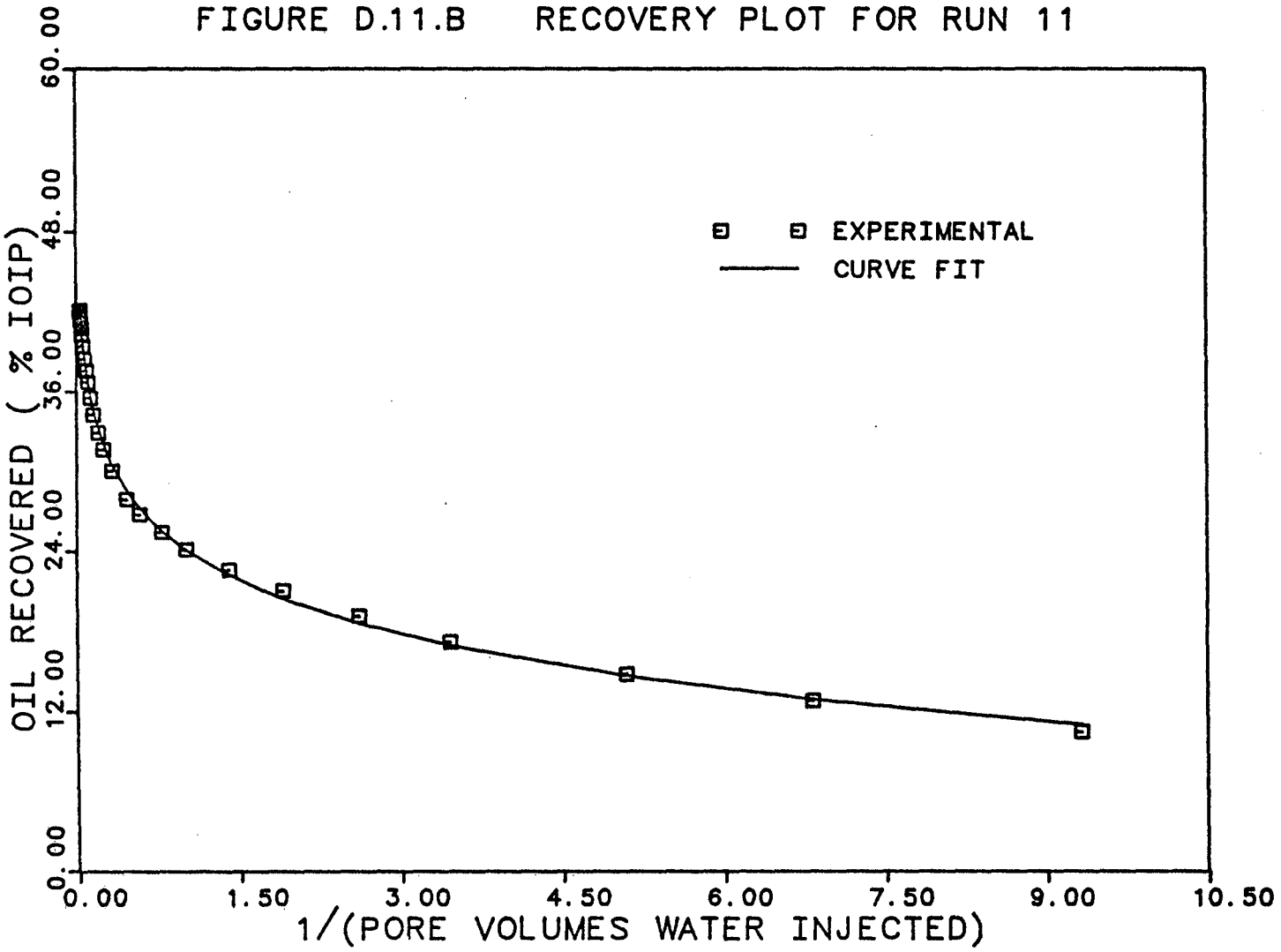

FIGURE D.12.A RECOVERY PLOT FOR RUN 12

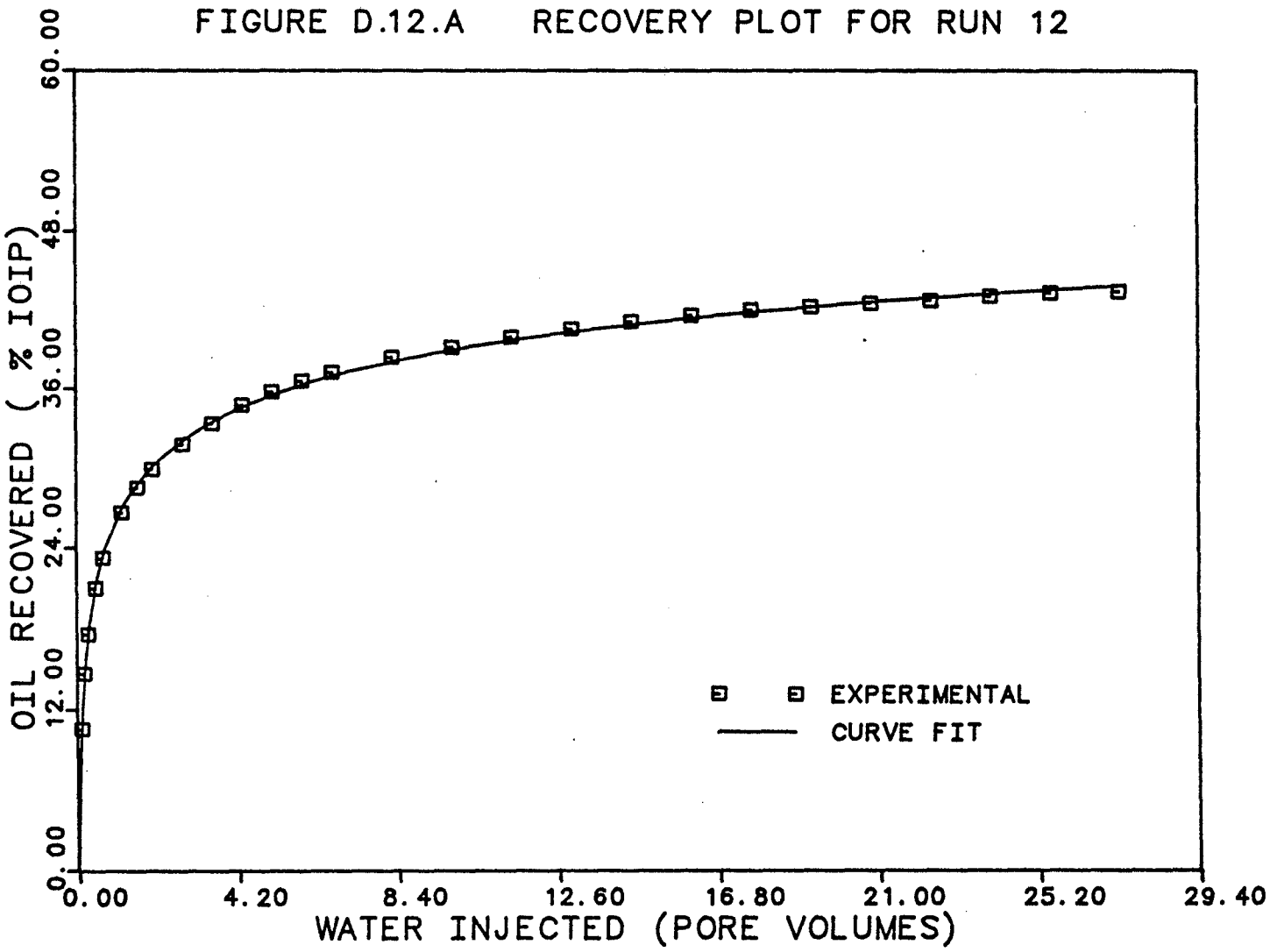

FIGURE D.12.B RECOVERY PLOT FOR RUN 12

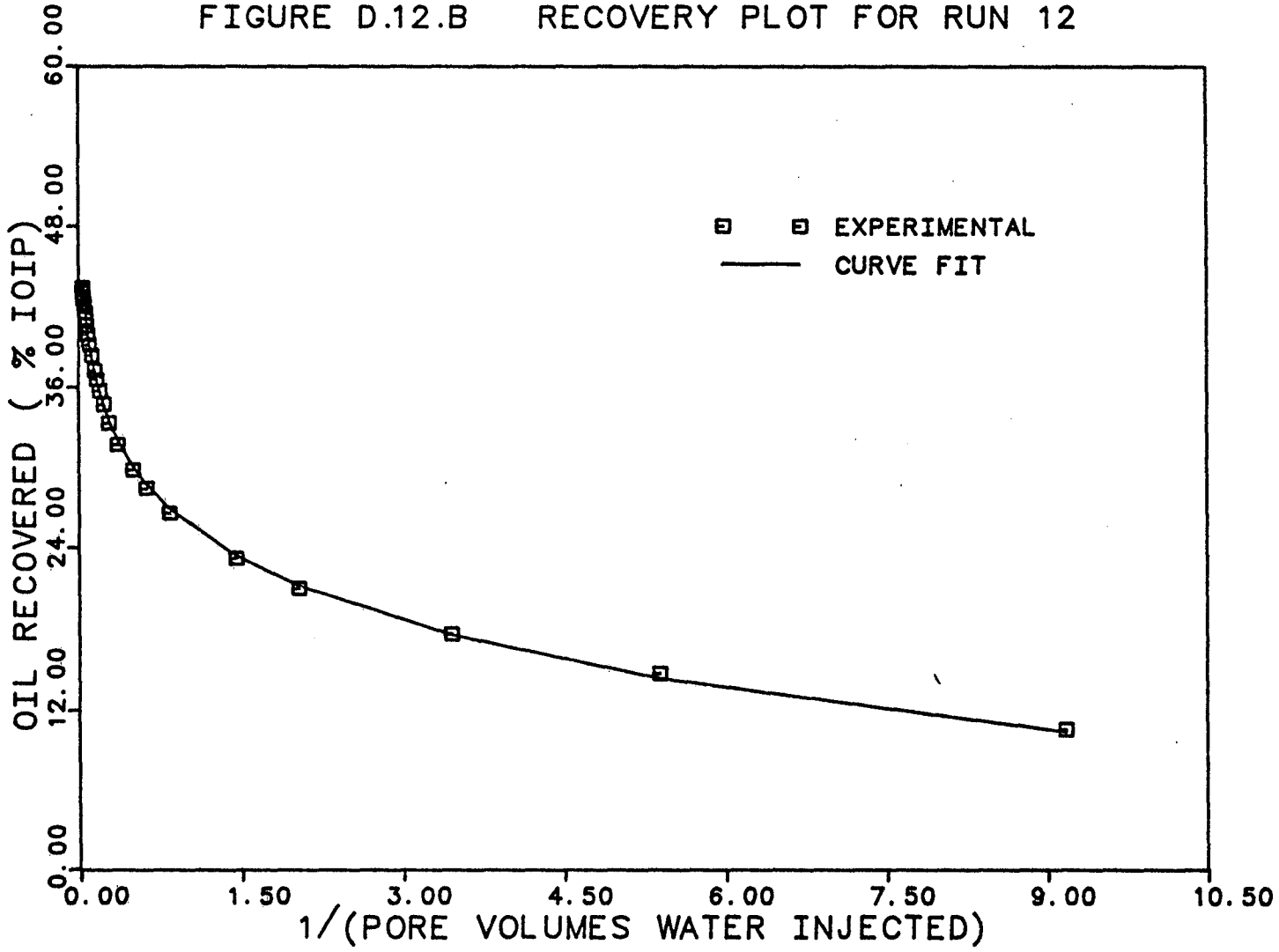

APPENDIX E

FIGURE E.2. A INJECTIVITY PLOT FOR RUN 2

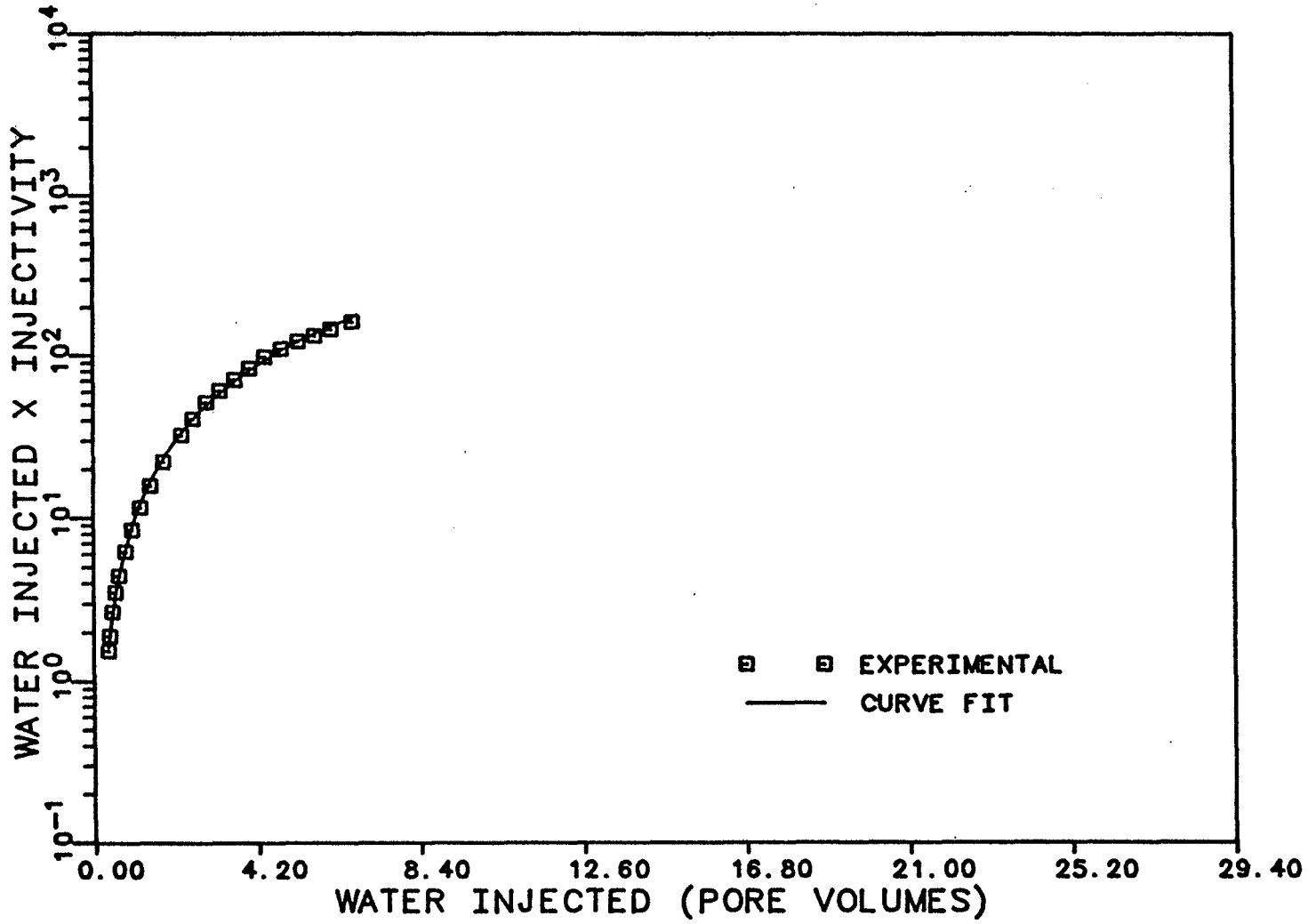

FIGURE E.2. B INJECTIVITY PLOT FOR RUN 2

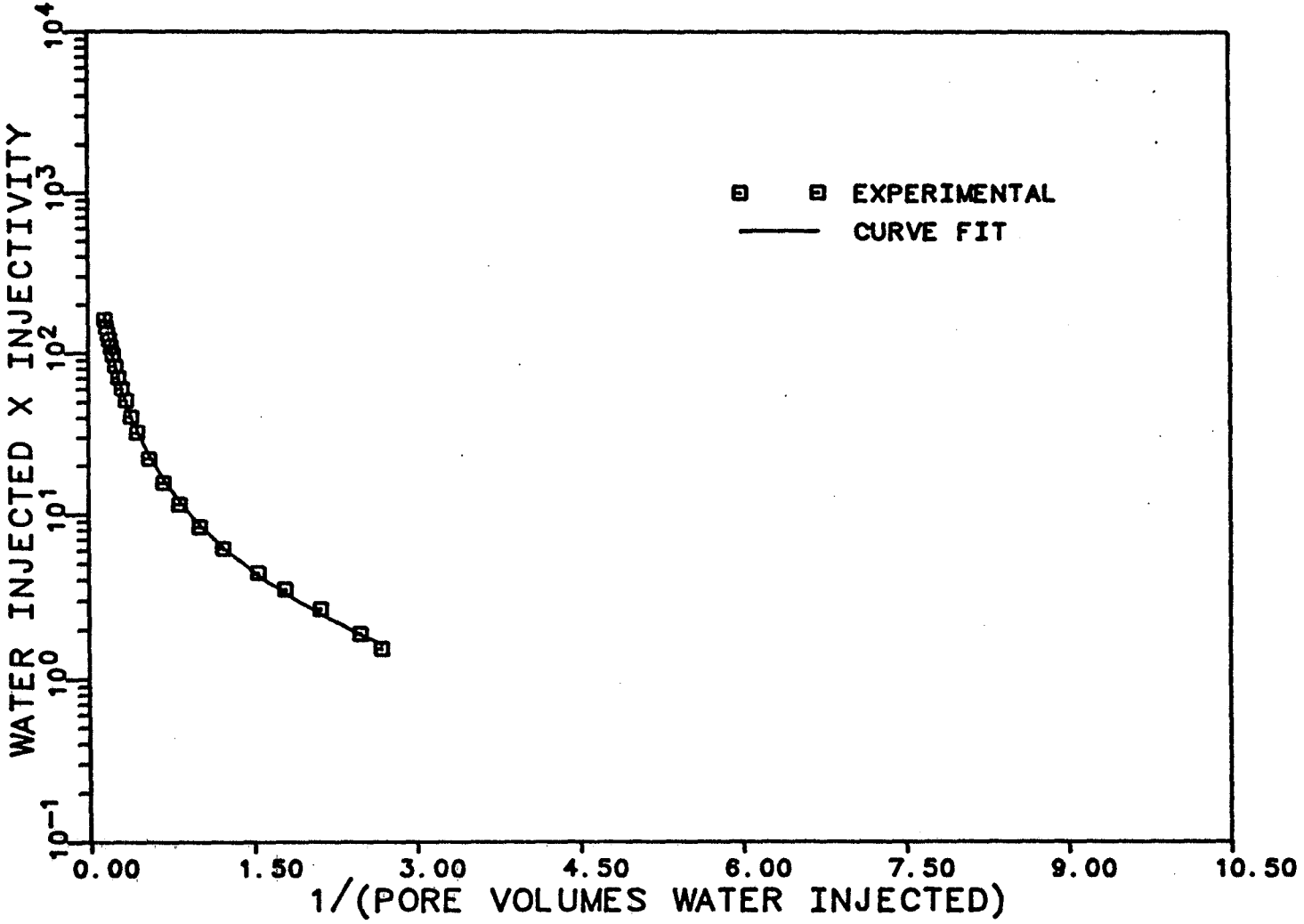

FIGURE E.3. A INJECTIVITY PLOT FOR RUN 3

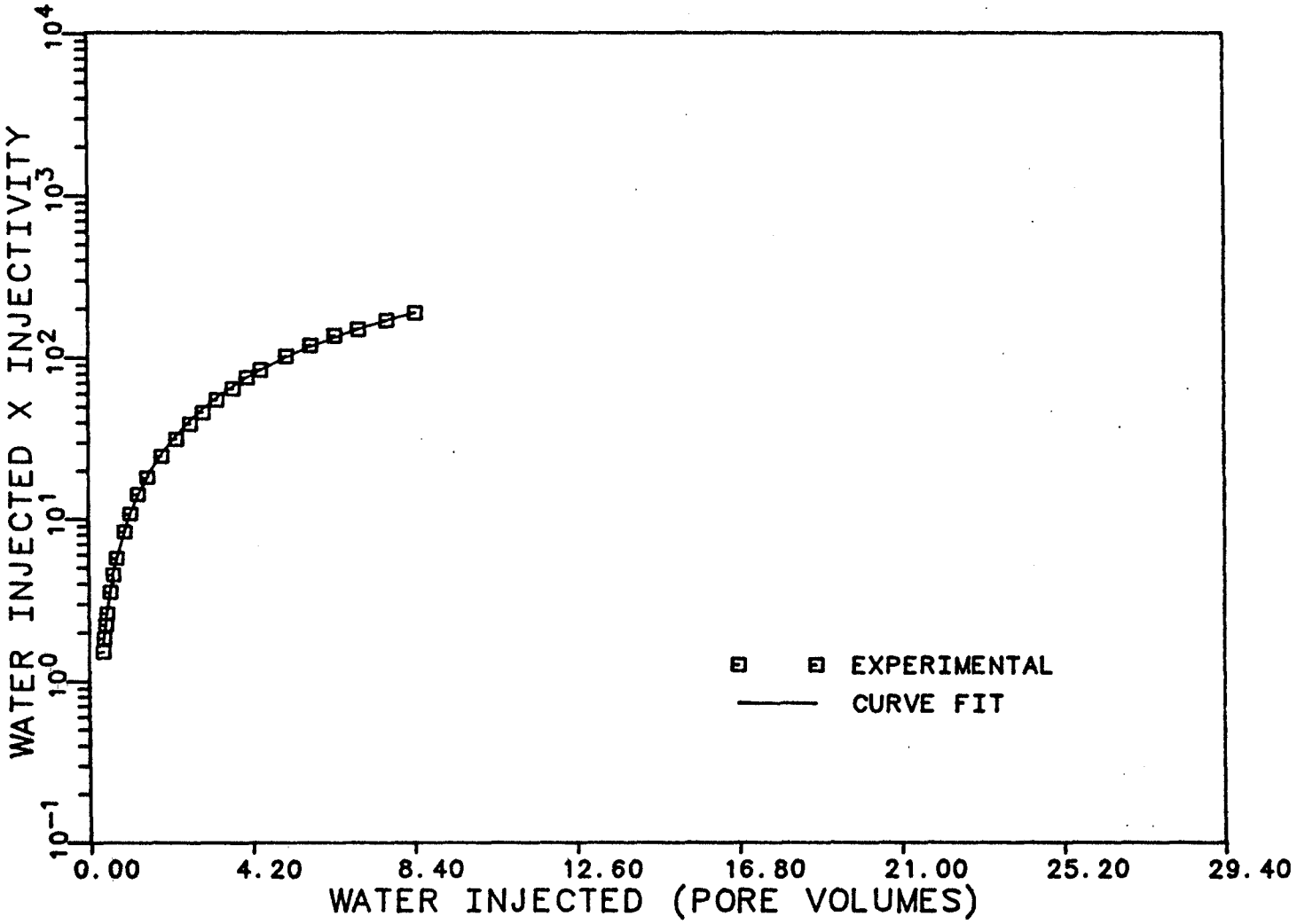

FIGURE E.3. B INJECTIVITY PLOT FOR RUN 3

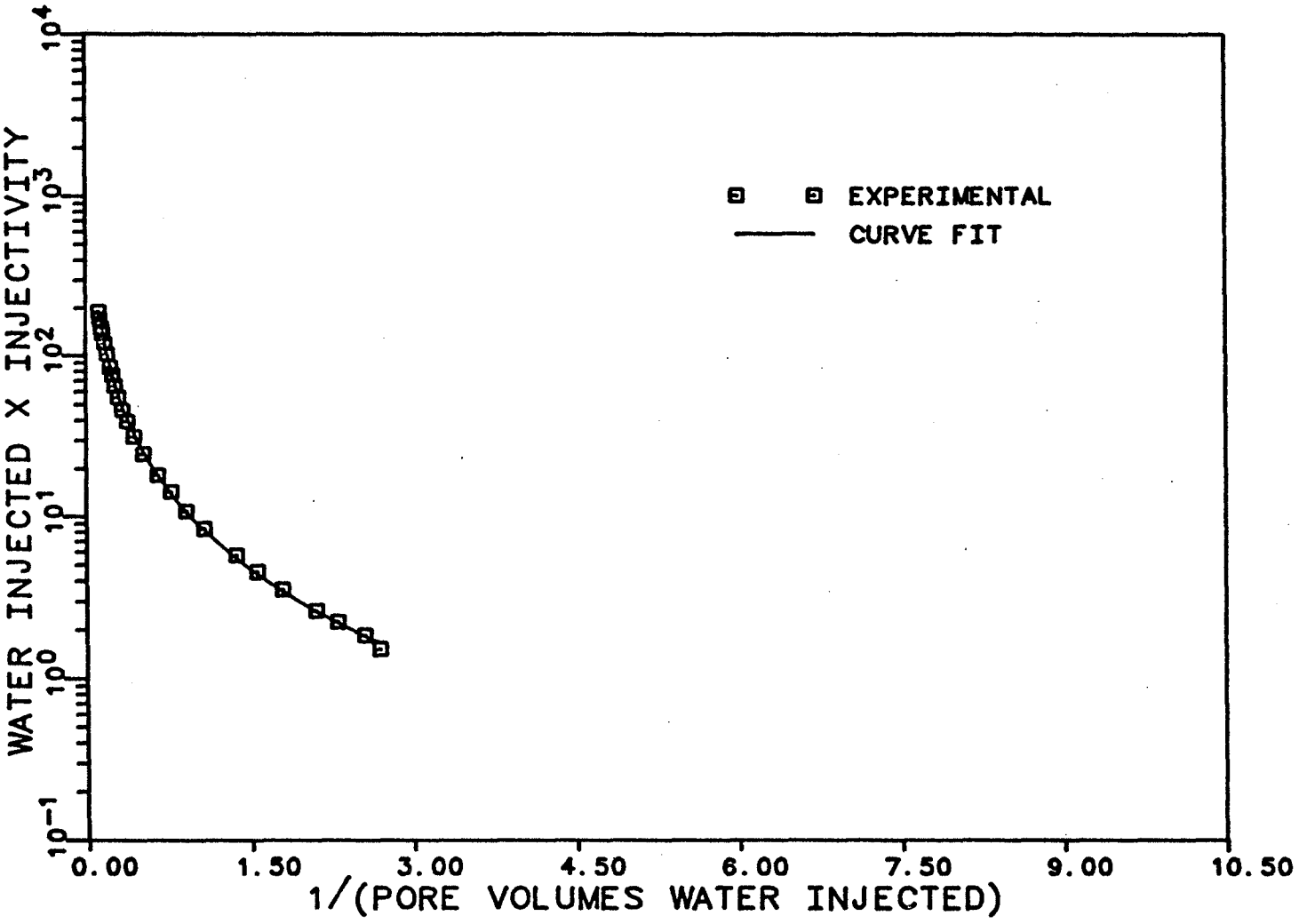

FIGURE E.4. A INJECTIVITY PLOT FOR RUN 4

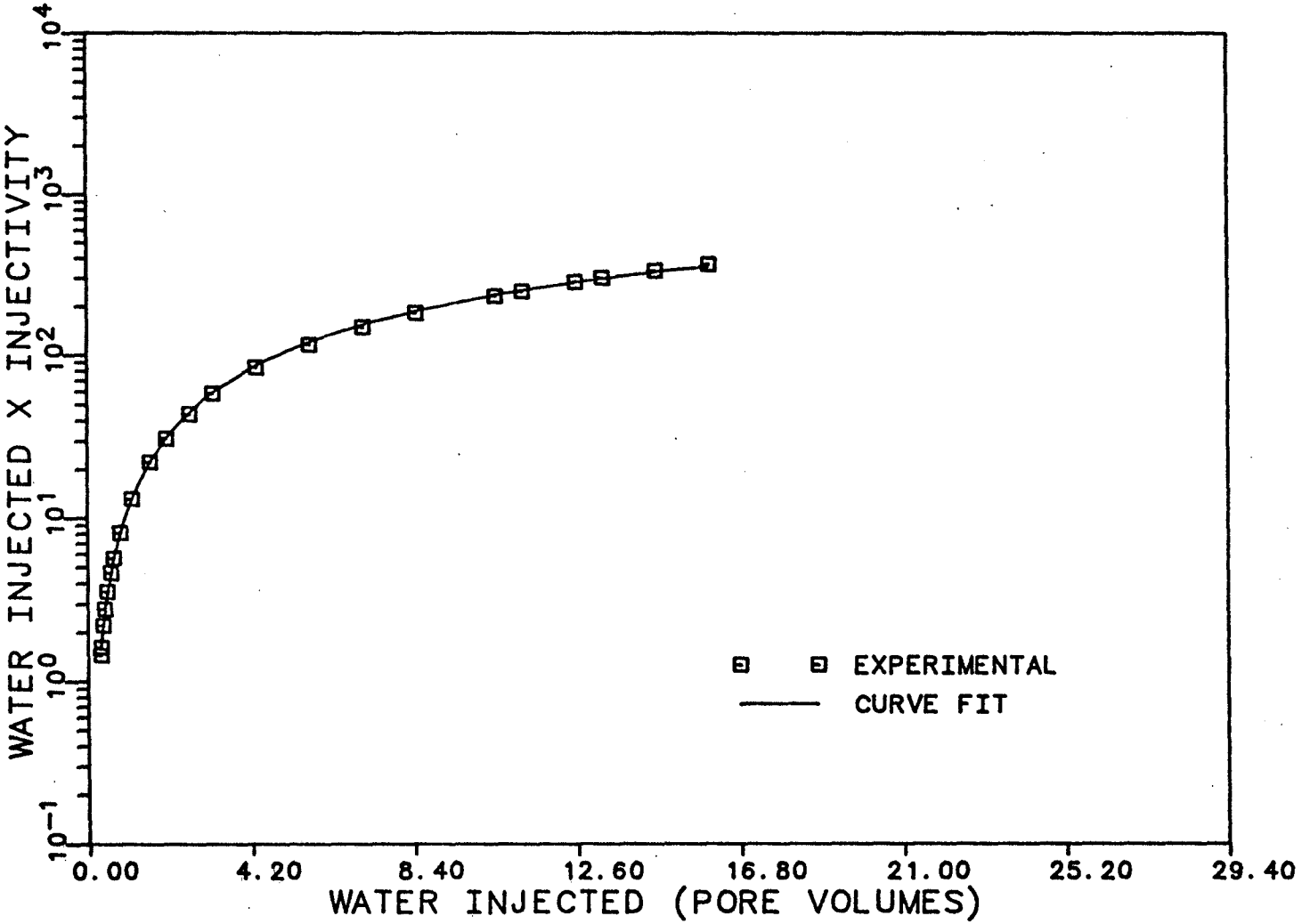

FIGURE E.4. B INJECTIVITY PLOT FOR RUN 4

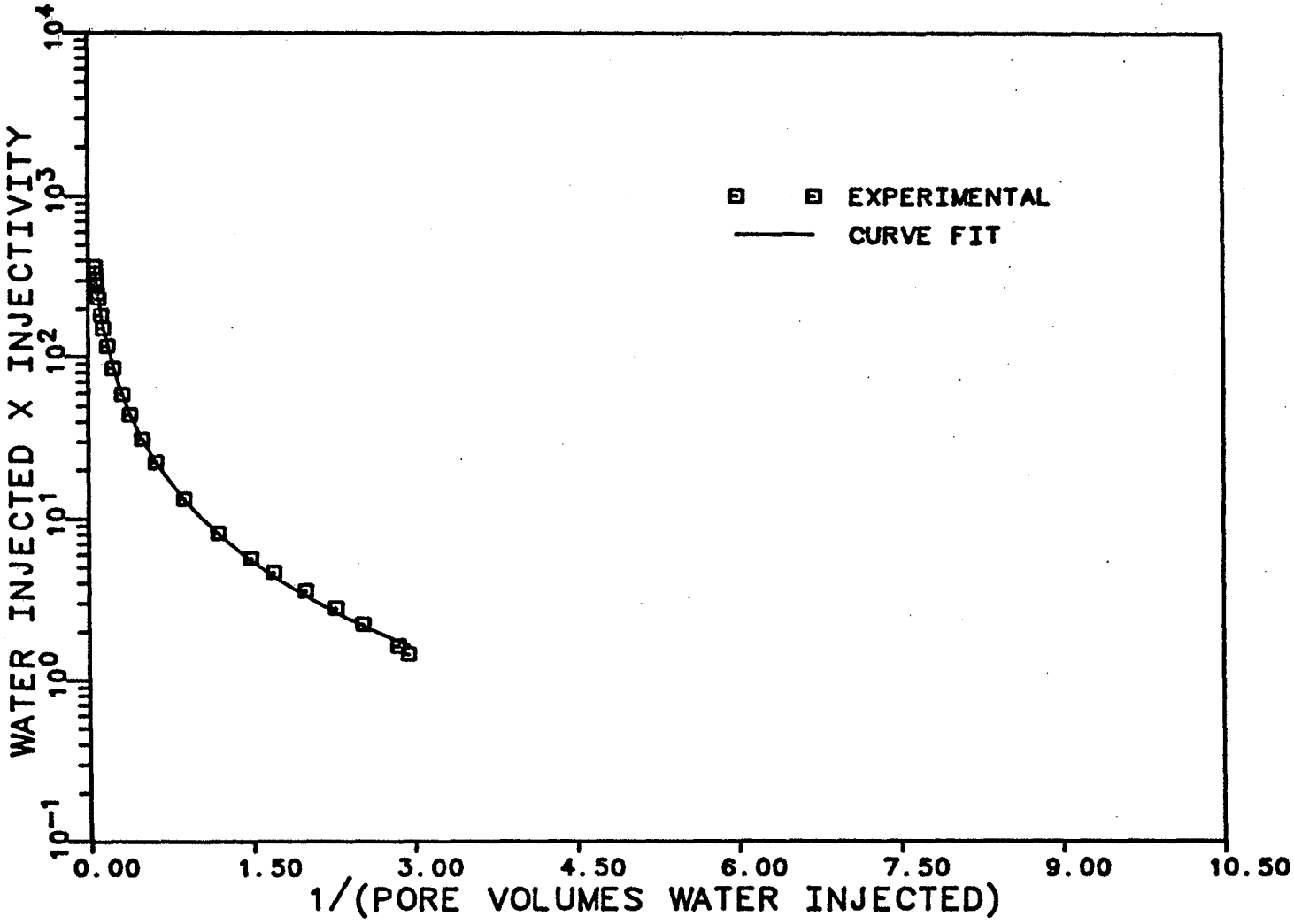

FIGURE E.5. A INJECTIVITY PLOT FOR RUN 5

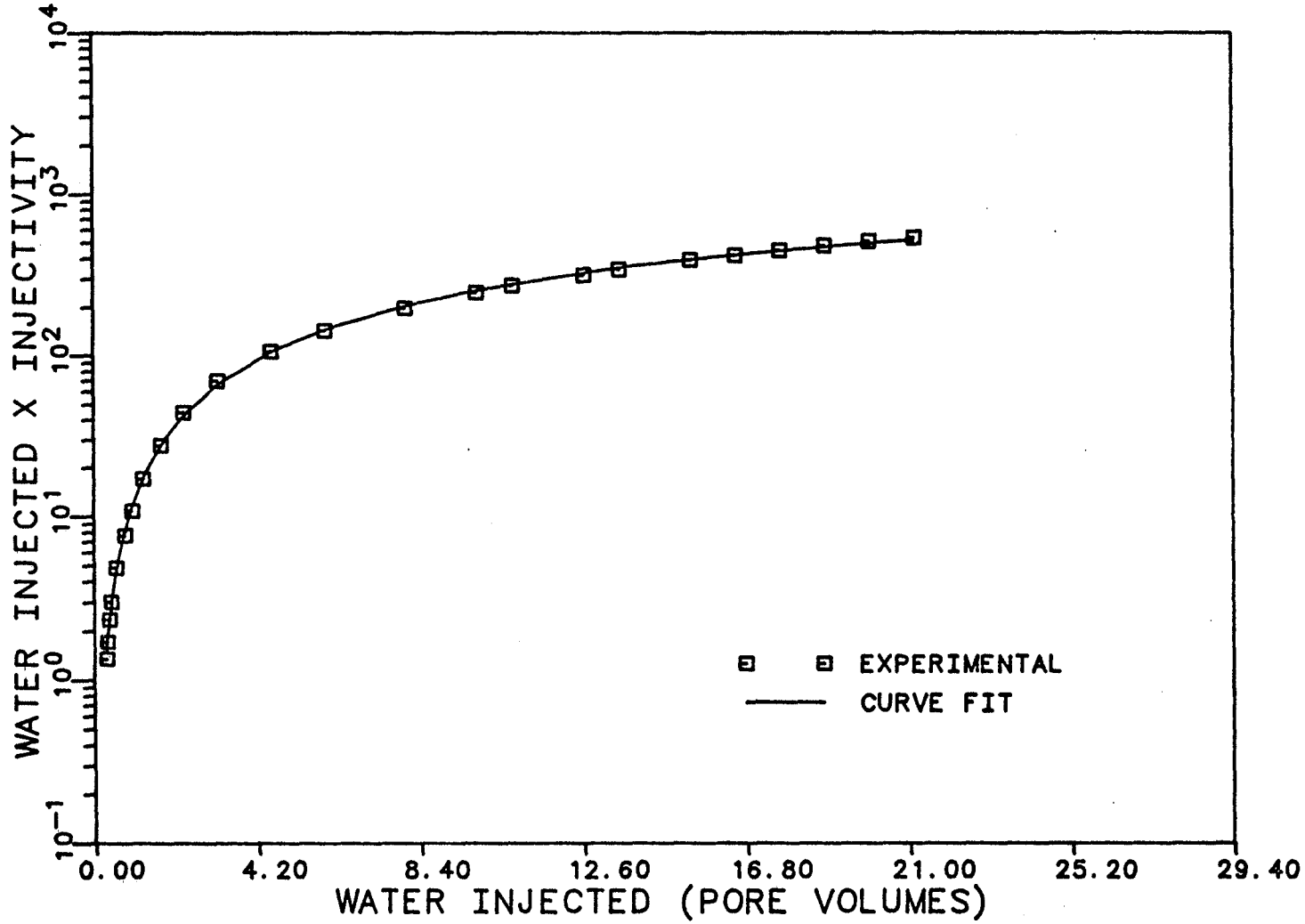

FIGURE E.5. B INJECTIVITY PLOT FOR RUN 5

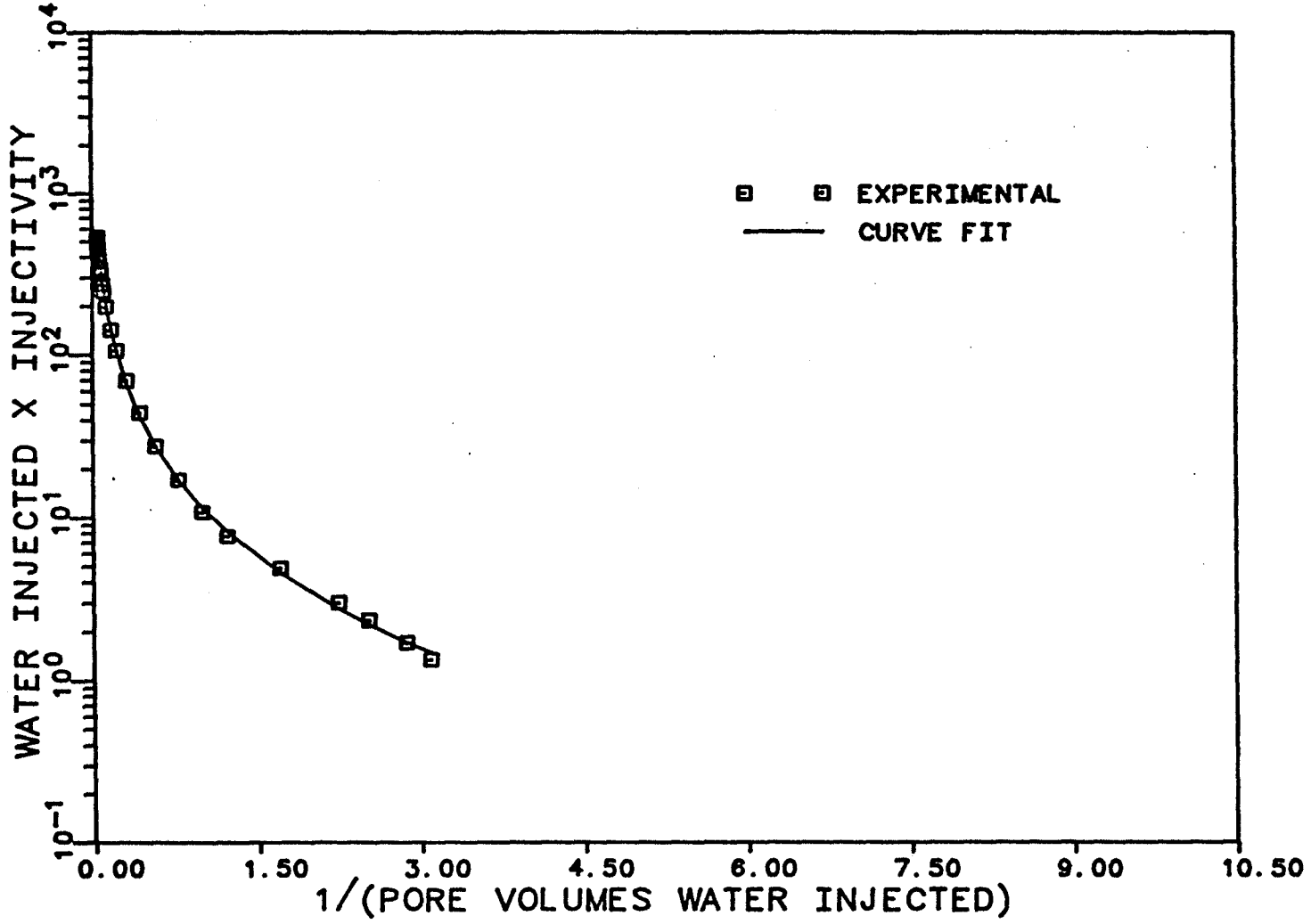

FIGURE E.6. A INJECTIVITY PLOT FOR RUN 6

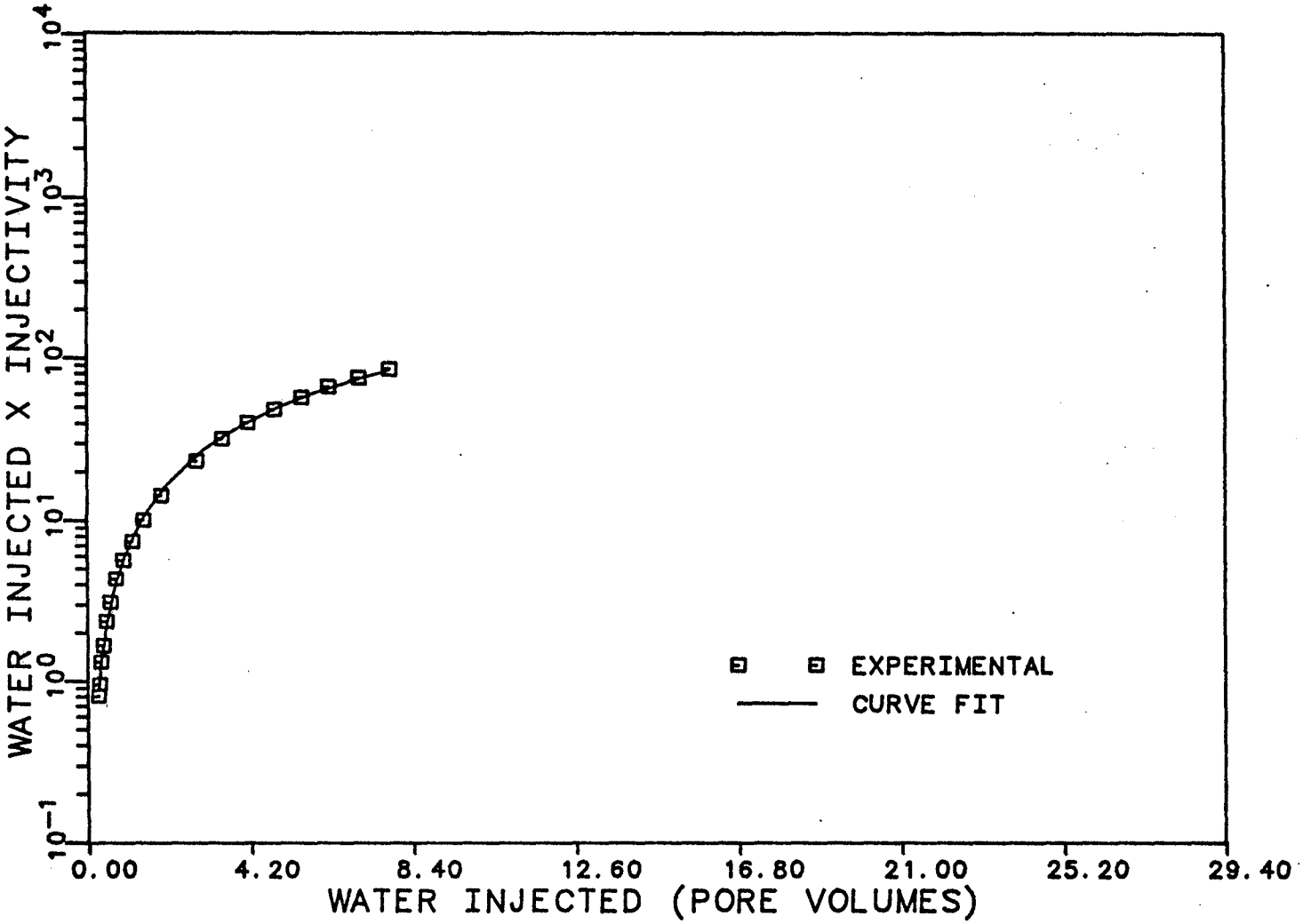

FIGURE E.6.B INJECTIVITY PLOT FOR RUN 6

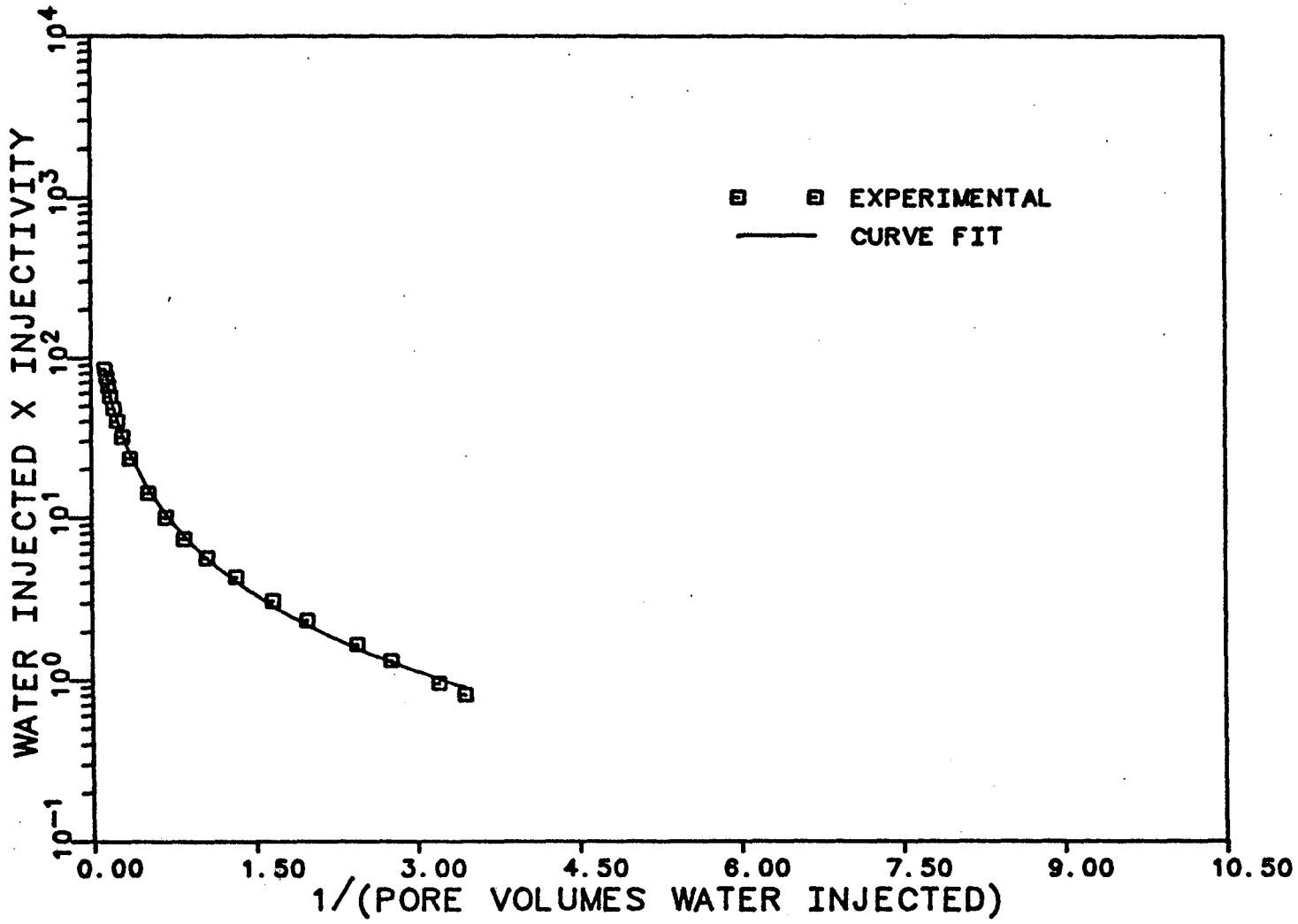

FIGURE E.7. A INJECTIVITY PLOT FOR RUN 7

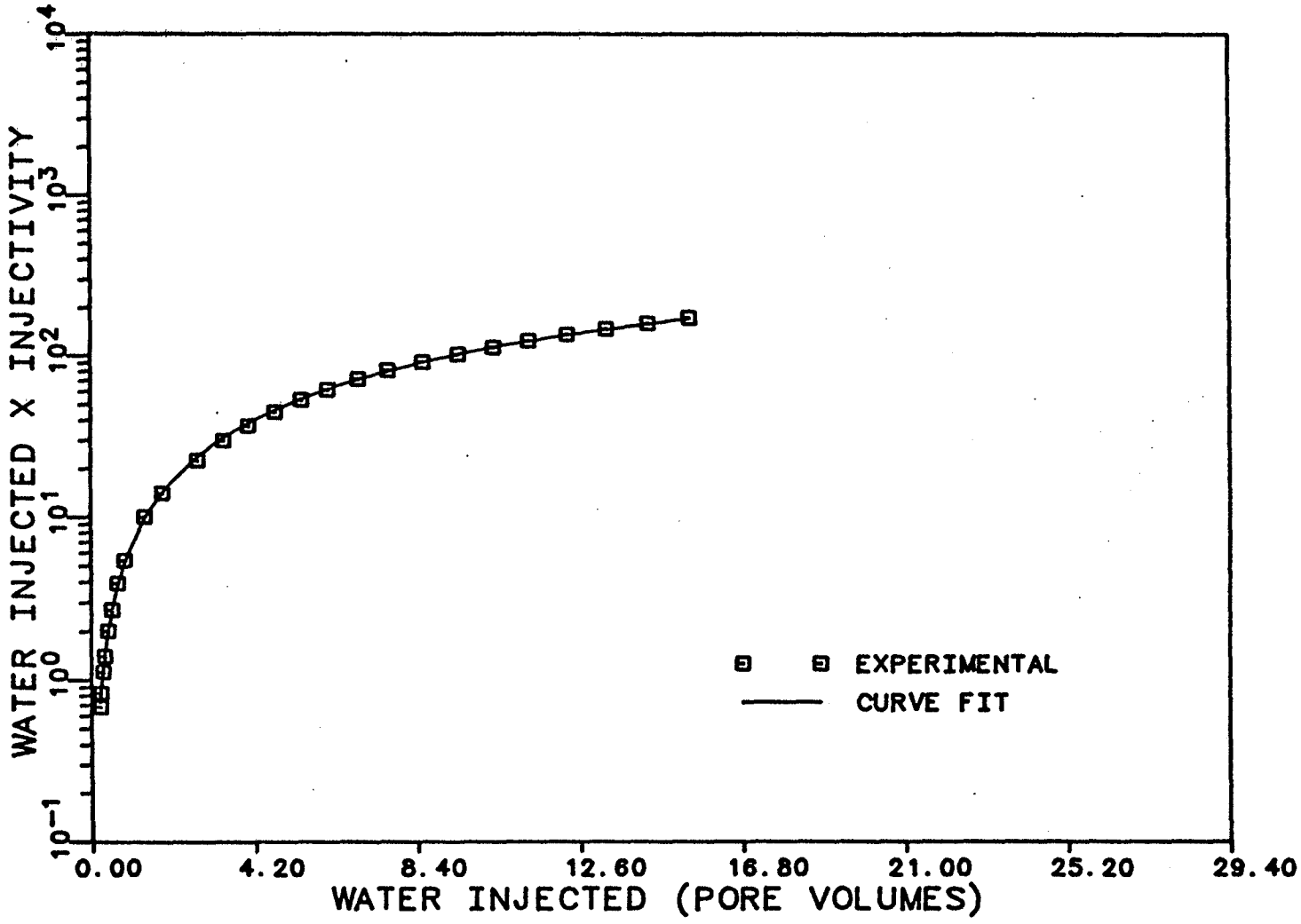

FIGURE E.7. B INJECTIVITY PLOT FOR RUN 7

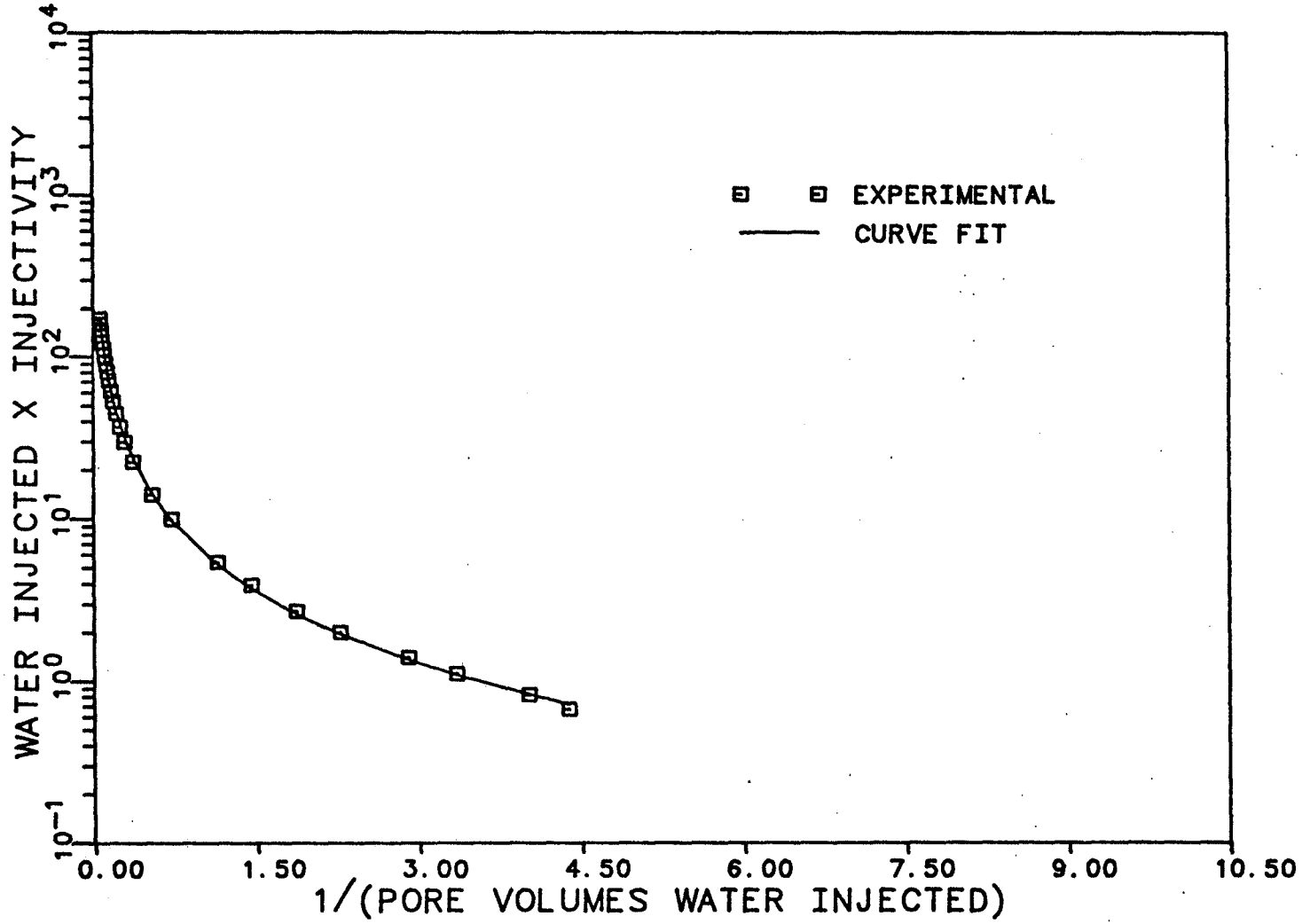

FIGURE E.8. A INJECTIVITY PLOT FOR RUN 8

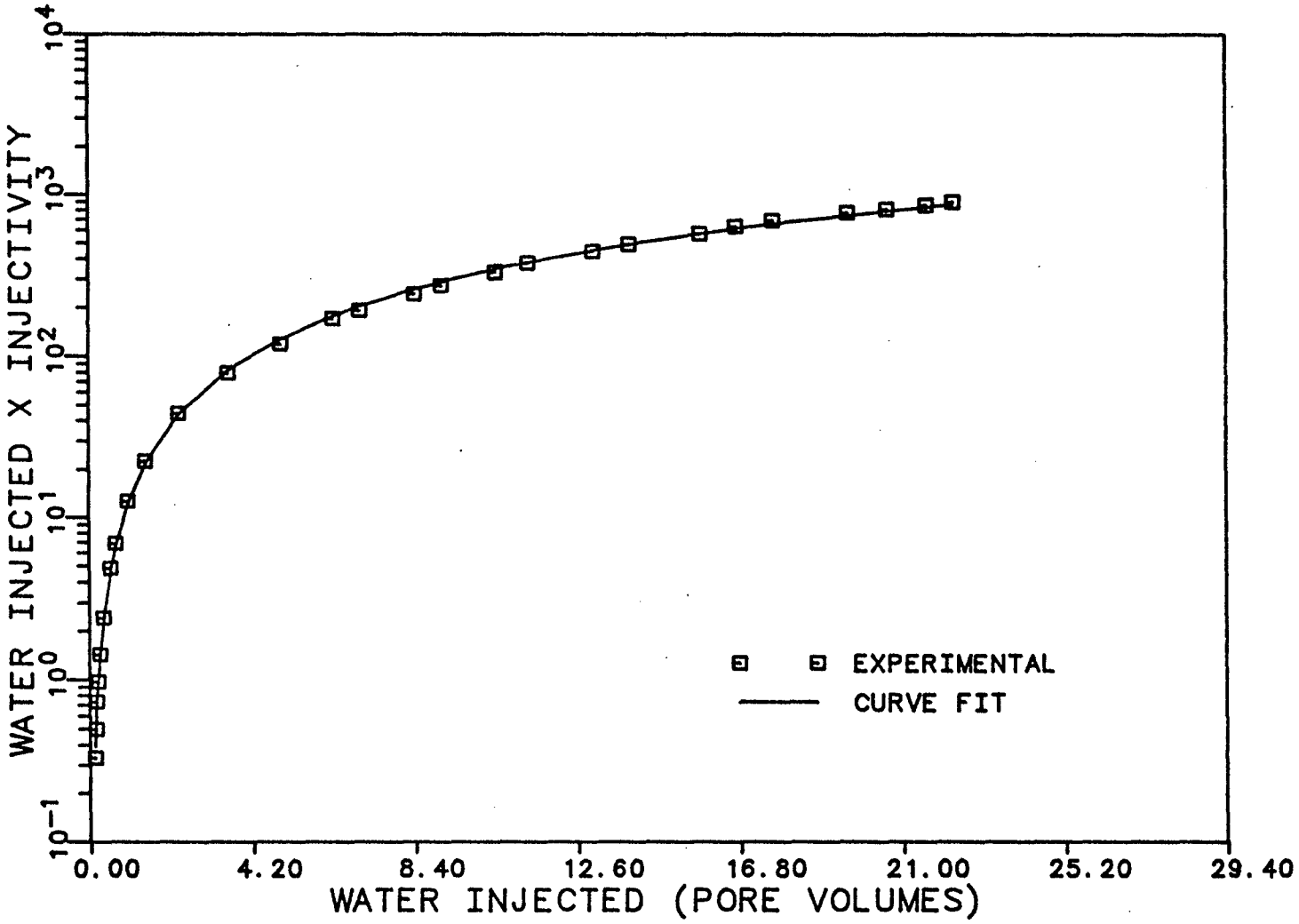

FIGURE E.8. B INJECTIVITY PLOT FOR RUN 8

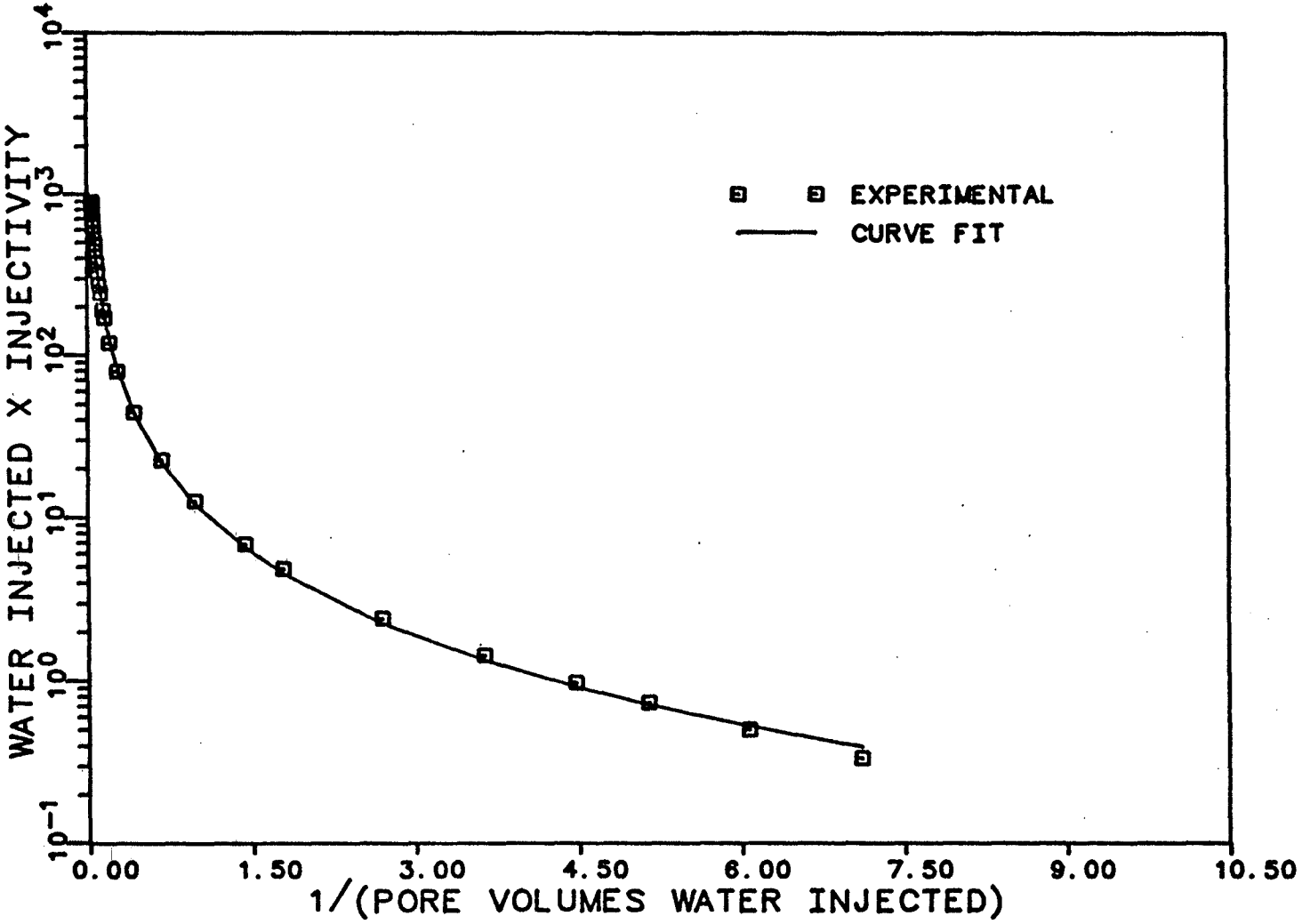

FIGURE E.9. A INJECTIVITY PLOT FOR RUN 9

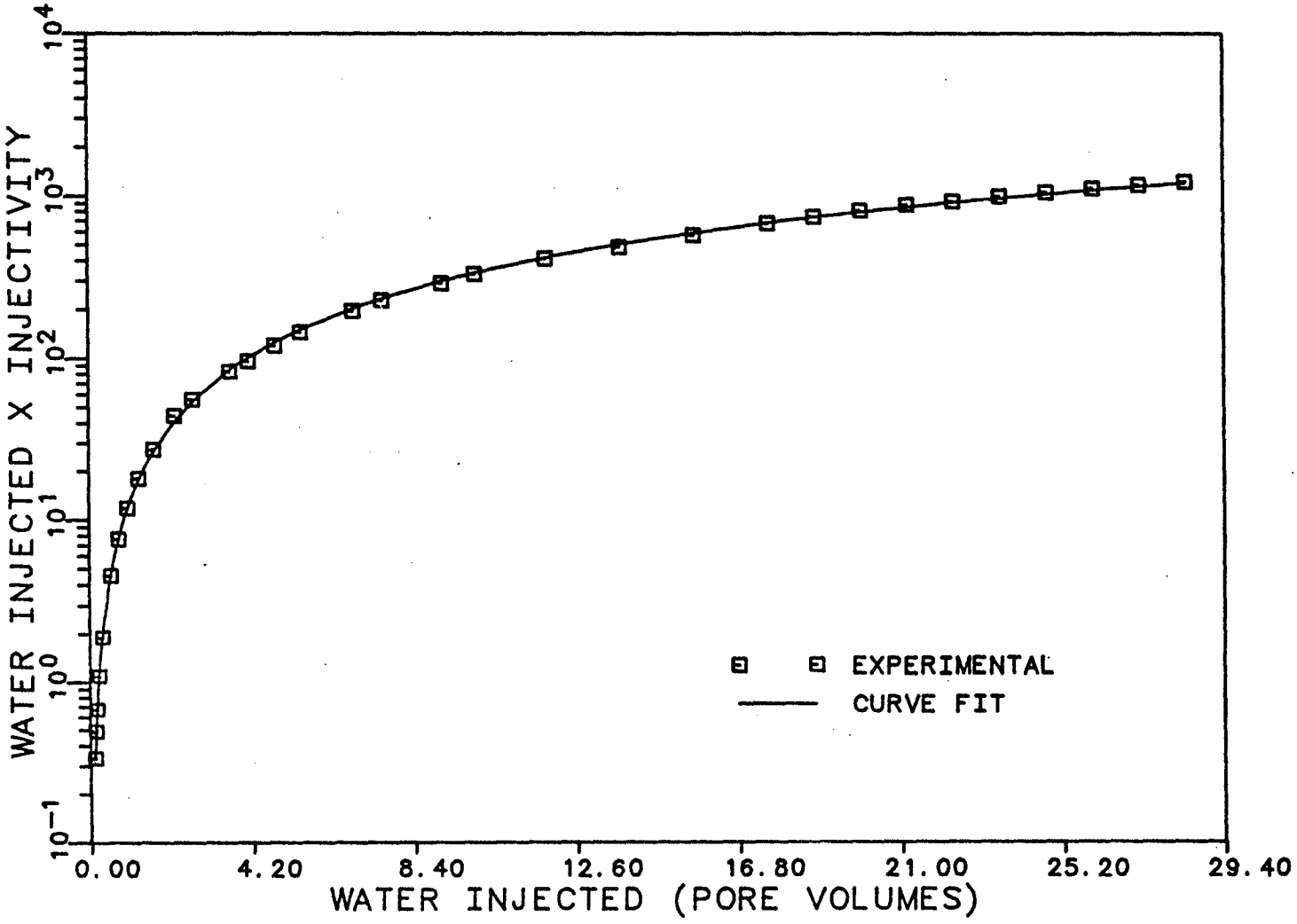

FIGURE E.9. B INJECTIVITY PLOT FOR RUN 9

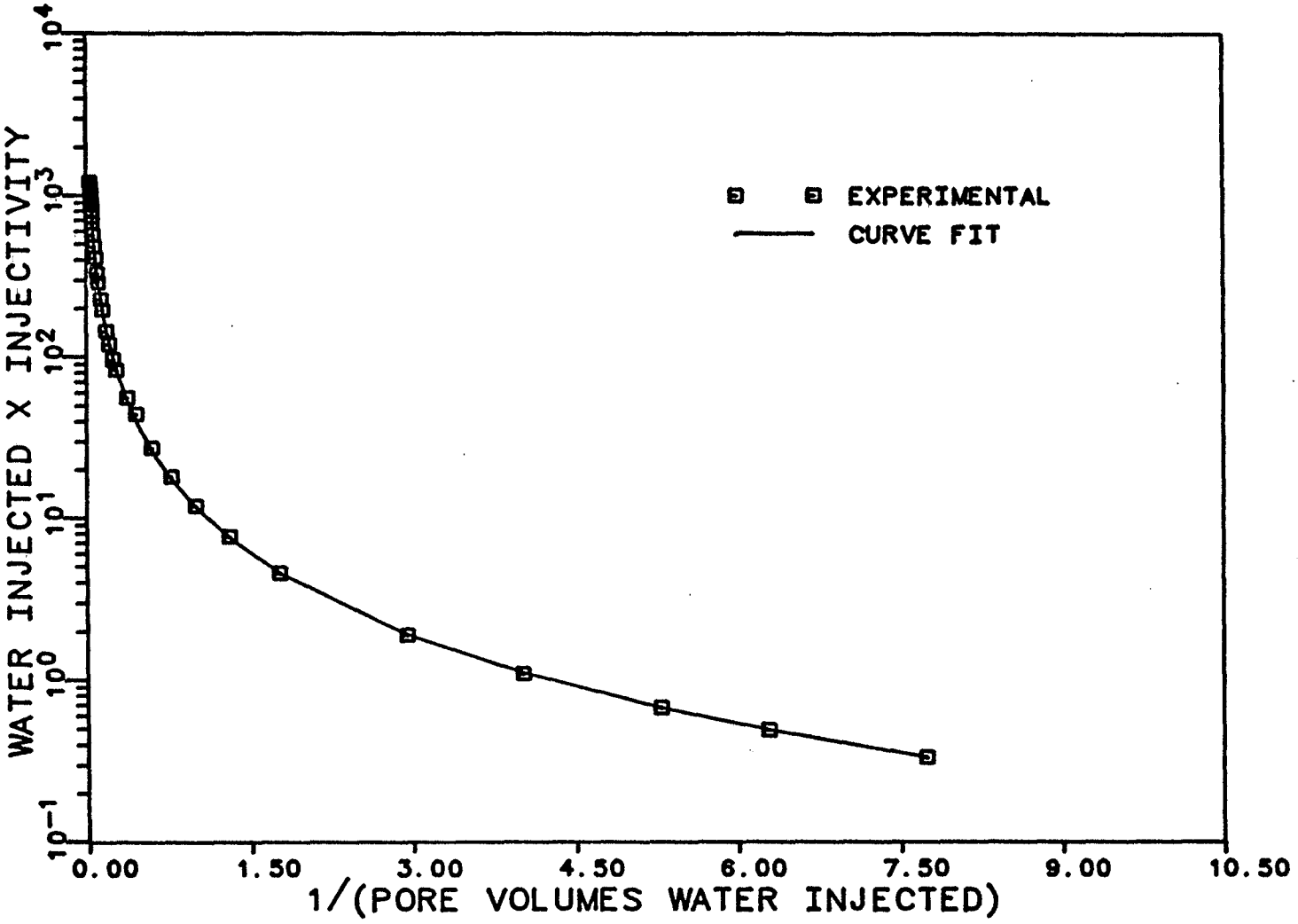

FIGURE E.10.A INJECTIVITY PLOT FOR RUN 10

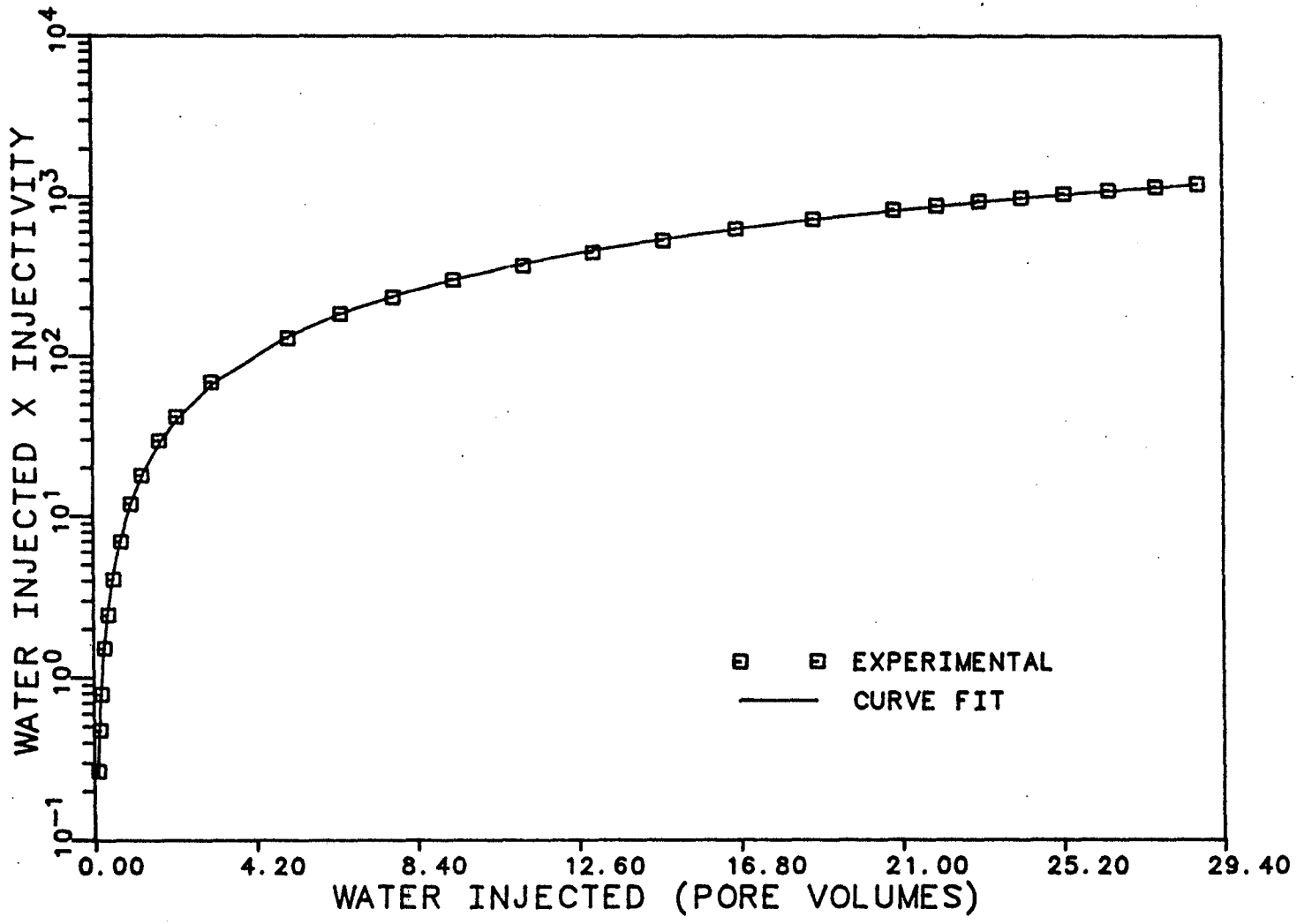

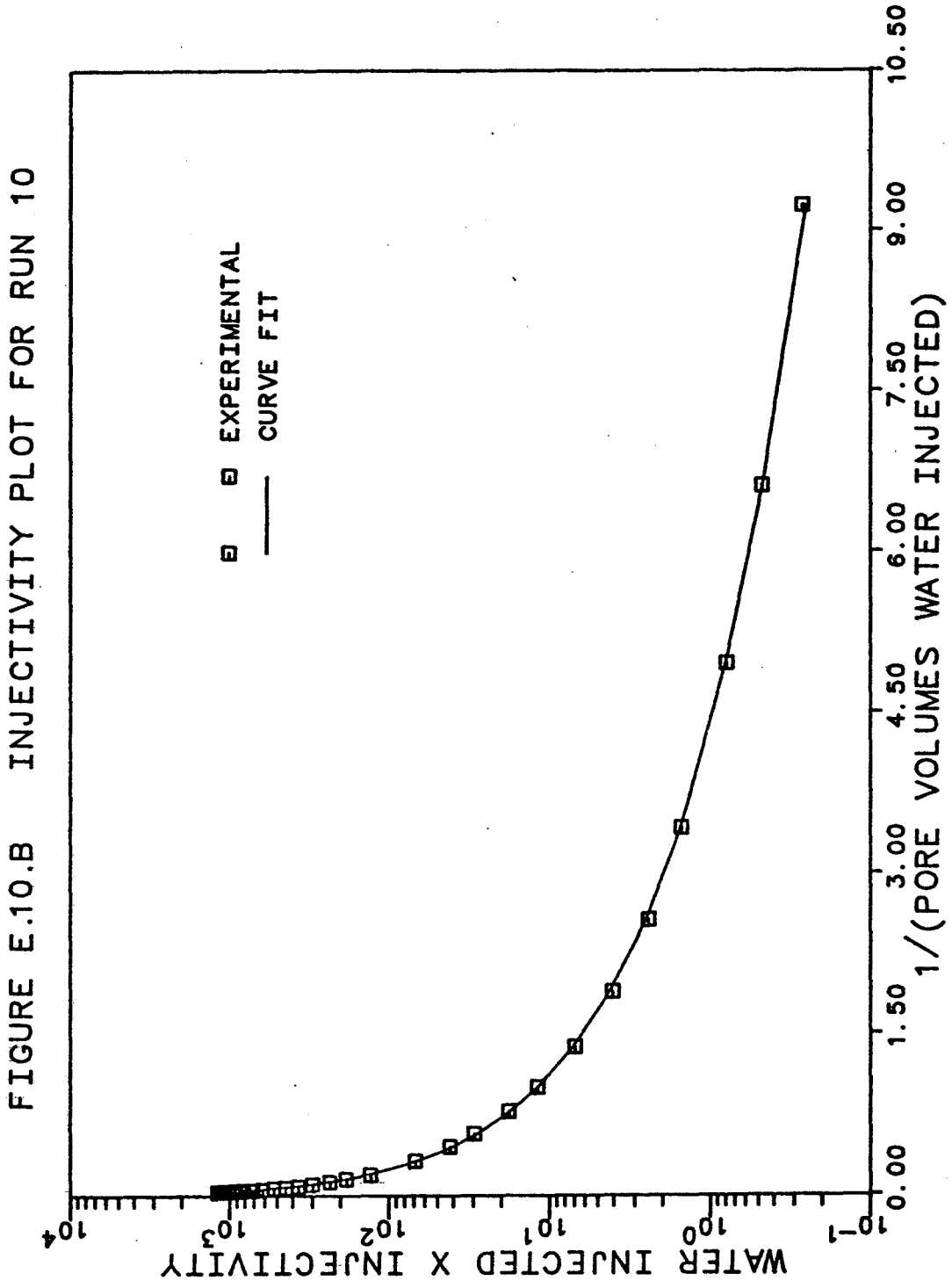
FIGURE E.10.B INJECTIVITY PLOT FOR RUN 10
EXPERIMENTAL
CURVE FIT
WATER INJECTED X INJECTIVITY
1/(PORE VOLUMES WATER INJECTED)
0.00
1.50
3.00
4.50
6.00
7.50
9.00
10.50

FIGURE E.11.A INJECTIVITY PLOT FOR RUN 11

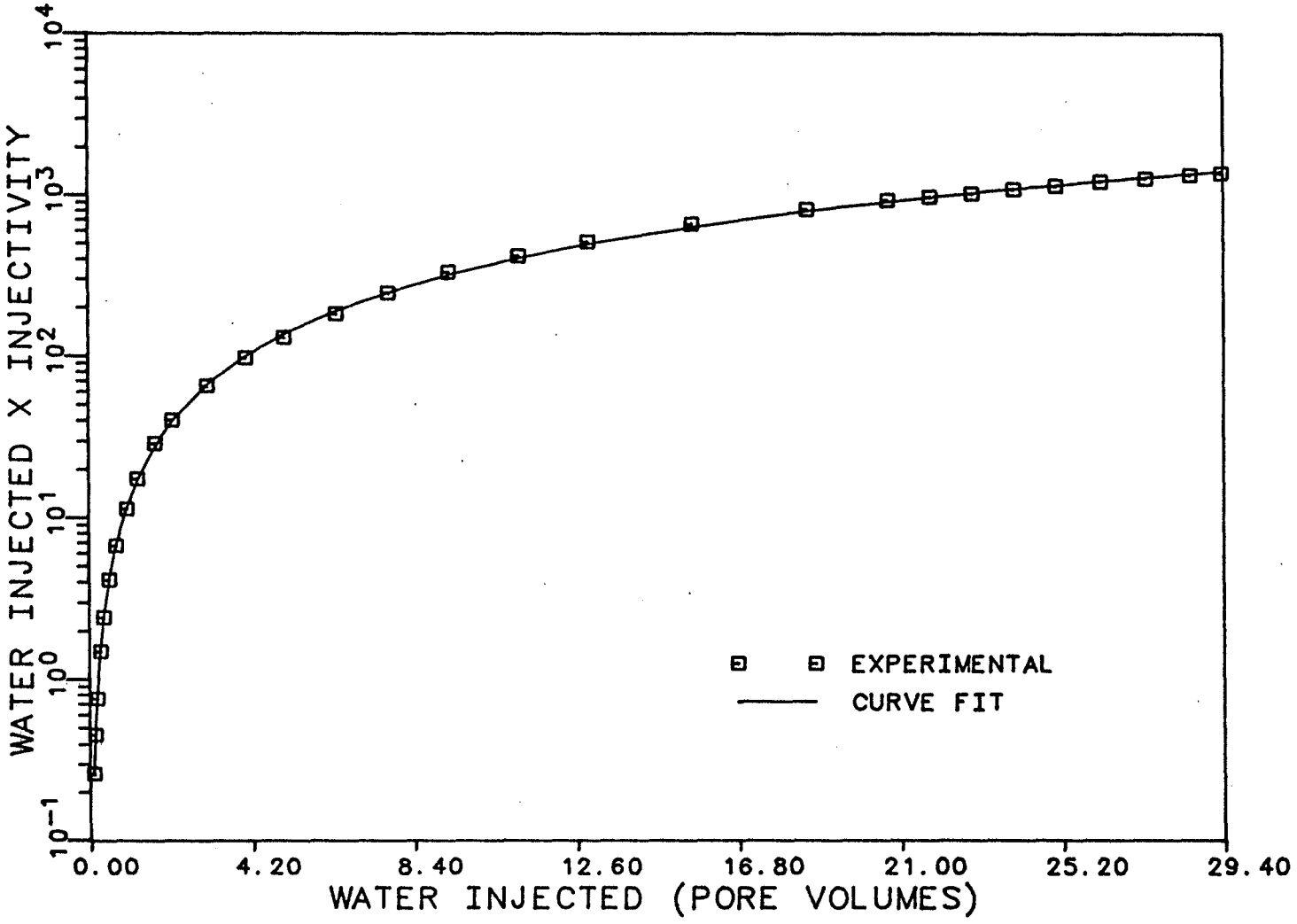

FIGURE E.11.B INJECTIVITY PLOT FOR RUN 11

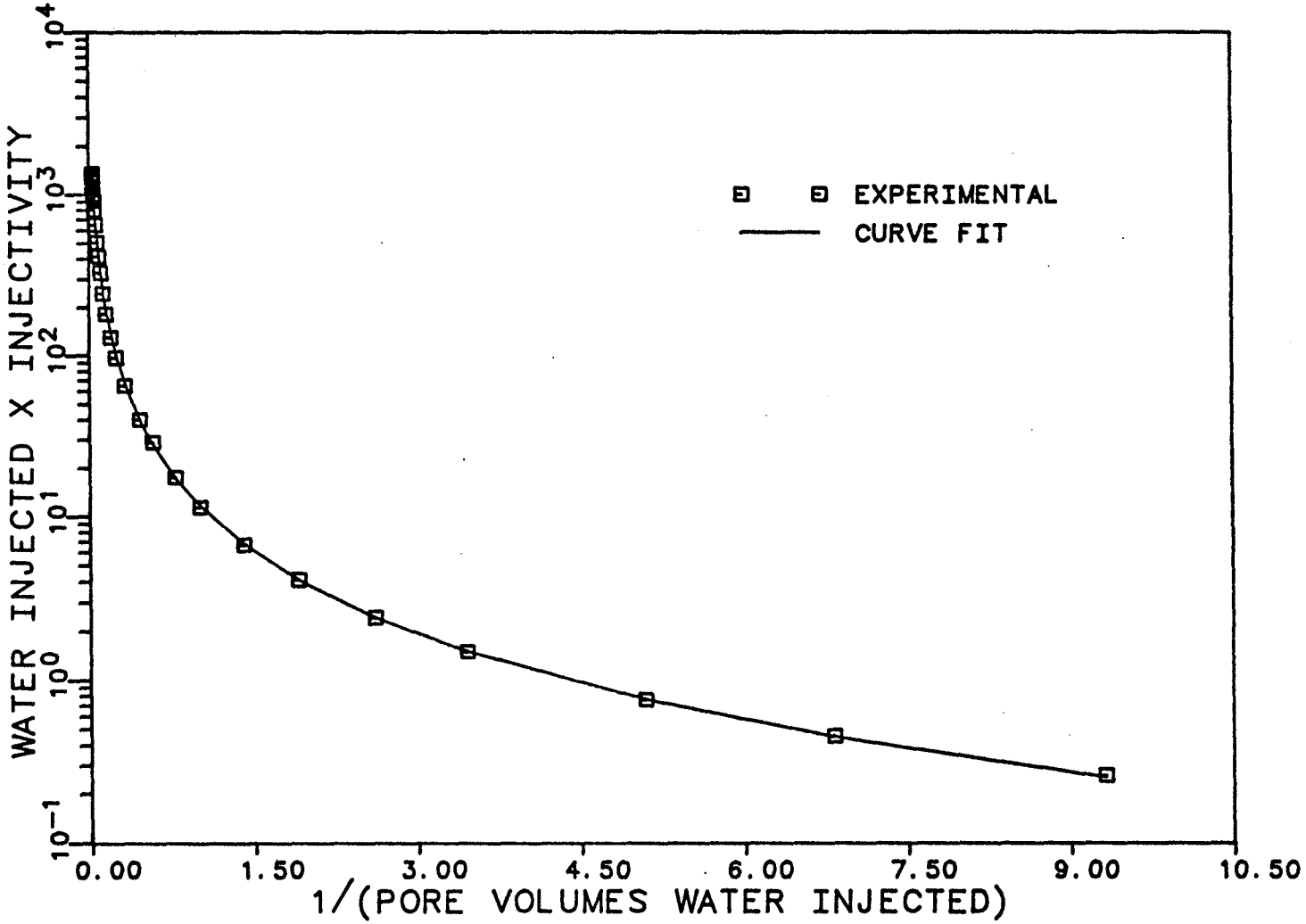

FIGURE E.12.A INJECTIVITY PLOT FOR RUN 12

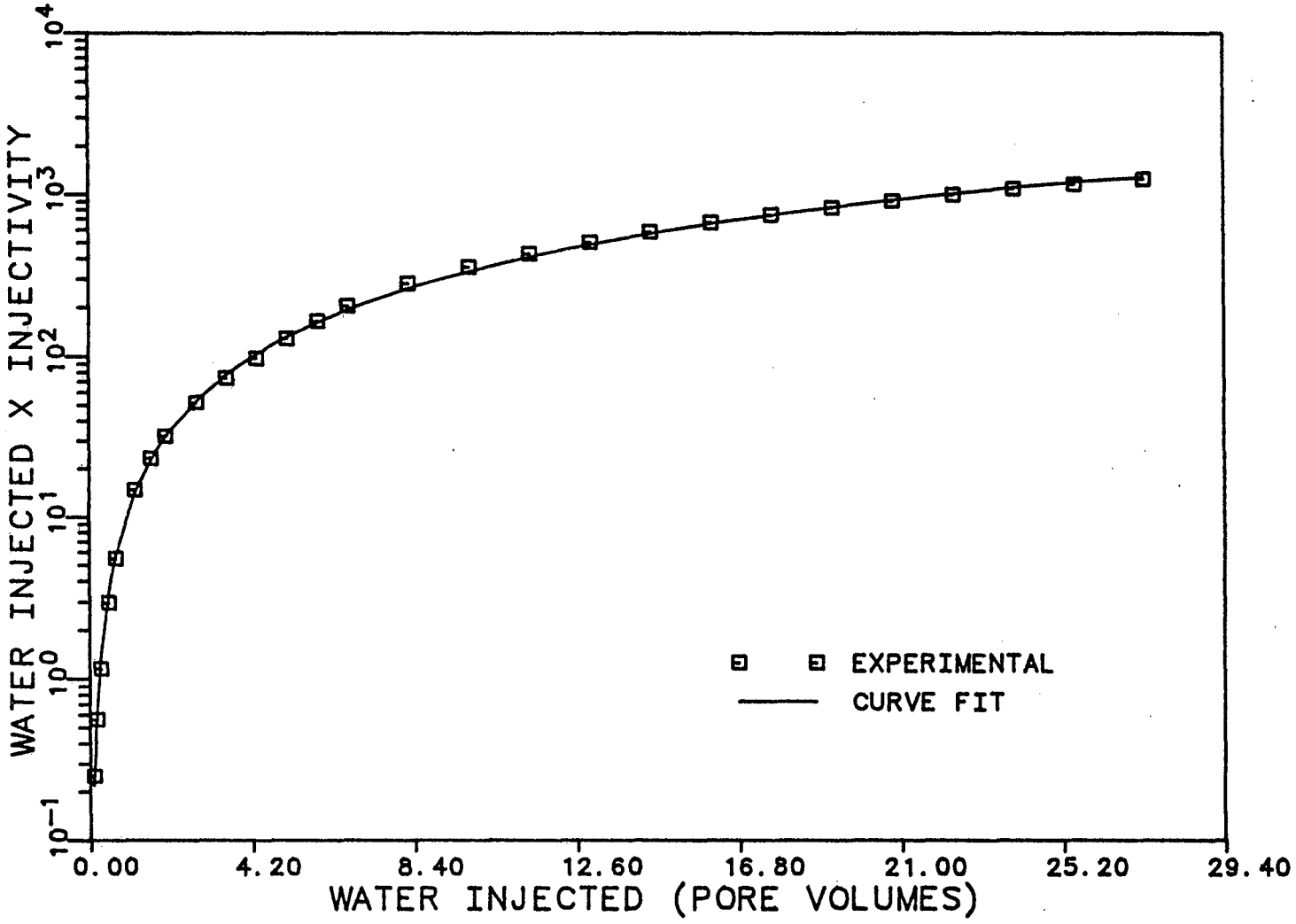

FIGURE E.12.B INJECTIVITY PLOT FOR RUN 12

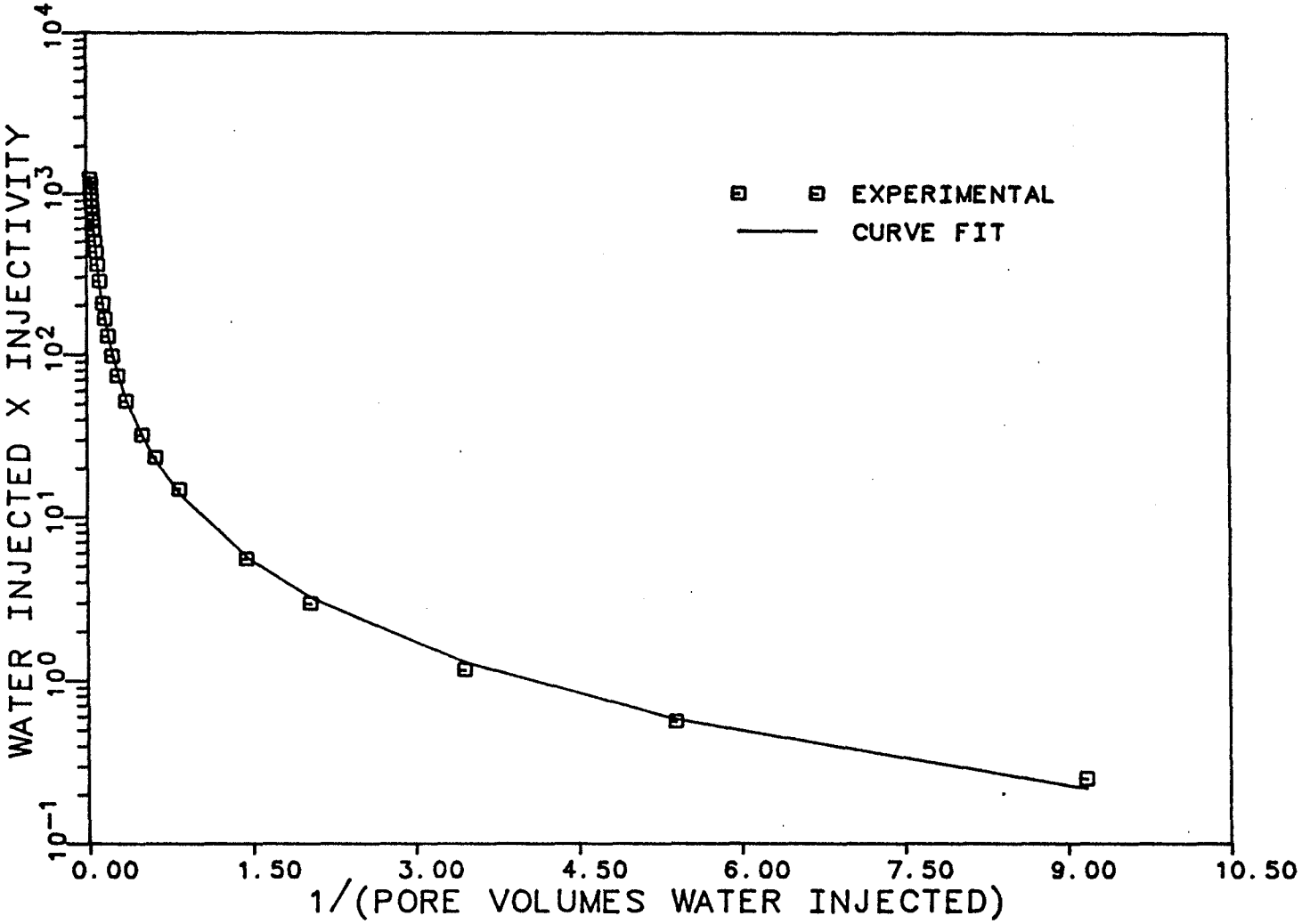

APPENDIX F

FIGURE F.1 STEADY STATE OIL-WATER RELATIVE PERMEABILITY CURVES FOR RUN NO. 1.

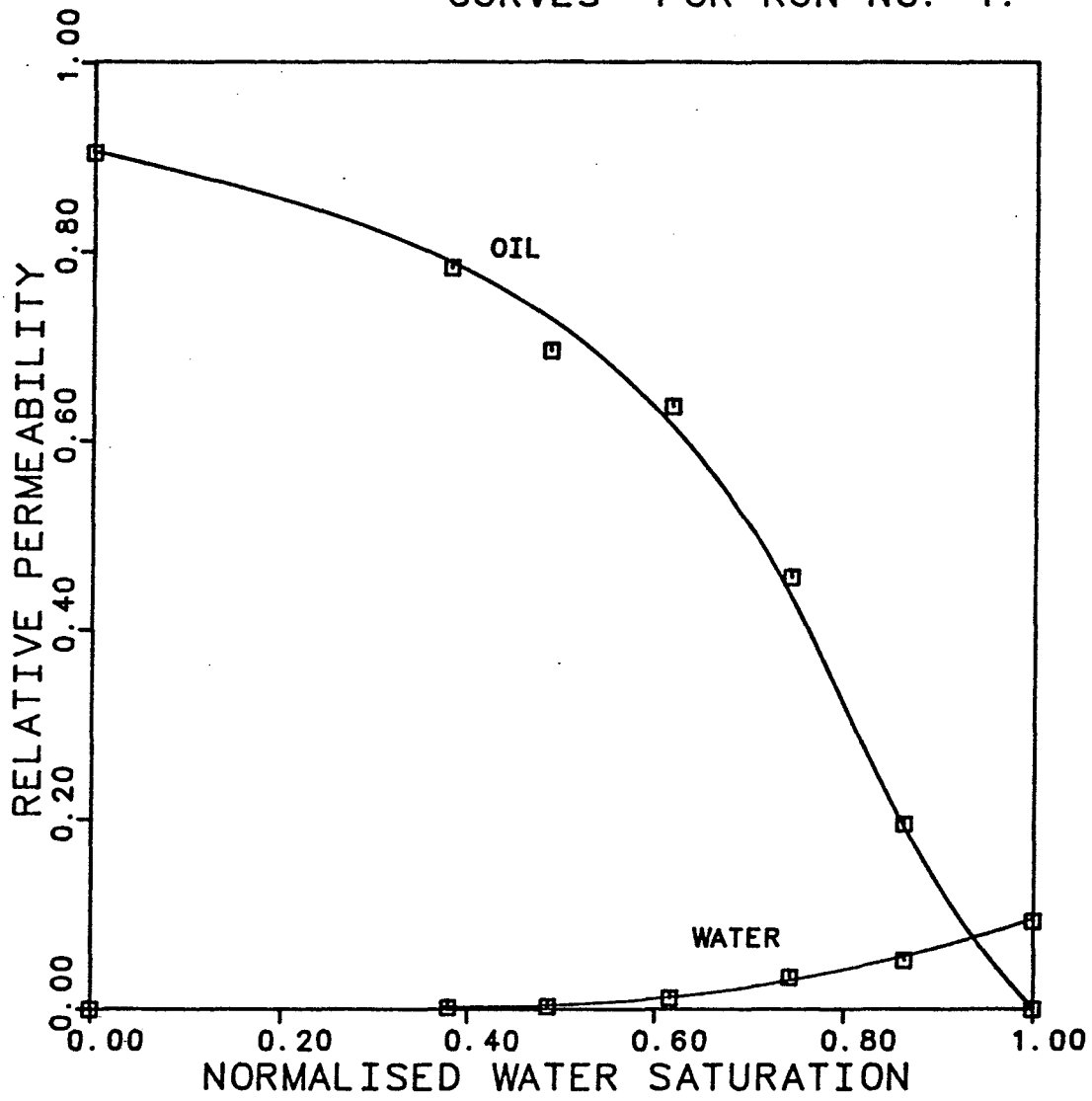

FIGURE F.2 DYNAMIC DISPLACEMENT OIL – WATER RELATIVE PERMEABILITY CURVES FOR RUN NO. 2.

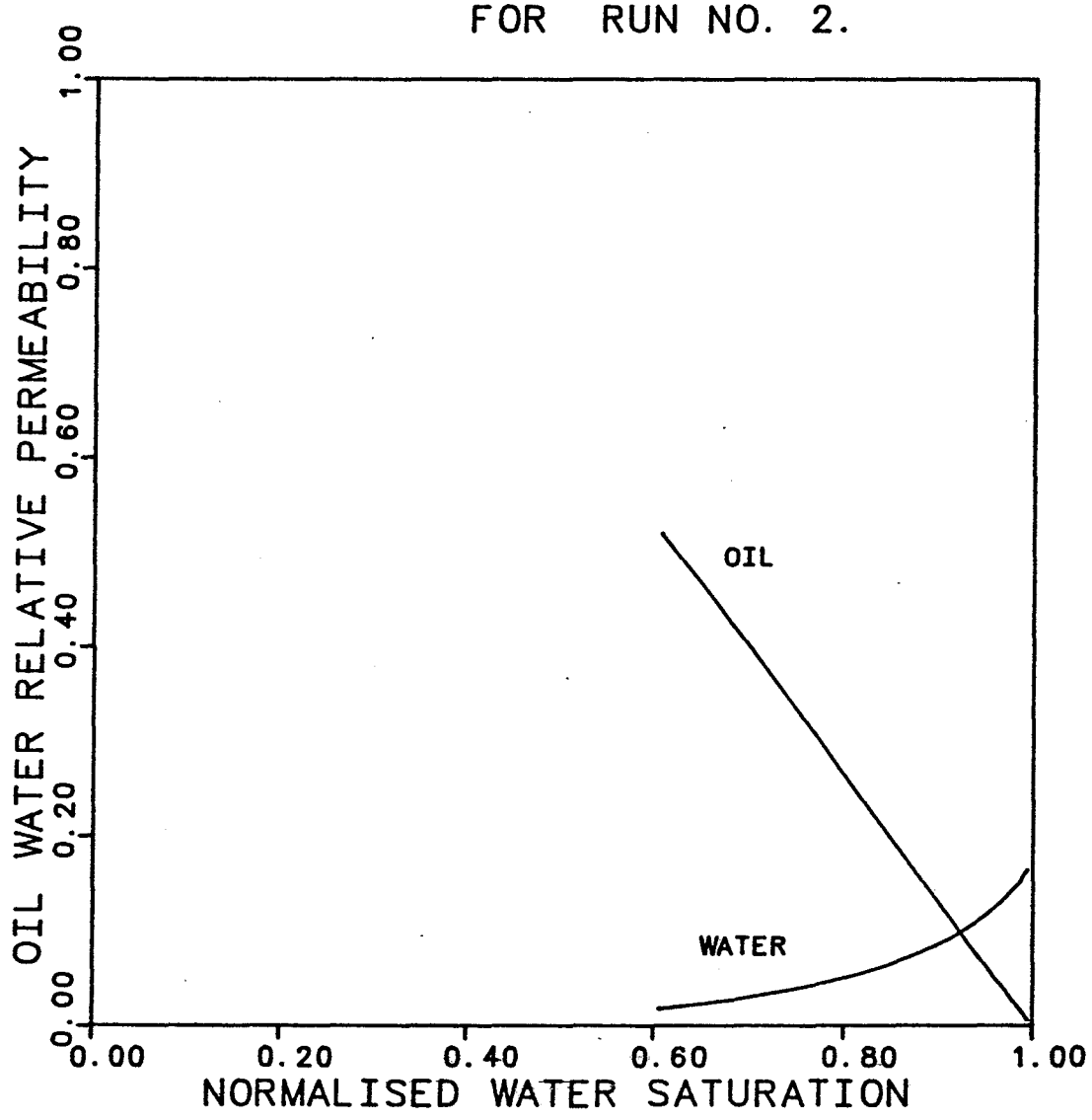

FIGURE F.3 DYNAMIC DISPLACEMENT OIL – WATER RELATIVE PERMEABILITY CURVES FOR RUN NO. 3.

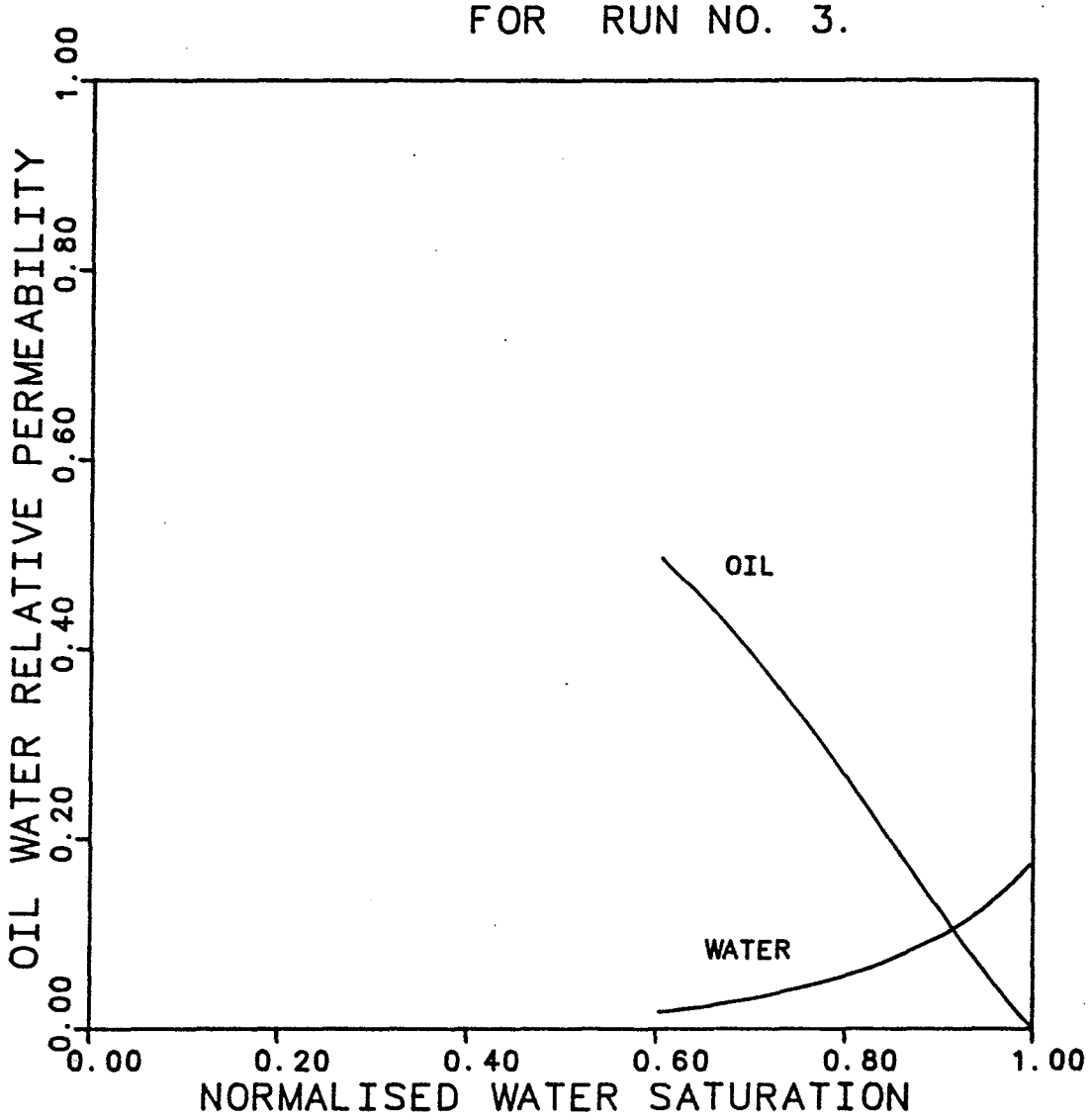

FIGURE F.4 DYNAMIC DISPLACEMENT OIL – WATER RELATIVE PERMEABILITY CURVES FOR RUN NO. 4.

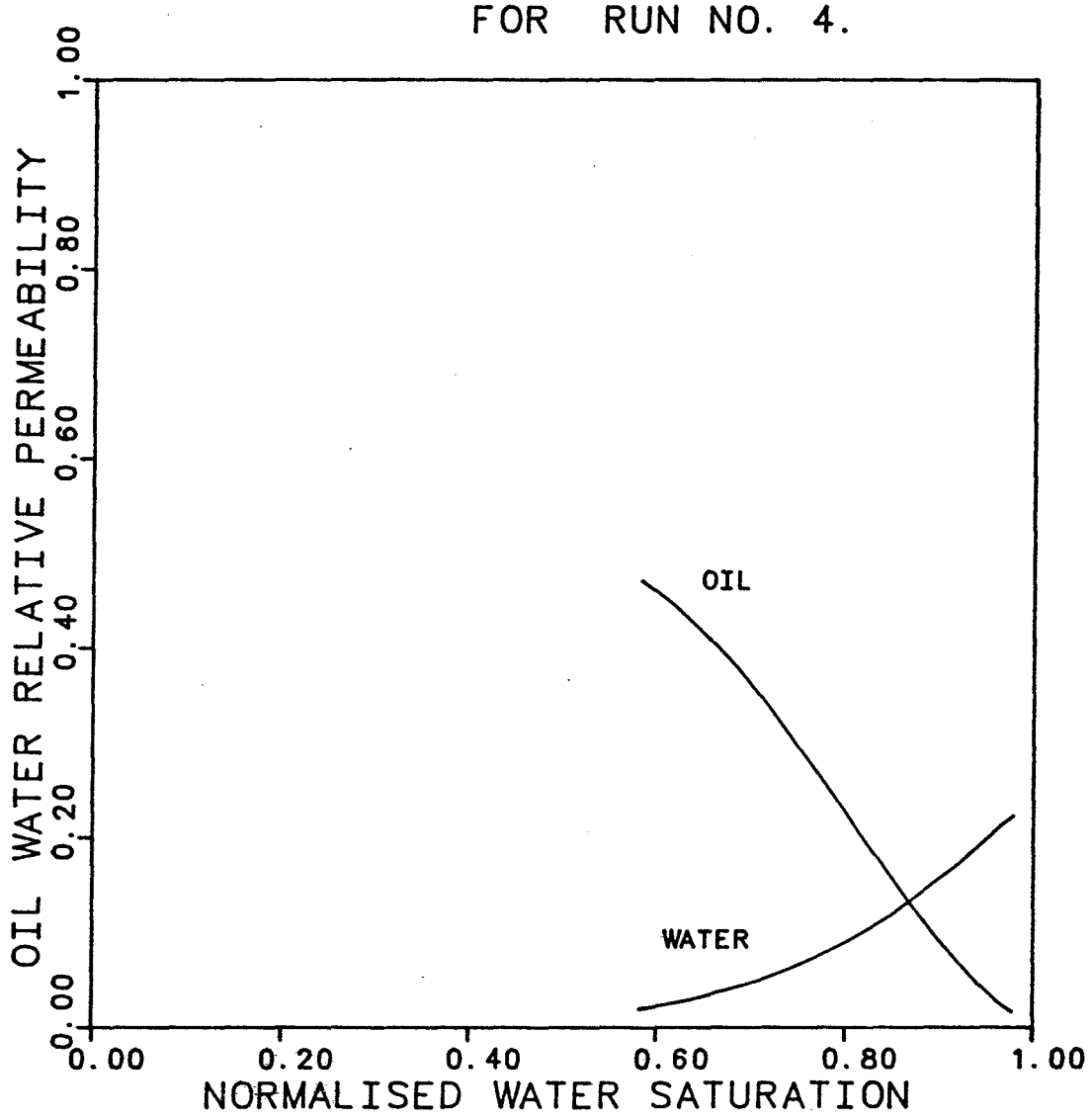

FIGURE F.5 DYNAMIC DISPLACEMENT OIL – WATER RELATIVE PERMEABILITY CURVES FOR RUN NO. 5.

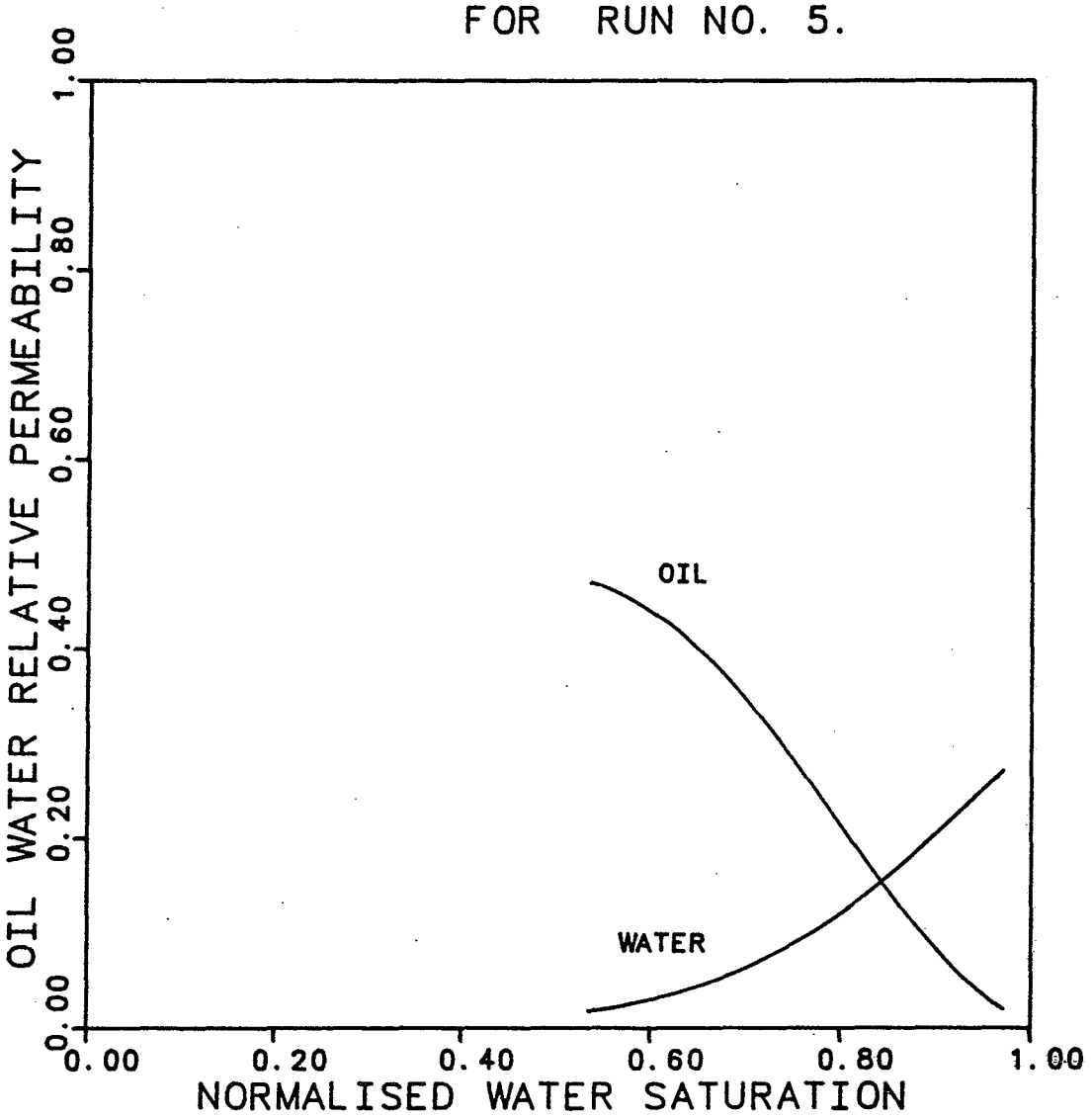

FIGURE F.6 DYNAMIC DISPLACEMENT OIL – WATER RELATIVE PERMEABILITY CURVES FOR RUN NO. 6.

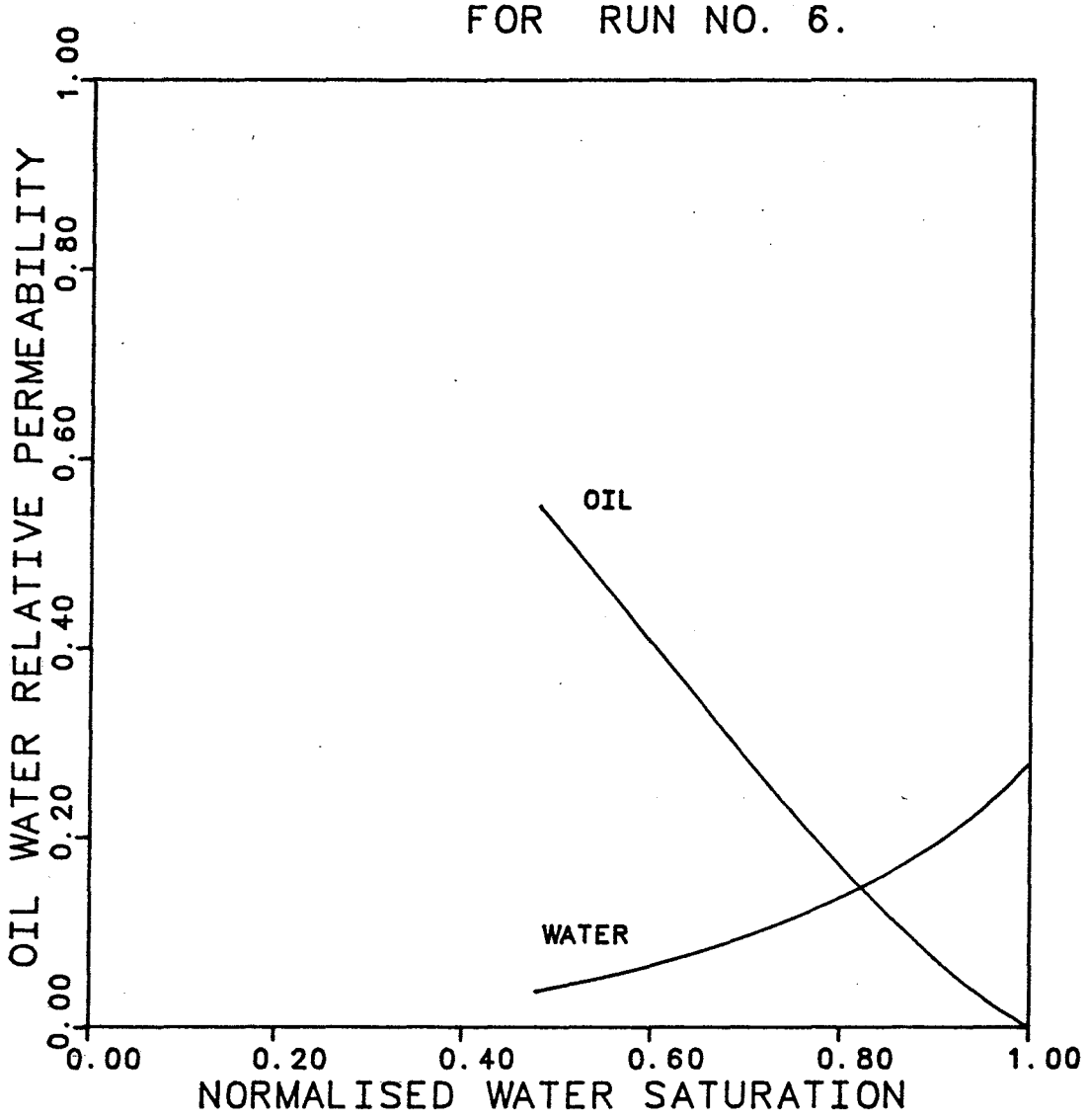

FIGURE F.7 DYNAMIC DISPLACEMENT OIL – WATER RELATIVE PERMEABILITY CURVES FOR RUN NO. 7.

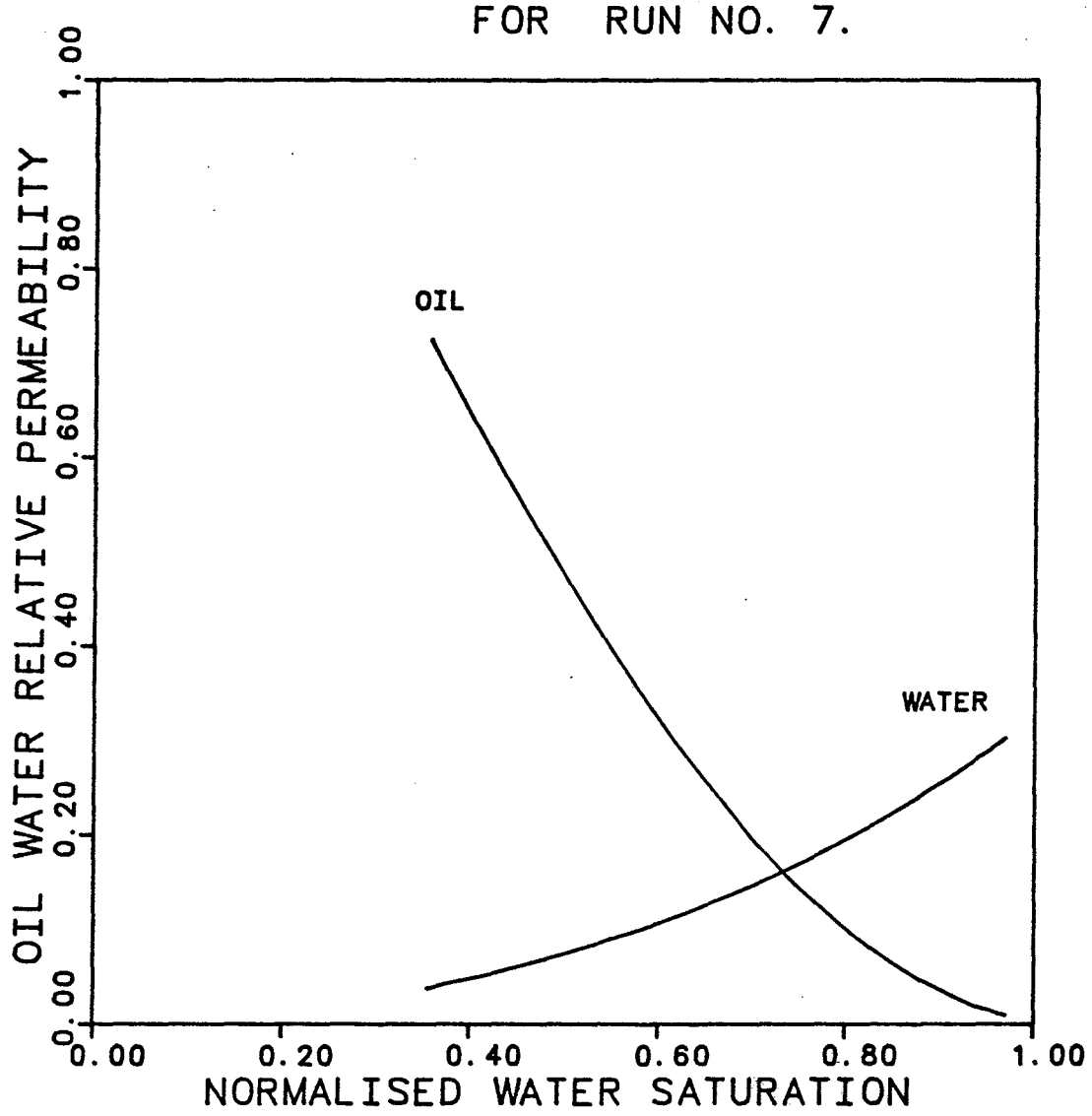

FIGURE F.8 DYNAMIC DISPLACEMENT OIL – WATER RELATIVE PERMEABILITY CURVES FOR RUN NO. 8.

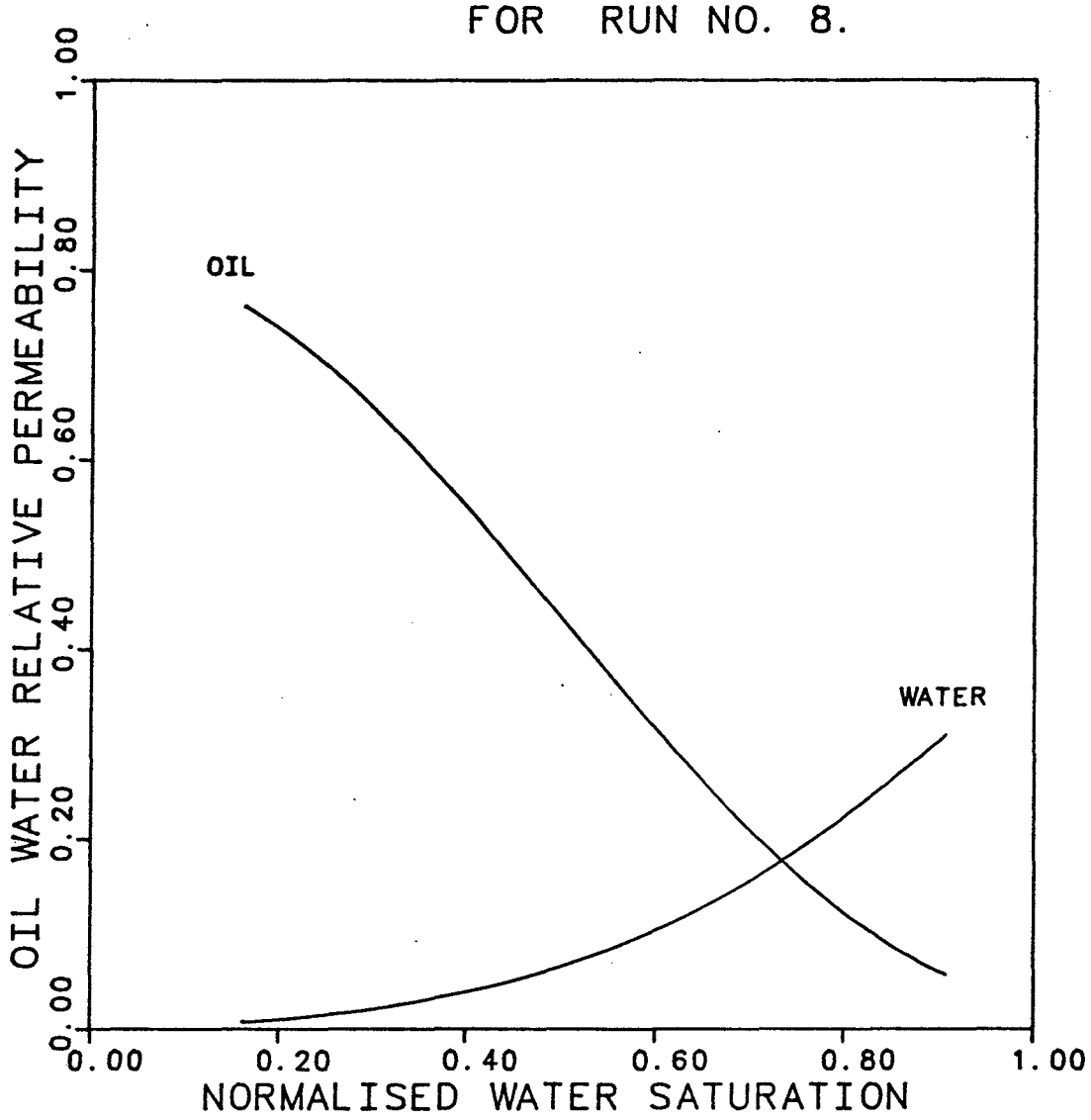

FIGURE F.9 DYNAMIC DISPLACEMENT OIL – WATER RELATIVE PERMEABILITY CURVES FOR RUN NO. 9.

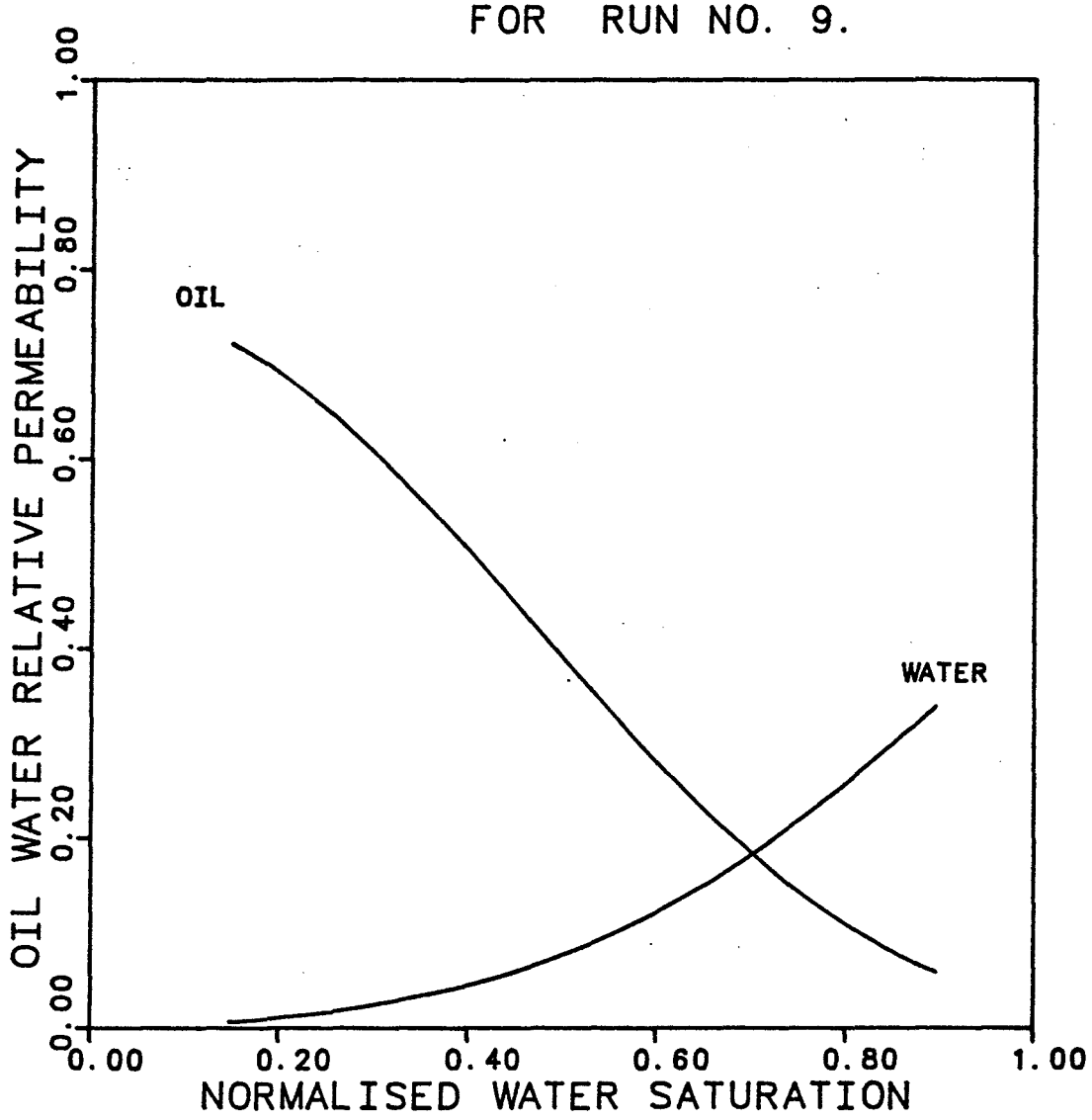

FIGURE F.10 DYNAMIC DISPLACEMENT OIL – WATER RELATIVE PERMEABILITY CURVES FOR RUN NO. 10.

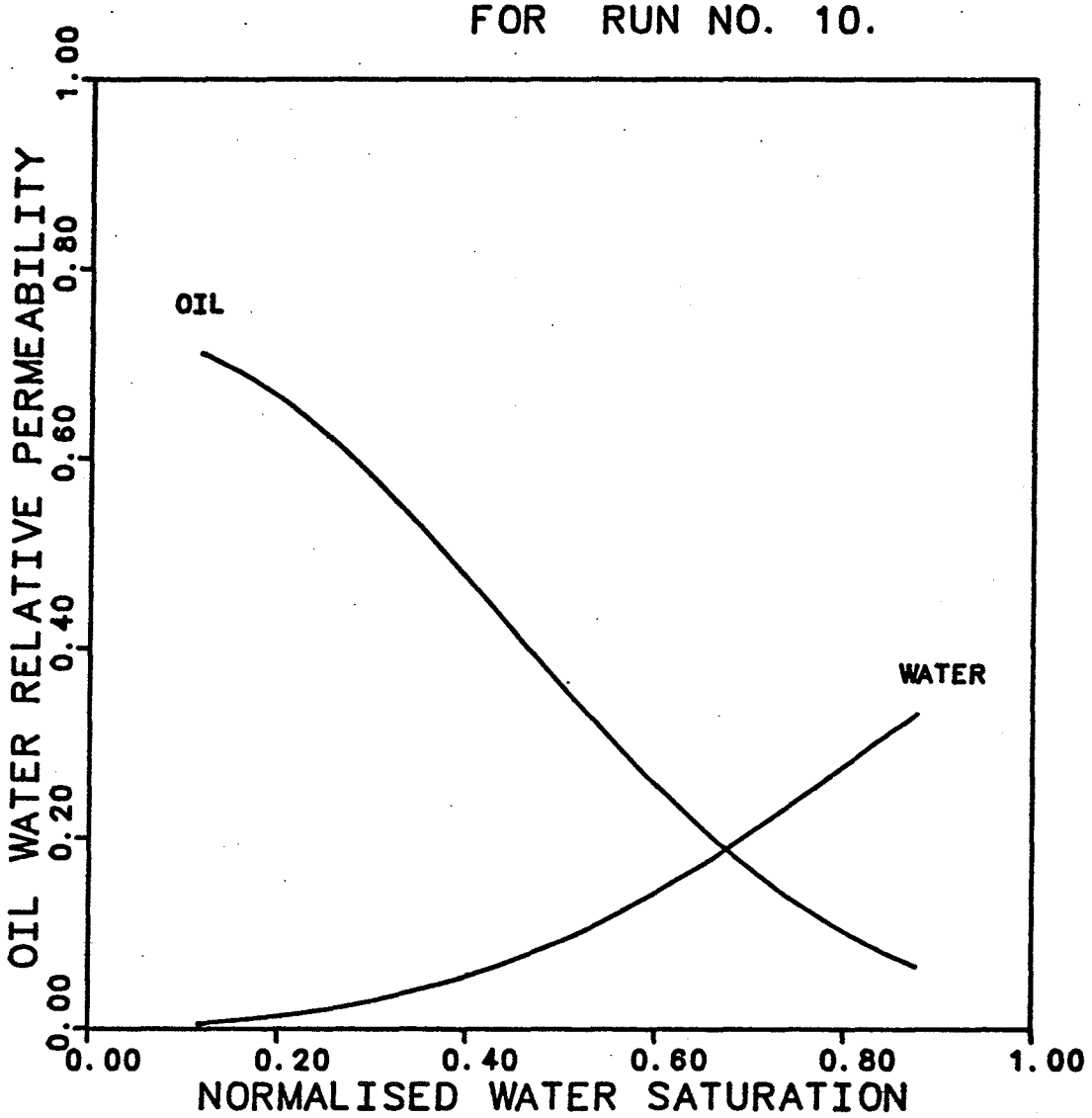

FIGURE F.11 DYNAMIC DISPLACEMENT OIL – WATER RELATIVE PERMEABILITY CURVES FOR RUN NO. 11.

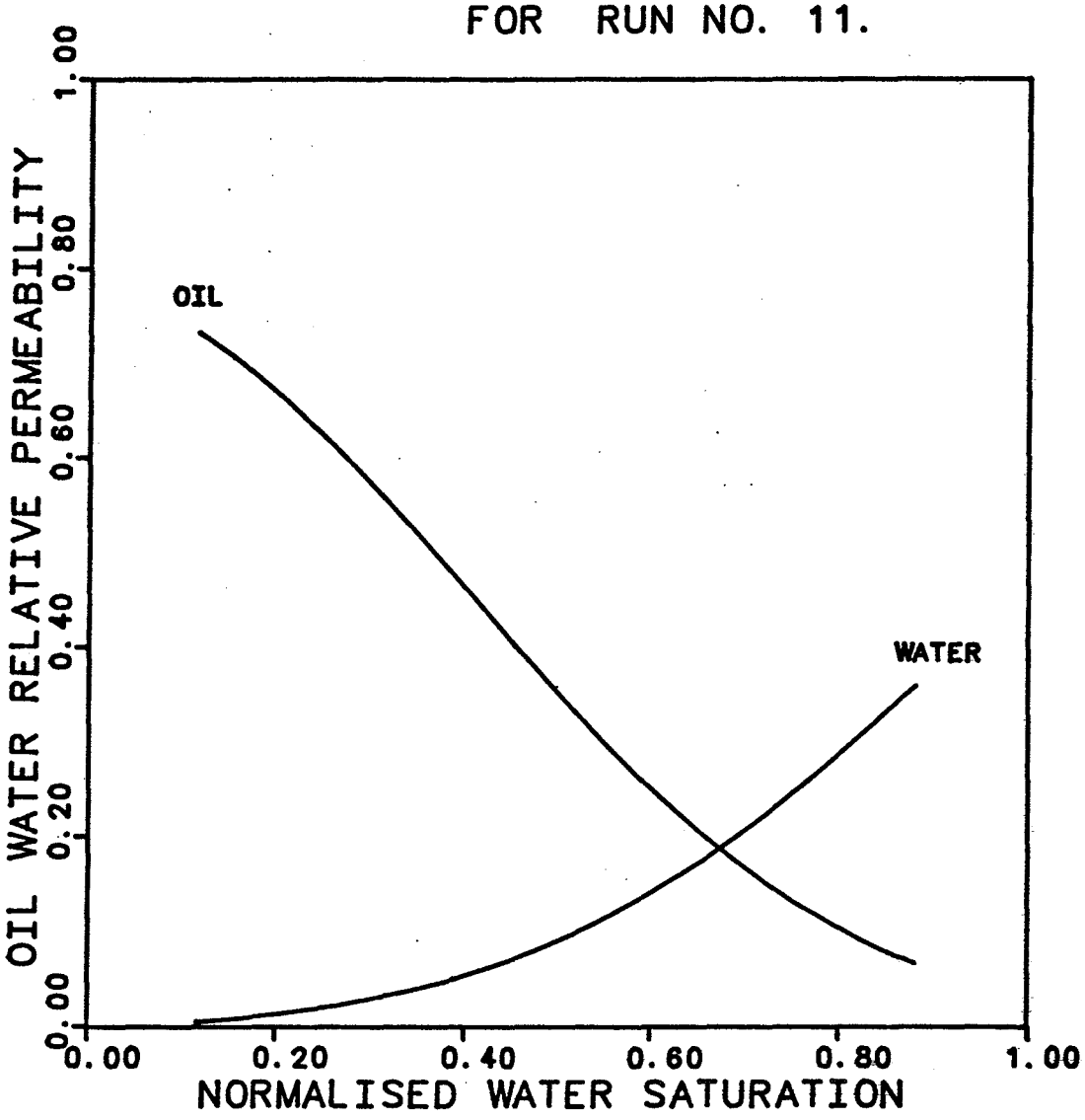

FIGURE F.12 DYNAMIC DISPLACEMENT OIL – WATER RELATIVE PERMEABILITY CURVES FOR RUN NO. 12.

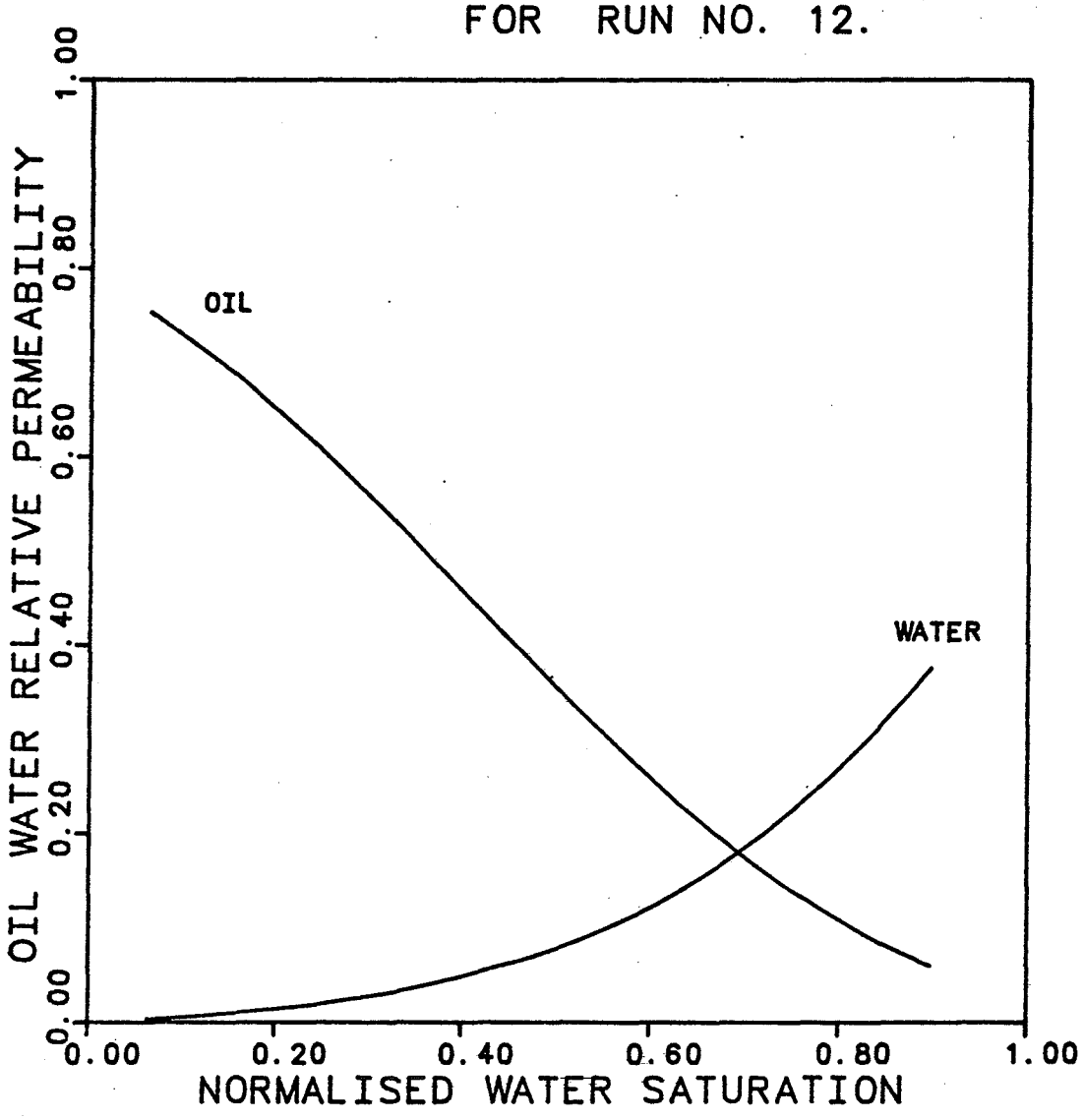

LIST OF REFERENCES

1. Welge, H. J.: "Displacement of Oil from Porous Media by Water or Gas", Trans., AIME (1949) 179, 133-145.

2. Johnson, E. F., Bossler, D. P. and Naumann, V. O.: "Calculation of Relative Permeability from Displacement Experiments", Trans., AIME (1959) 216, 370-372.

3. Buckley, S. E. and Leverett, M. C.: "Mechanism of Fluid Displacement in Sands", Trans., AIME (1942) 146, 107-116.

4. Perkins, F. M.: "An Investigation of the Role of Capillary Forces in Laboratory Waterfloods", Trans., AIME (1957) 210, 409-411.

5. Fayers, F. J. and Sheldon, J. W.: "The Effect of Capillary Pressure and Gravity on Two Phase Fluid Flow in a Porous Medium", Trans., AIME (1959) 216, 147-155.

6. Osoba, J. S., Richardson, J. G., Kerver, J. K., Hafford, J. A. and Blair, P. M.: "Laboratory Measurements of Relative Permeability", Trans., AIME (1951) 192, 47-56.

7. Jones, S. C. and Roszelle, W. O.: "Graphical Techniques for Determining Relative Permeability from Displacement Experiments", J. Pet. Tech. (May 1978), 807-817.

8. Miller, M. A. and Ramey, H. J., Jr.: "Effect of Temperature on Oil/Water Relative Permeabilities of Unconsolidated and Consolidated Sands", paper SPE 12116, presented at the SPE 58th Annual Technical Conference and Exhibition, San Fransisco, Oct. 5-8, 1983.

9. Engelberts, W. F. and Klinkenberg, L. J.: "Laboratory Experiments on the Displacement of Oil by Water from Packs of Granular Materials", Proc. Third World Petroleum Congress, Sec. II, (1951), 544-554.

10. van Meurs, P.: "The Use of Transparent Three-Dimensional Models for Studying the Mechanism of Flow Pro-

cesses in Oil Reservoirs", Trans., AIME (1957) 210, 295-301.

11. van Meurs, P. and van der Poel, C.: "A Theoretical Description of Water-Drive Processes Involving Viscous Fingering", Trans., AIME (1958) 213, 103-112.

12. Chouke, R. L., van Meurs, P. and van der Poel, C.: "The Instability of Slow, Immiscible, Viscous Liquid-Liquid Displacements in Permeable Media", Trans., AIME (1959) 216, 188-194.

13. Peters, E. J. and Flock, D. L.: "The Onset of Instability during Two Phase Immiscible Displacement in Porous Media", Soc. Pet. Eng. J. (April 1981), 249-258.

14. Jones-Parra, J., Stahl, C. D. and Calhoun, J. C., Jr.: "A Theoretical and Experimental Study of Constant Rate Displacements in Water-Wet Systems", Prod. Monthly (Jan. 1954), 18-26.

15. Caudle, B. H., Slobod, R. L. and Brownscombe, E. R.: "Further Developments in the Laboratory Determination

of Relative Permeability", Trans., AIME (1951) 192, 83-88.

16. Sandberg, C. R., Gourney, L. S. and Sippel, R. F.: "The Effect of Fluid-Flow Rate and Viscosity on Laboratory Determinations of Oil-Water Relative Permeabilities", Trans., AIME (1958) 213, 36-43.

17. Rapoport, L. A. and Leas, W. J.: "Properties of Linear Waterfloods", Trans., AIME (1953) 198, 139-148.

18. Kyte, J. R. and Rapoport, L. A.: "Linear Waterflood Behavior and End Effects in Water-Wet Porous Media", Trans., AIME (1958) 213, 423-426.

19. Calhoun, J. C., Jr. and LaRue, J. W.: "The Effect of Velocity in Waterflooding", Prod. Monthly (April 1951), 20-29.

20. Fulcher, R. A., Jr., Ertekin, T. and Stahl, C. D.: "The Effect of the Capillary Number and Its Constituents on Two-Phase Relative Permeability Curves", paper SPE 12170, presented at the SPE 58th Annual Technical Conference and Exhibition, San Fransisco, Oct. 5-8, 1983.

21. Sufi, A. S., Ramey, H. J., Jr. and Brigham, W. E.: "Temperature Effects on Relative Permeabilities of Oil-Water Systems", paper SPE 11071, presented at the SPE 57th Annual Technical Conference and Exhibition, New Orleans, Sept. 26-29, 1982.

22. Peters, E. J.: "Stability Theory and Viscous Fingering in Porous Media", Ph.D. Dissertation, University of Alberta, 1979.

23. Bentsen, R. G. and Saeedi, J.: "Liquid-Liquid Immiscible Displacement in Unconsolidated Porous Media", J. Can. Pet. Tech. (Jan.-Mar. 1981), 93-103.

24. Levine, J. S.: "Displacement Experiments in a Consolidated Porous System", Trans., AIME (1954) 201, 57-66.

25. Odeh, A. S.: "Effect of Viscosity Ratio on Relative Permeability", Trans., AIME (1959) 216, 346-353.

26. Baker, P. E.: "Discussion of 'Effect of Viscosity Ratio on Relative Permeability'", Trans., AIME (1960) 219, 404-405.

27. Downie, J. and Crane, F. E.: "Effect of Viscosity on Relative Permeability", Soc. Pet. Eng. J. (June 1961), 59-60.

28. Lefebvre du Prey, E. J.: "Factors Effecting Liquid-Liquid Relative Permeabilities of a Consolidated Porous Medium", Soc. Pet. Eng. J. (Feb. 1973), 39-47.

29. Amaefule, J. O. and Handy, L. L.: "The Effect of Interfacial Tensions on Relative Oil-Water Permeabilities of Consolidated Porous Media", paper SPE/DOE 9783, presented at the SPE/DOE Second Joint Symposium on Enhanced Oil Recovery, Tulsa, OK., April 2-5, 1981.

30. Owens, W. W. and Archer, D. L.: "The Effect of Rock Wettability on Oil-Water Relative Permeability Relationships", J. Pet. Tech. (July 1971), 873-878.

31. Broman, J. A.: "An Experimental Verification of the Onset of Instability in Rectangular Porous Media", M.S. Thesis, University of Texas at Austin, 1984.

BIBLIOGRAPHY

1. Abrams, A.: "The Influence of Fluid Viscosity, Interfacial Tension, and Flow Velocity on Residual Oil Saturation Left by Waterflood", Soc. Pet. Eng. J. (Oct. 1975), 437-447.

2. Amyx, J. W., Bass, D. M., Jr. and Whiting, R. L.: "Petroleum Reservoir Engineering - Physical Properties", McGraw Hill Book Company, New York City, 1960.

3. Bardon, C. and Longeron, D. G.: "Influence of Very Low Interfacial Tensions on Relative Permeability", Soc. Pet. Eng. J. (Oct. 1980), 391-401.

4. Batycky, J. P., McCaffery, F. G., Hodgins, P. K. and Fisher, D. B.: "Interpreting Relative Permeability and Wettability from Unsteady-State Displacement Measurements", Soc. Pet. Eng. J. (June 1981), 296-308.

5. Benham, A. L. and Olson, R. W.: "A Model Study of Viscous Fingering", Soc. Pet. Eng. J. (June 1963), 138-144.

6. Dake, L. P.: "Fundamentals of Reservoir Engineering", Elsevier Scientific Publishing Company, New York, 1978.

7. de Haan, H. J.: "Effect of Capillary Forces in the Water Drive Process", Proc. Fifth World Petroleum Congress, 1959, Vol. II, 1-13.

8. Geffen, T. M., Owens, W. W., Parrish, D. R. and Morse, R. A.: "Experimental Investigation of Factors Affecting Laboratory Relative Permeability Measurements", Trans., AIME (1951) 192, 99-110.

9. Hagoort J.: "Displacement Stability of Water Drives in Water-Wet Connate-Water-Bearing Reservoirs", Soc. Pet. Eng. J. (Feb. 1974), 63-74.

10. Heaviside, J. and Black, C. J. J.: "Fundamentals of Relative Permeability: Experimental and Theoretical Considerations", paper SPE 12173, presented at the 58th Annual Technical Conference and Exhibition, San Fransisco, Oct. 5-8, 1983.

11. Hovanessian, S. A. and Fayers, F. J.: "Linear Waterflood with Gravity and Capillary Effects", Soc. Pet. Eng. J. (March 1961), 32-36.

12. Jerauld, E. R., Davis, H. T. and Scriven, L. E.: "Frontal Structure and Stability in Immiscible Displacement", paper SPE/DOE 12691, presented at the SPE/DOE 4th Symposium on Enhanced Oil Recovery, Tulsa, OK., April 15-18, 1984.

13. Labasite, A., Guy, M., Delclaud, J. P. and Iffly, R.: "Effect of Flow Rate and Wettability on Water-Oil Relative Permeabilities and Capillary Pressure", paper SPE 9236, presented at the SPE 55th Annual Fall Technical Coference and Exhibition, Dallas, TX, Sept. 21-24,1980.

14. Leverett, M. C.: "Capillary Behavior in Porous Solids", Trans., AIME (1941) 142, 152-169.

15. Morse, R. A., Terwilliger, P. L. and Yuster, S. T.: "Relative Permeability Measurements on Small Core Samples", Prod. Monthly (Aug. 1947), 19-25.

16. Mungan, N.: "Role of Wettability and Interfacial Tension in Waterflooding", Soc. Pet. Eng. J. (June 1964), 115-123.

17. Mungan, N.: "Certain Wettability Effects in Laboratory Waterfloods", J. Pet. Tech. (Feb. 1966), 247-252.

18. Mungan, N.: "Interfacial Effects in Immiscible Liquid-Liquid Displacement in Porous Media", Soc. Pet. Eng. J. (Sept. 1966), 247-253.

19. Naar, J., Wygal, R. J. and Henderson, J. H.: "Imbibition Relative Permeability in Unconsolidated Porous Media", Soc. Pet. Eng. J. (March 1962), 13-17.

20. Perkins, T. K. and Johnston, O. C.: "A Study of Immiscible Fingering in Linear Models", Soc. Pet. Eng. J. (March 1969), 39-46.

21. Rachford, H. H., Jr.: "Instability in Waterflooding Oil from Water-Wet Porous Media Containing Connate Water", Trans., AIME (1964) 231, 133-148.

22. Richardson, J. G., Kerver, J. K., Hafford, J. A. and Osoba, J. S.: "Laboratory Determination of Relative Permeability", Trans., AIME(1952) 195, 187-196.

23. Sayre, A. T., Jr. and Yuster, S. T.: "A Study of the Effects of Connate Water Saturation on Waterflooding", Prod. Monthly (Oct. 1949), 19-26.

24. Sheldon, J. W.: "On the Fingering of Slow, Immiscible, Viscous Liquid-Liquid Displacements", paper SPE 1552G, presented at the 35th Annual Fall Meeting of SPE-AIME, Denver, Colorado, Oct. 2-5, 1960.

25. Wagner, O. R. and Leach, R. O.: "Effect of Interfacial Tension on Displacement Efficiency", Soc. Pet. Eng. J. (Dec. 1966) 335-344.

VITA

Santanu Khataniar was born at Dibrugarh, Assam, India, on May 1, 1961, the son of Hiranya Prova Khataniar and Sobhan Chandra Khataniar. He completed the High School Leaving Certificate Examination from Cotton Collegiate Higher Secondary School of Gauhati, Assam, India, in 1976 and the Pre-University Examination from Cotton College, Gauhati, Assam, India, in 1978. He received the degree of Bachelor of Technology in Petroleum Engineering from The Indian School of Mines, Dhanbad, India, in 1983. After receiving his Bachelor's degree, he entered the Graduate School of The University of Texas at Austin.

Permanent Address: Pub Sarania
Gauhati-781003
Assam
INDIA.

This thesis was typed by Santanu Khataniar.